Sustainable Energy Technology

Study of amine degradation in direct air capture

Arya Kumar Gowda

Confidential

TU Delft

ZEF

Study of amine degradation in direct air capture

by

Arya Kumar Gowda

to obtain the degree of Master of Science
at the Delft University of Technology,
to be defended publicly on Tuesday April 7th, 2020 at 10:30 AM.

Student number:	4718577	
Project duration:	January 15, 2019 – April 7, 2020	
Thesis committee:	Prof. dr. ir. W. de Jong,	TU Delft, Chair
	Prof. dr. ir. E. Goetheer,	TU Delft
	dr. B. Eral,	TU Delft
	ir. J. van Kranendonk,	ZEF .BV, daily supervisor

TU Delft

Abstract

The extensive use of fossil fuels and the emission of greenhouse gases have resulted in severe issues such as global warming and climate change. The energy and transport sector generate the major share of greenhouse gases globally. Though renewable energy can supply some of the energy demands, fossil fuels are still considered as a primary source to balance the world energy requirements. CO_2 being the major constituent of the greenhouse gases, carbon capture process (from the source of emission and from air) has been proposed as a promising technology to alleviate the effects of global warming in the near future. Alongside, technologies have been developed to produce fuels or other useful chemicals from the captured CO_2. This process is called carbon re-utilization. Zero Emission Fuels (ZEF. B.V) is a company in the Netherlands that is working towards developing a system that produces Methanol from CO_2 and water captured from ambient air viz. Direct air capture (DAC).

In the ZEF DAC process, polyethylenimine (PEI) and tetraethylenepentamine (TEPA) are used as CO_2 absorbents. These amines capture CO_2 and water at ambient conditions (absorption phase). The CO_2 and water is then stripped from the amine at elevated temperature (desorption pahse) and the gases are used for methanol production. During the process of absorption and desorption, the amines undergo losses such as evaporation and degradation. This leads to decrease in the efficiency of the DAC system over time. This thesis is focused on determining the evaporation and CO_2 induced degradation losses that might occur of PEI and TEPA during the direct air capture process

To determine the losses in PEI and TEPA, it is necessary to understand the behaviour of amines in a cyclic absorption-desorption. PEI and TEPA were subjected to 30 cycles of alternative absorption and desorption processes. Regarding evaporation losses, both PEI and TEPA showed significant loss of mass during the desorption process (80 °C, 120 °C were the selected desorption temperatures). Theoretically, the partial pressure of CO_2 and water absorbed by the amine reduces the evaporation rate of the mixture (amine+water+CO_2). But, during the desorption process, as the CO_2 and water are stripped out of the amine, the evaporation rate of the mixture increases. To, determine the maximum evaporation that could take place under negligible partial pressure of CO_2 and water, pure samples of PEI and TEPA were heated at 80 °C, 100 °C, 120 °C. Results showed that, in a long term operation, both PEI and TEPA might undergo evaporation losses (relatively, TEPA evaporates faster than PEI) and replacing the amine frequently would increase the cost of DAC process. Another important observation was that a significant mass of CO_2 remained in the sample after every desorption cycle. PEI accumulated more CO_2 than TEPA. This suggested that the process of desorption carried out during the experiment was inefficient. A hypothesis was proposed to explain the accumulation taking place in both the amines. Furthermore, Fourier Transform Infrared Spectroscopy (FTIR) was carried out on the samples subjected to cyclic experiments to identify the formation of degradation products. Results showed that during the cyclic absoprtion-desorption process, TEPA might have degraded when desorbed at 120°C. PEI samples did not show any indications of degradation.

Finally, future experiments are proposed to understand the degradation losses which might help in deciding the suitable amine for the DAC process.

Acknowledgements

Firstly I would like to thank Jan van Kranendonk, Ulrich Starke and Hessel Jongebreur for giving me an opportunity to work on my master thesis at Zero emission fuels.

I would also like to thank professor Wiebren de Jong and professor Earl Goetheer for guiding me throughout the research process and helping me tune my scientific writing skills.

Thank you Arjen Huizinga (TNO) for your assistance during my experiments. Without your support, the completion of this thesis would have been difficult.

Thank you Dr Janameyjaya Channegowda for being my mentor from the start of my master's journey. I am always grateful for your constant support and timely motivation which kept me on track.

This section would be incomplete without mentioning my friends Karthik Badarinath, Anurag, Varun and Samruddhi. Their love and affection has made my master's journey much easier. I would also like to thank Sushanth mama, Sharab, Kishan, Kushal,Nikhilesh, Arvind, Anoosh, Akhilesh and Sid for being a part of my Delft life.

Thank you Yashvanth Pochareddy for your moral support and feedback on the thesis manuscript.

I would also like to thank Shasish Bhai, Mrigank Bhai and Marieke for creating a positive environment in the work space. This helped to relieve the stress of the bottlenecks during the experimental phase.

Finally, I would take this opportunity to express my love and gratitude to my parents who has always believed in me.

Contents

List of Figures

List of Tables

Nomenclature

CCS -Carbon Capture Sequestration

D_w -Molecular diffusivity of water

DAC -Direct Air Capture

H_v -Heat of vaporization

k_m -Mass transfer coefficient

P_v -Vapour pressure

PEI -Polyethylenimine

R -Universal gas constant

Re -Reynolds number

Sc -Schmidt number

Sh -Sherwood number

$TEPA$ -Tetraethylenepentamine

1 Introduction

1.1. CO_2 emissions and Global warming

Global warming is a major issue that has become a subject of public concern. This is caused due to the presence of greenhouse gases (GHG's) in the atmosphere, which traps the heat within the lower atmosphere and at the earth's surface [1]. The greenhouse gases includes water vapor, methane, carbon dioxide, nitrous oxide and chloroflurocarbons (CFC's) [1]. Global warming changes the earth's energy balance which leads to climate change [2]. Some of the evidences of climate changes are: rise in global temperatures, extreme changes in the frequency of weather conditions [3], and rise in sea level due to glacier meltdowns [4]. Thus, climate change is disturbing the balance of the ecosystem [5].

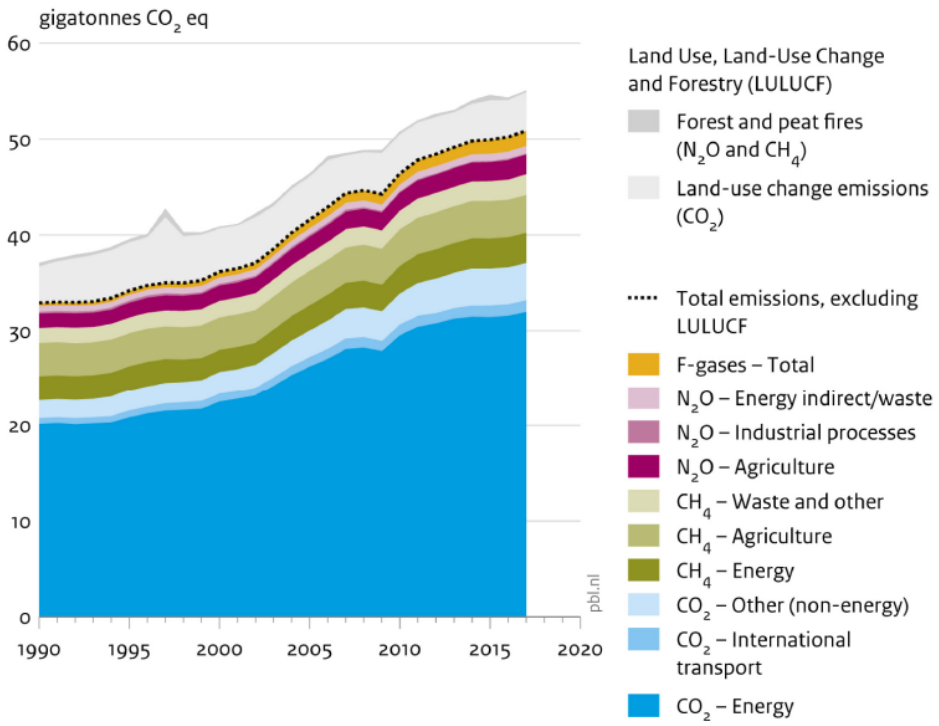

Figure 1.1: Greenhouse gas emission by different sectors [6]

It can be seen from figure 1.1 that the green house gas composition consists largely of CO_2. This level of CO_2 concentration in the atmosphere is a result of emissions caused by extensive use of fossil fuels [1, 7]. The permitted levels of CO_2 in the atmosphere is about 300 ppm, but studies carried out in 2010 showed that the CO_2 concentrations had crossed 400 ppm [8]. The Intergovernmental Panel on Climate Change (IPCC) suggests that the levels of CO_2 concentrations in the atmosphere must be restricted to 450 ppm by 2100 in order to mitigate the global temperature rise, greater than 1.5°C [9]. As shown in Figure 1.1, we can see that the energy sector is the major contributor to CO_2 emissions.

Replacing the fossil fuels with renewable energy could help in reducing the carbon dioxide concentrations. Currently, the world renewable energy system contributes to 17% of the total

consumption and the remainder is supplied by petroleum, coal and natural gas [3]. Figure 1.2 shows the dependence on different energy sources in the year 2017. It can be clearly seen that oil and natural gas provide a major share in the human energy demands. Therefore, fossil fuels are still the major sources for energy production [2].

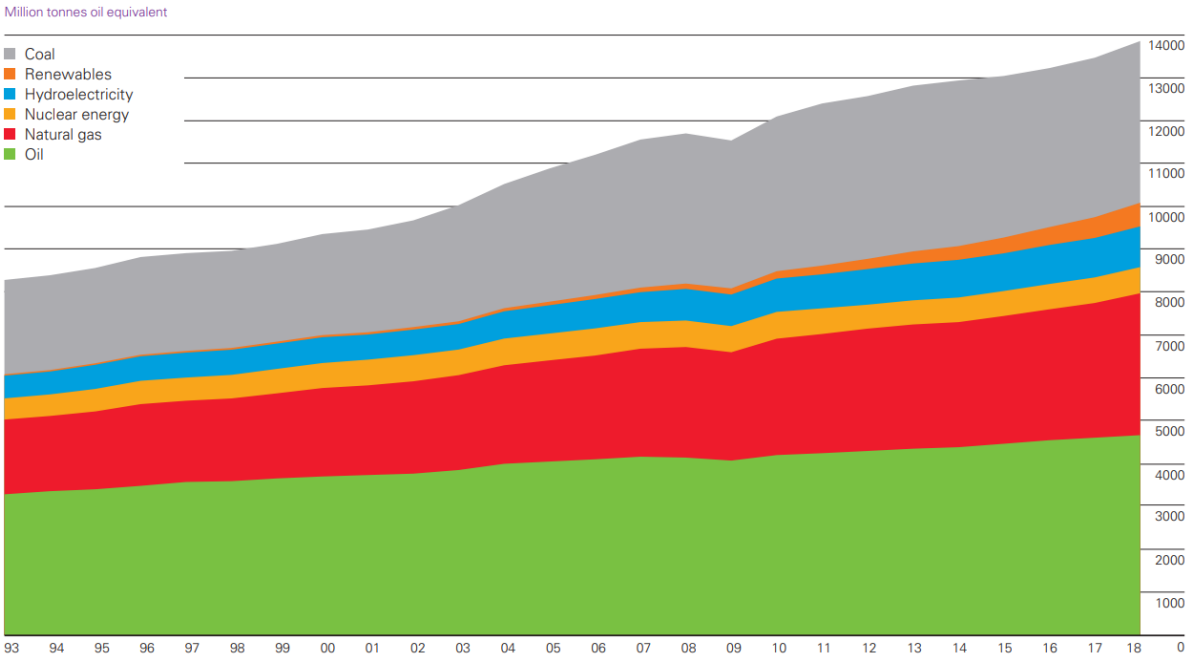

Figure 1.2: World primary energy consumption [10]

Considering the dependency on the fossil fuels as sources of energy and the consequences of their extensive usage, an alternative method to mitigate the carbon dioxide levels in the atmosphere is by capturing and storing it [11, 12]. This method includes capturing CO_2 at the source of emission, generally called as carbon capture and sequestration (CCS), and direct air capture. This process is explained in Section 1.2. **It is important to note that this thesis is focused on direct air capture process**. Thus, only a brief description on CCS will be given in Section 1.2. Further, the captured CO_2 can be used to produce value added products. This process is called “carbon re-utilization”. A brief explanation on the process will be explained in Section 1.3.

1.2. Carbon capture

The carbon capture process can be broadly classified into carbon capture and sequestration and direct air capture. A brief description on both the process is given in Section 1.2.1 and 1.2.2, respectively.

1.2.1. Carbon Capture Sequestration (CCS)

Conventionally, the application of carbon capture technology was mainly focused on limiting the CO_2 emissions from large stationary sources (eg: oil refineries, fossil fuel power plants, iron industries etc) [13]. Different techniques are employed to capture CO_2 from different emitting sources and this can be seen in figure 1.3.

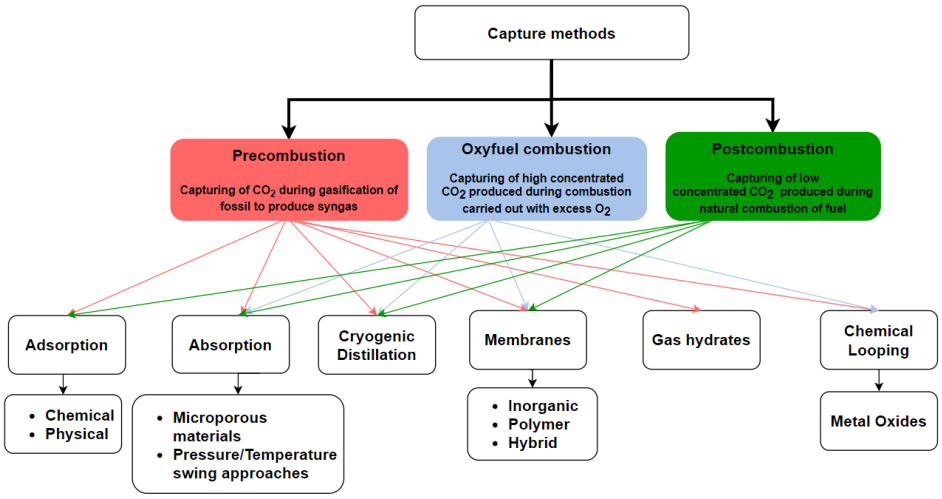

Figure 1.3: Carbon capture techniques [14]

The sources of CO_2 seen in figure 1.3 are the exhaust gases produced during different processes. The exhaust gases vary with CO_2 concentration, temperature and pressure. The variation in process parameters can be found in table 1.1.

Table 1.1: Typical pressure, temperature and CO_2 concentrations of gas streams found in CCS technology [15]

Source	Precombustion	oxy-fuel combustion	Postcombustion
Pressure (atm)	>5	>50	1
Temperature °C	>100	<50	<100
CO_2 (vol %)	35	>90	4-14

From table 1.1, we can see that the process condition of the gas stream vary largely from one source to another. Thus, different procedures and absorbing materials must be used to effectively capture the CO_2 from different sources. The details on the process of carbon capture sequestration are not included in this report. A review on CCS techniques can be found in literature of Perez et.al [13], Gao et.al [3], Yu et.al [7], Singh [16] , Ko et.al [17] and Wanga et.al [18].

The captured CO_2 is pressurized and transported either by pipelines or ships. Further, they are stored in depleted oil reservoir or saline aquifers [19]

Although the CCS technology helps to reduce the CO_2 emissions, it is suitable mainly for large stationary sources. A significant level of emissions are caused by sources such as small industries, transportation sector, houses etc. As the parameters of the distributed sources vary from one another, the application of CCS to individual source becomes difficult and is not economically viable [20].

1.2.2. Direct Air Capture (DAC)

This is a complimentary technique to CCS, which helps to remove CO_2 directly from ambient air [21, 22]. This technique has an advantage over CCS as it can be used to capture CO_2 irrespective of the nature and location of the emitting source [12].

One of the key challenges to the DAC process is that the process takes place with dilute or ultradilute concentrations of CO_2 (400 ppm) and under ambient conditions [23]. Thus, this process is different from flue-gas capture (CCS) and requires different operating conditions and CO_2 scrubbing/absorbing material. Materials such as aqueous hydroxides, alkali carbonates, oxide supported amines are used to capture CO_2 in direct air capture process. Information on different DAC techniques and materials used can be found in literature of

Pirez et.al [13].

1.3. CO_2 re-utilization

The CO_2 captured through the techniques mentioned in Section 1.2 are generally stored in underground reservoirs. But, a better way is to convert CO_2 into methanol [3]. The methanol can be either used as fuel or as a precursor to produce other useful chemicals [24]. Figure 1.4 shows a simple process of converting CO_2 and re-utilization.

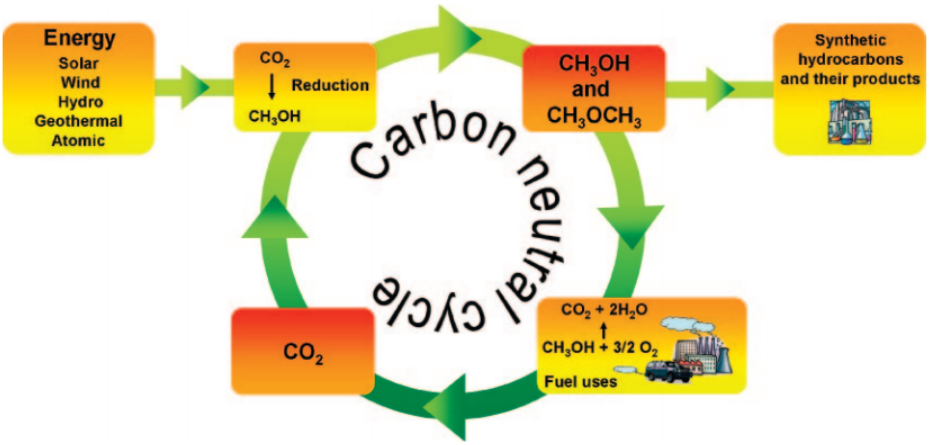

Figure 1.4: Process for achieving carbon neutral fuel[24]

It can be seen in figure 1.4 that the energy demands of the CO_2 conversion process are supplied by renewable energy. Thus, by integrating renewable energy, carbon capture and re-utilization the need to use fossil fuel can substantially reduced and consequently the new CO_2 emissions. This is called **carbon neutral cycle** and fuel produced is called **carbon neutral fuel**

Zero Emission fuels (ZEF B.V) is one such company which is trying to produce carbon neutral fuel by integrating solar energy, direct air capture and re-utilization techniques. Brief details on the company can be found in Section 1.4.

1.4. Zero Emission Fuels

Zero Emission Fuels BV (ZEF BV) [25] is a startup from Delft, the Netherlands, working towards developing a small scale carbon neutral fuel (methanol) production system. This production unit consists of the following subsystems [25]:

- **Direct air Capture (DAC):** This subsystem captures water and carbon dioxide from ambient air
- **Electrolyser:** The water captured by DAC subsystem is split into H_2 and O_2
- **Methanol reactor:** CO_2 and H_2 are converted into methanol at elevated pressures and temperatures
- **Compressor :** CO_2 and water are compressed to 50 bar pressure as it is the selected operating condition of the electrolyser and methanol rector

The energy requirements of the whole system are delivered by the solar energy. An overview of integrated subsystems in the methanol production plant can be seen in figure 1.5.

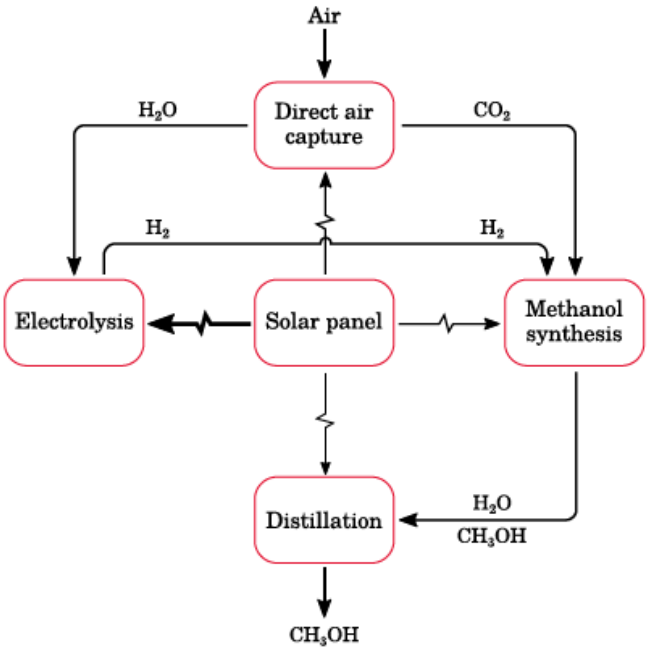

Figure 1.5: Overview of the ZEF methanol production plant [26]

As mentioned in Section 1.1, this project and report focuses on the DAC subsystem. Section 1.4.1 gives a brief description on the DAC process, materials used for CO_2 capture operational conditions.

1.4.1. DAC at ZEF

As explained in Section 1.4, the captured CO_2 is re-utilized to produce methanol. Thus, the DAC at ZEF includes both carbon capture (absorption) and regeneration (desorption) process. Polyethylenimine (PEI) and tetraethylenepentamine (TEPA) are the two polyamines considered for the process of carbon capture. The overview of the process followed in DAC at ZEF is shown in figure 1.6.

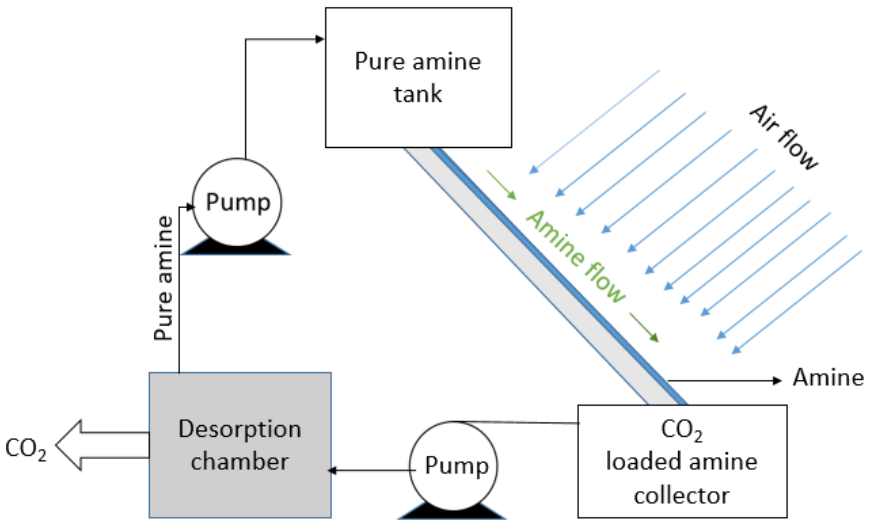

Figure 1.6: Overview of ZEF DAC system

As seen in figure 1.4.1, a thin layer of pure amine flows on a plate and is exposed to am-

bient air. CO_2 and moisture are absorbed as the amine flows down. The CO_2 loaded amine is then carried to the desorption chamber where amine is separated from CO_2 and moisture by application of heat. This process is similar to amine scrubbing technique. The process of CO_2 absorption-desorption through amine scrubbing technique is explained in Section 2.2.1.

The selection of amine is a critical part in developing a carbon capture system. Figure 1.7 shows certain important parameters to be considered before selecting an amine absorbent. These parameters must be studied for PEI and TEPA in-order to decide which amine can perform efficiently in the ZEF DAC system for a longer duration.

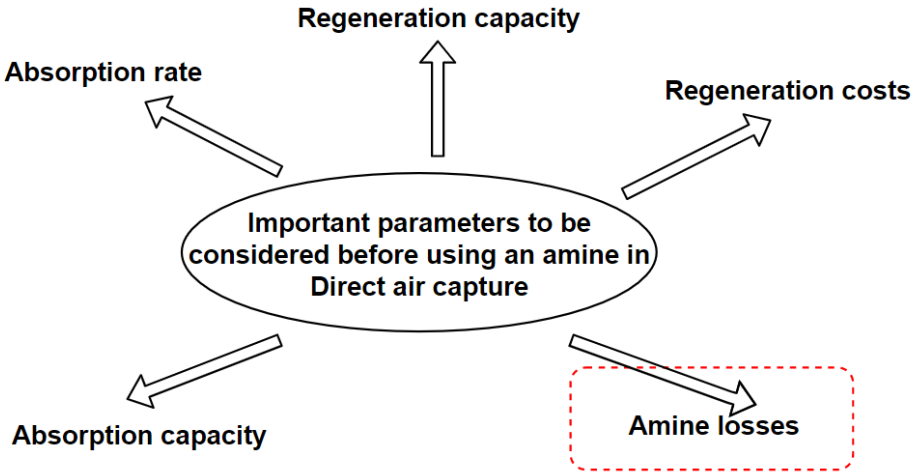

Figure 1.7: Parameters to be considered while selecting an amine absorbent for DC process

The studies on PEI and TEPA have been carried at ZEF. The absorption of CO_2 and water in PEI/TEPA and its influence on the physical properties of the amine was studied by Sinha [27]. Ovaa studied the behaviour of amine during desorption of CO_2 and water [28]. The important observations are given in section 2.5. In the above mentioned studies, the amine behaviour was studied with respect to only one absorption or desorption cycle. This thesis focuses on studying the behaviour of amine when subjected to multi-cycle process and the losses that might occur during the process.

1.5. Thesis objectives

The thesis objective is to identify the suitable amine (PEI or TEPA) regarding the amine losses that takes places in DAC process. Figure 1.8 gives an overview of the thesis objective.

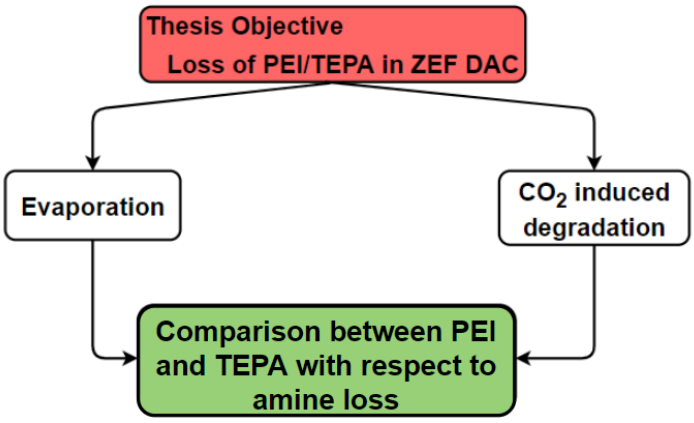

Figure 1.8: Overview of thesis objectives

The above mentioned objectives can be achieved by answering the following questions:

- Understand the behaviour of PEI and TEPA, when used as bulk absorbents, in cyclic absorption desorption process
- Determine the evaporation rates of PEI and TEPA at different temperatures
- Determine which amine is more resistant to CO_2 induced degradation

1.6. Thesis scope

The behaviour of the amine might vary with change in parameters such as pressure, temperature, moisture, concentrations of CO_2 and other gases. This change is applicable at both absorption and desorption stages. The experimental procedures followed were:

- Ambient air was used during absorption phase of the experiment. The variation in concentrations of CO_2, moisture and absorption temperature was not regulated. Thus, the effects of different concentrations on amine degradation cannot be observed.
- Only concentrations of CO_2 and moisture were measured during experiments. Absorption of any other gases was not studied.
- This thesis focuses only on evaporation and CO_2 induced degradation. Other important loses such as O_2 induced degradation were not studied.
- During the desorption process of the cyclic experiments, N_2 gas was used to purge the desorbed gases. The pressure of the outgoing gases was not measured. Thus, the influence of pressure cannot be determined.

1.7. Report outline

Figure 1.9 shows an overview of the report structure.

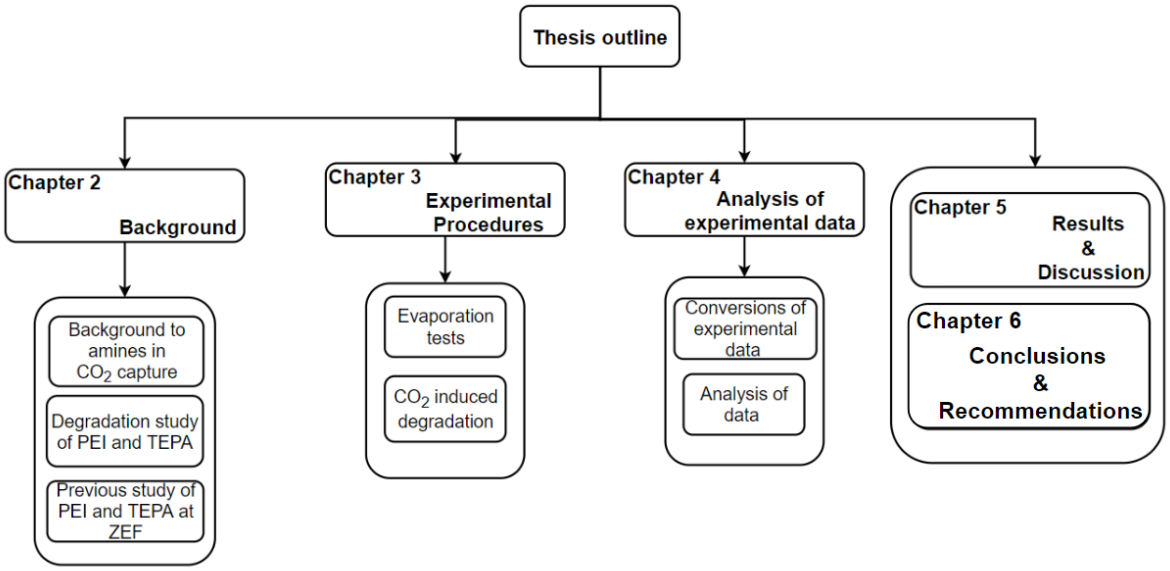

Figure 1.9: Overview of the thesis report

The relevant literature on DAC process can be found in Chapter 2. Chapter 3 explains the experimental procedures followed to determine the amine losses occurring during the DAC process. The data obtained during the experiments were analysed and the methods of analysis are given in Chapter 4. Chapter 5 presents the important results obtained during the experiments. Further, the implications of the thesis in ZEF DAC system and recommendations for future experiments are given in chapter 6.

2

Background

This literature studied to understand the application of amines in the process of carbon capture (from both stationary source and from air) are presented in this chapter. Figure 2.1 shows the structure of the chapter. The topics covered in this chapter provides an insight into the basic principles and the state of the art research on amines in carbon capture process.

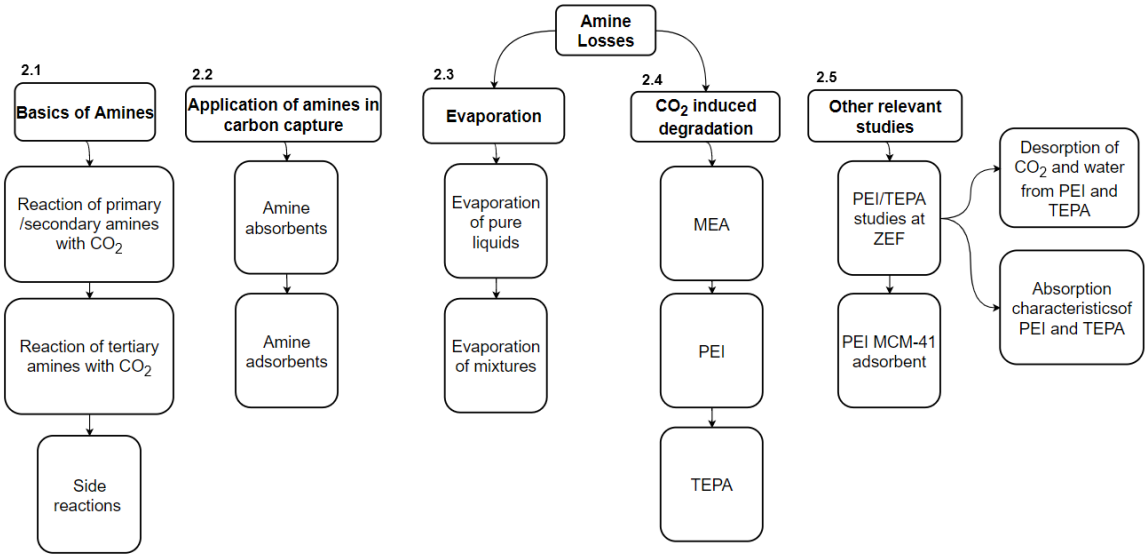

Figure 2.1: Overview of chapter 2

2.1. Basics of Amines

Amines are derived from ammonia NH_3 where one or more hydrogen atoms are substituted by an alkyl or aryl groups [29]. The substitutes are called functional groups. Amines can be classified as primary, secondary and tertiary amines. Descriptions of amine classification and functinal groups are shown below.

Primary amines: Primary amines are derived by replacing one of the hydrogen in ammonia with a functional group. Methyl amine is a basic primary amine with a functional group of methane.

Secondary amines: Secondary amines are derived by replacing two hydrogens in ammonia with two functional groups. Dimethylamine is a basic example of secondary amine.

Tertiary amines: Tertiary amines are derived by replacing all hydrogen with functional groups. Trimethyl amine is a basic example. Molecular representation of primary, secondary and tertiary amines can be seen in figure 2.2.

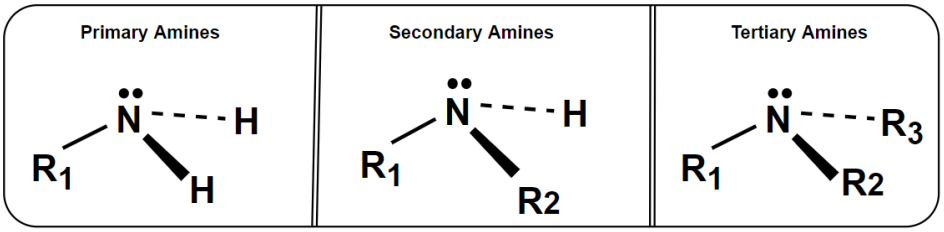

Figure 2.2: Molecular representation of primary, secondary and tertiary amines. R1,R2,R3 are functional groups

2.1.1. Reaction of CO_2 with primary and secondary amines

The reaction mechanism for amine based absorbents was introduced by Caplow in 1968 [30]. The reaction takes place in two steps which are represented as shown below:

$$CO_2 + R_1R_2NH \rightleftharpoons R_1R_2NH^+COO^- \tag{2.1}$$

$$R_1R_2NH^+COO^- + B \rightleftharpoons R_1R_2NCOO^- + BH^+ \tag{2.2}$$

R_1R_2NH is the aqueous amine (secondary amine in this case). R_1 and R_2 are the substituted groups. The $R_1R_2NH^+COO^-$ seen in Equation 2.1 is called zwitterion. In Equation 2.2, $R_1R_2NCOO^-$ is the carbamate formed by removal of a proton by B. B is a base molecule which can be water, amine or hydroxyl ion (OH^-). Caplow assumed that the amines must be hydrated or, the presence of water is necessary to form carbamates at faster rate. That is, the base molecule in Equation 2.2 should be water [30]. The molecular representation of zwitterion formation given by Caplow is shown in figure 2.3.

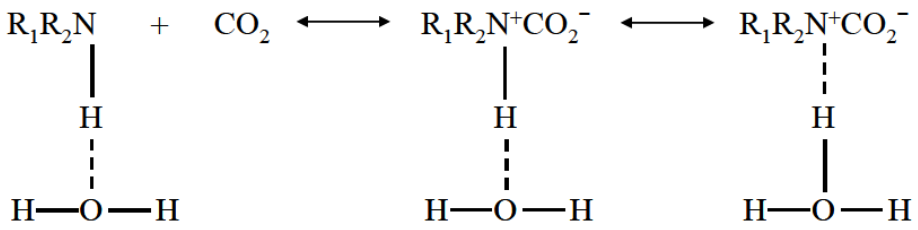

Figure 2.3: Reaction of amine with CO_2 to form zwitterion, represented by Caplow [16]

Danckwerts suggested that the carbamate formation can be reduced to a single step process by considering the base molecule to be an amine [31]. This study showed improved kinetics in carbamate formation resulting in considering the zwitterion as a quasi-steady state. Yoshida et al. and Svendsen da Silva separately carried out quantum mechanical calculations on zwitterion and suggested that such species are highly unstable or exist in a transition state [32, 33].

Following Danckwerts, Crooks and Donnellan suggested a single step termolecular mechanism for amine reaction [34] represented in Equation 2.3. Figure 2.4 shows the simultaneous bonding of amine/CO_2 and transfer of proton. Here, B is again a base molecule.

$$CO_2 + R_1R_2NH + B \rightleftharpoons R_1R_2NCOO^- + BH^+ \tag{2.3}$$

Further, the carbamates undergo hydrolysis to form bicarbonates [16]. Equation 2.4 shows the hydrolysis of carbamates to form bicarbonates.

$$R_1R_2NCOO^- + H_2O \rightleftharpoons R_1R_2NH + HCO_3^- \tag{2.4}$$

The rate of formation of bicarbonates by hydrolysis of carbamates depends on several factors such as temperature, the basicity of amines, amine chain length. The rate limiting factors of bicarbonate formation is currently beyond the scope of this report. A Brief explanation can be found in the work of Singh [16].

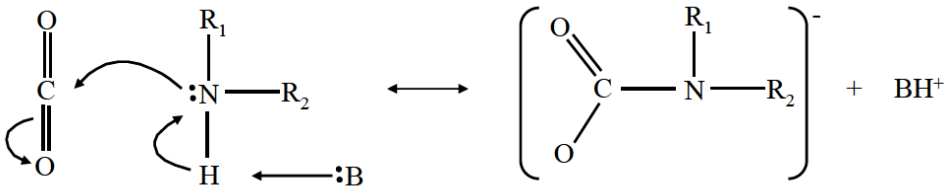

Figure 2.4: Molecular representation of single step carbamate formation [16]

2.1.2. Reaction of CO_2 with tertiary amines

The tertiary amines lack a free proton which hinders the direct reaction of CO_2 to form carbamates [35]. Nguyen and Donaldsen suggested that the hydration of CO_2 is catalyzed by the tertiary amine resulting in the formation of bicarbonates [36]. The reaction mechanism is as follows:

$$CO_{2(aq)} + H_2O \rightleftharpoons H_2CO_3 \tag{2.5}$$

$$CO_{2(aq)} + OH^- \rightleftharpoons HCO_3^- \tag{2.6}$$

$$CO_2^+ R_1R_2R_3N + H_2O \rightleftharpoons R_1R_2R_3N^+H + HCO_3^- \tag{2.7}$$

The reaction of tertiary amines with CO_2 is found to be less exothermic when compared to reactions with primary and secondary amines [37]. Shyu and Lin reported that, in comparison to primary and secondary amines, the tertiary amines show less degradation and loss of capacity when subjected to regeneration cycles [38].

The carbonates are formed by deprotonating the bicarbonates with a base molecule. Equation 2.8 shows the carbonate formation in the presence of a base molecule.

$$HCO_3^- + B \rightleftharpoons CO_3^- + B \tag{2.8}$$

2.1.3. Side reactions

Apart from the reactions involving the formation of bicarbonates, carbamates, carbonates, important side reactions such as ionization of water and protonation of amines also take place in the aqueous media [16]. The following equations represent the side reactions taking place.

$$Ionization : H_2O \rightleftharpoons OH^- + H_3O^+ \tag{2.9}$$

$$Protonation : R_1R_2NH + H_2O \rightleftharpoons R_1R_2NH_2^+ + OH^- \tag{2.10}$$

The hydroxyl ions formed during side reactions are responsible for bicarbonate formation in case of tertiary amines shown in Equation 2.6. Figure 2.5 shows an overview of the reaction mechanisms of CO_2 with primary, secondary and tertiary amine.

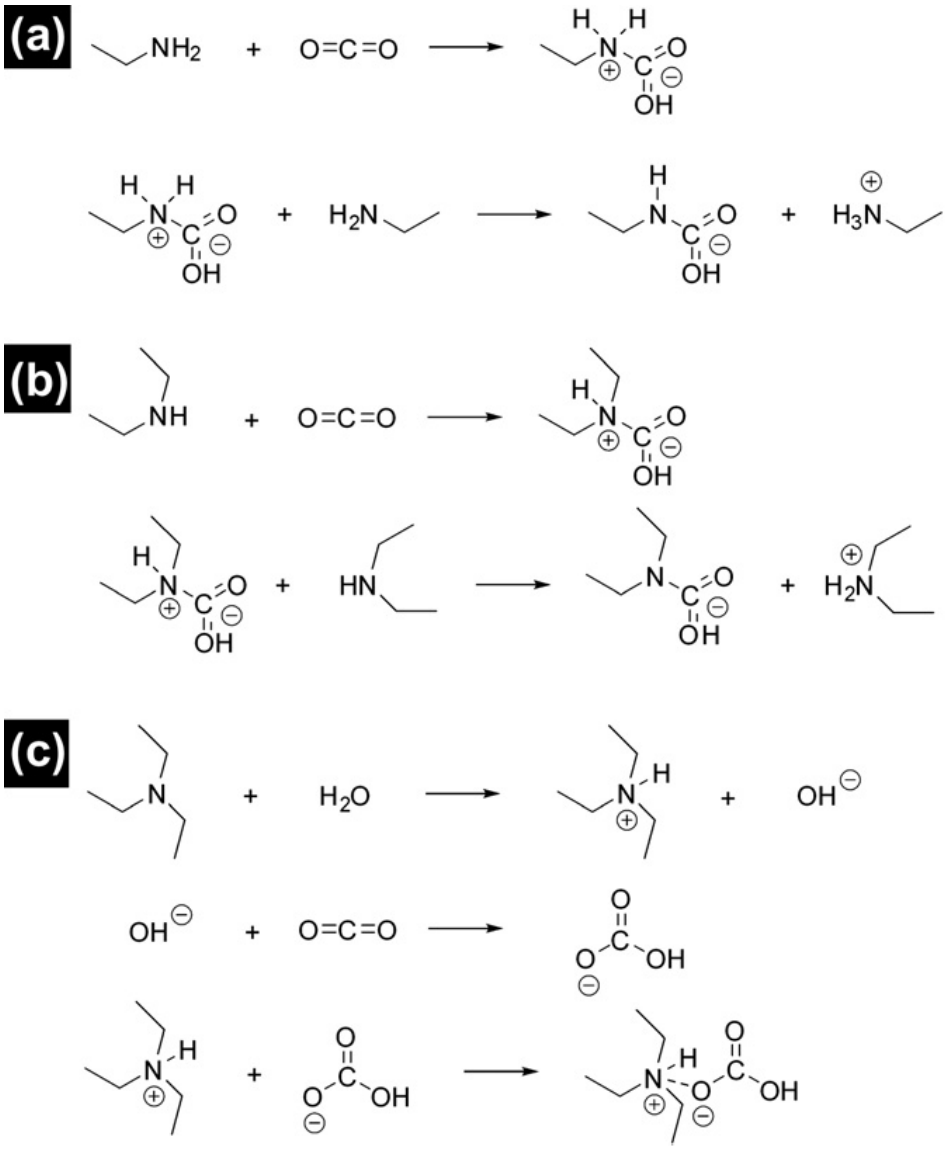

Figure 2.5: Reaction mechanism of CO_2 with (a) primary amine (dry condition), (b) secondary amine (dry condition), (C) tertiary amine (hydrated) [39]

2.2. Application of amines in carbon capture process

As explained in Section 2.1.1, the reaction of CO_2 with amines forms stable carbamate ions. These reactions can be reversed and CO_2 can be regenerated [40]. This characteristics of amines makes it suitable for carbon capture and re-utilization process [41]. Amine scrubbing is one such process where liquid amines are used for CO_2 capture process. Details on amine scrubbing can be found in Section 2.2.1.

2.2.1. Amine scrubbing

The process of amine scrubbing process using monoethanolmine (MEA) was started with the work of Bottoms which was patented in 1930 [42]. The figure 2.6 shows the process layout of the amine scrubbing plant.

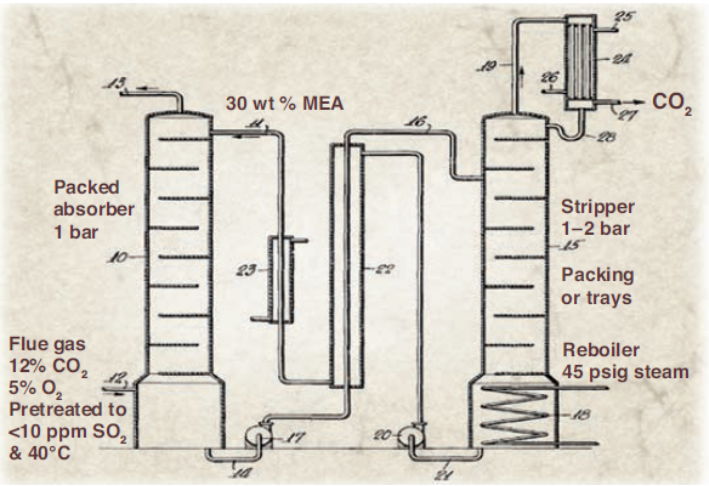

Figure 2.6: Amine scrubbing process layout by R.R. Bottoms [43]

A typical amine scrubber consists of an absorber column and a stripper column. CO_2 gas and aqueous amines flow counter- currently across a packed bed in the absorber column. This process takes place as ambient temperature and pressure. Once the CO_2 is absorbed by the amine, the absorbent is transported to the stripper column. The CO_2 is separated from the amine at a temperature range of 100^0C to 120^0C. The pure amine is again pumped back to the absorber column for cyclic use. The DAC process at ZEF mentioned in Section 1.4.1 is conceptually similar to the amine scrubbing technique.

The first commercially available absorbent for amine scrubbing technique was triethanolamine (TEA) [16]. Amines like monoethanolamine (MEA), diethanolamine(DEA) and methyldiethanolamine (MDEA) were also of commercial interest [42]. These amines showed several limitations which are represented in figure 2.7.

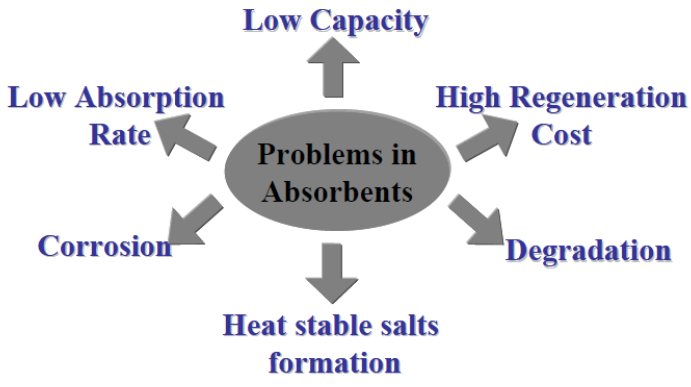

Figure 2.7: Various factors affecting the amine efficiency in CO_2 capture. [16]

The limitations of the absorbents used in amine scrubbing have been detailed in the works of Resnik [44] and Haszeldine [45]. To overcome the problems mentioned in figure 2.7, the amines are used as solid sorbents or adsorbents. Details on adsorbents are given in Section 2.2.2.

It must be noted that in this the report, the word **absorbent** and **absorption** is used when speaking about processes like **amine scrubbing**. In Section 2.2.2, **adsorption** technique is introduced where amines are supported by solid structures. Here the amine along with the support structure is called **adsorbent**. The words absorption and adsorption **cannot be used interchangeably**.

2.2.2. Use of amines as solid adsorbents

In the state of the art research on carbon capture, amines are used as solid sorbents or adsorbents. In this technique, the amines are supported by porous materials such as silica. Grafting , physical impregnation or in-situ polymerization methods are used to produce the solid sorbents [46].

Research has shown that the adsorbents exhibit higher CO_2 capture and regeneration ability, resistance towards degradation and low energy consumption when compared to other amine scrubbing techniques [47–50]. This report dose not focus on comparing the absorbents and adsorbents techniques. As mentioned in Section 1.5, the aim of this research is to study the amine losses that might occur in PEI and TEPA (when used as absorbents) during DAC process. Evaporation and CO_2 induced degradation are the losses considered in this study. The recent developments in carbon capture uses PEI/TEPA as adsorbents and studies on PEI/TEPA absorbents were not found. Thus, amine loss related studies on different absorbents and adsorbents were considered to develop experimental procedures to test PEI/TEPA absorbents and to analyse the results. Section 2.3 gives an abstract on how different studies were used to understand the behaviour of the amine at ZEF DAC.

2.3. Amine losses

As mentioned in Section 1.5, this thesis is focused on evaporation and CO_2 induced degradation. Section 2.3.1 gives a brief explanation on the principles of evaporation and the theoretical methods to determine the evaporation rates. Section 2.4 gives an over view of the state of art research on amine degradation.

2.3.1. Evaporation

The process by which molecules at the surface of the liquid breaks the liquid phase inter-molecular force and escapes into gas phase is called evaporation. Evaporation of a substance is influenced by factors such as given below: A brief description on how the evaporation rate varies with liquid mixture is included in Section 2.3.1.

Factors influencing evaporation

- **Vapour pressure** - This parameter indicates the tendency of molecules to escape from the liquid surface. High evaporation of liquid takes place if its vapour pressure is high.
- **Temperature** - As temperature increases the kinetic energy of the liquid molecules also increase. This results in faster evaporation.
- **Surface area** - Evaporation is a surface phenomena. As the surface area increases, more molecules tend to escape at the liquid-gas interface.
- **Flow rate** - Increase in the flow rate of the gases above the liquid surface results in higher evaporation rate. This is because, the gases flowing above the liquid surface enhances the mass transfer of liquid vapor into the gas phase.
- **Inter-molecular forces** - Liquids with strong inter-molecular forces exhibits lower evaporation

Determining evaporation rates

The evaporation rates of the liquids can be calculated using the equation shown below [51].

$$E = k_m * \frac{M_i * P_v(T)}{R * T} \tag{2.11}$$

Here, E = rate of evaporation ($kg\,m^{-2}\,s^{-1}$), P_v = vapour pressure at temperature T(Pa), k_m = mass transfer coefficient ($m\,s^{-1}$), R = gas constant ($8314\,m^3\,Pa\,K^{-1}\,kmol^{-1}$), M_i = molecular weight of the liquid ($kg\,kmol^{-1}$), T = temperature of the liquid (K).

The factor $\frac{M_i * P_v(T)}{R * T}$ signifies the mass of chemical vapour present in a unit volume above the liquid surface at a unit time. k_m signifies the rate at which the vapour molecules diffuses into the purge gas. In order to use this simplified equation to verify the experimental data certain assumptions were made such as:

- The chemical vapours obey ideal gas laws
- There are no temperature gradient within the liquid pool
- The temperature of the gas flowing above the liquid is neglected
- The energy interaction between the vapour and the gas flowing above the liquid is neglected

Further, the mass transfer coefficient k_m can be calculated using Sherwood number (Sh).

$$Sh = \frac{k_m * d_l}{D} \tag{2.12}$$

Here, d_l = surface diameter of the liquid (m), D = diffusion coefficient of vapour in air ($m^2\,s^{-1}$).

Diffusion coefficient of chemical vapour can be determined using Graham's law of molecular diffusivity [52].

$$D = D_w * \sqrt{\frac{M_w}{M_i}} \tag{2.13}$$

D_w = molecular diffusivity of water ($m^2\,s^{-1}$), M_w = mass of water ($kg\,kmol$), M_i = molecular weight of the liquid ($kg\,kmol^{-1}$).

Sherwood number (Sh) can also be calculated using Schmidt (Sc) and Reynolds (Re) number:

$$Sc = \frac{\nu}{D} \tag{2.14}$$

ν = kinematic viscosity of air ($m^2\,s^{-1}$)

$$Re = \frac{v * d_l}{\nu} \tag{2.15}$$

v = velocity of air over the liquid ($m\,s^{-1}$).

Sherwood number can be calculated using the following equations presented by Bennett et.al [53].

$$\text{For laminar flow} \quad Sh = 0.66 * Re^{0.5} * Sc^{0.33} \tag{2.16}$$

$$\text{For turbulent flow} \quad Sh = 0.0365 * Re^{0.8} * Sc^{0.5} \tag{2.17}$$

By using the above equations, the evaporation rates of a liquid at a particular temperature can be calculated. As seen in Equation 2.11, the vapour pressure used to determine the

evaporation rate is a function of temperature. The relation between vapour pressure and temperature can be determined by **Clausius-Clapeyron** Equation 2.18.

$$\ln \frac{P_1}{P_2} = (\frac{\delta H_v}{R}) * (\frac{1}{T_2} - \frac{1}{T_1}) \tag{2.18}$$

P_1 and P_2 are the vapour pressures at temperatures T_1 and T_2. H_v is the heat of vaporization of the liquid ($J\,mol^{-1}$).

The above equations can be useful to determine the evaporation rate of a pure liquid. Liquid mixtures exhibits different evaporation behaviour. Section 2.3.1 gives a brief explanation on evaporation of liquid mixtures.

Evaporation in liquid mixtures

In a liquid mixture, the liquid is considered as a solvent and the impurities added are called solute. Figure 2.8 and 2.9 shows the liquid molecular arrangement of pure (solvent) and liquid mixture (solvent and solute) respectively.

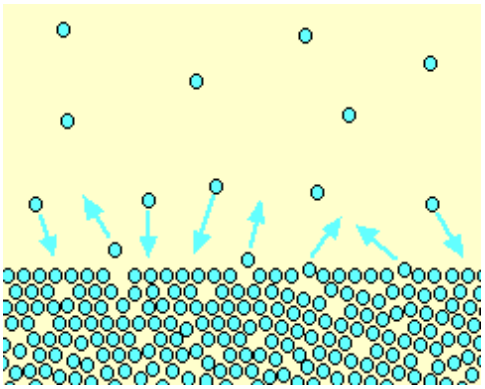

Figure 2.8: Pure liquid

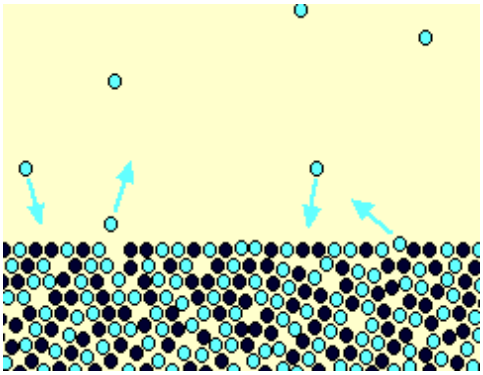

Figure 2.9: Liquid mixture

Comparing the figures 2.8 and 2.9, we can see that the pure liquid evaporates faster than liquid mixture. This reduction in evaporation rate can be explained by **Raoult's law** of partial pressures. The relation is shown in Equation 2.19

$$P_n = x_{solvent} * P^0_{solvent} \tag{2.19}$$

$x_{solvent}$ is the mole fraction of the solvent in the mixture. $P^0_{solvent}$ is the vapour pressure of the solvent at temperature T. P_n is the partial pressure of the solvent at temperature T. The relation between solute and solvent mole fractions are given in Equation 2.20.

$$x_{solvent} = \frac{m_{solvent}}{m_{solvent} + m_{solute}} \tag{2.20}$$

The increase in solute molecules will reduce the partial pressure of the solvent. This leads to reduction in evaporation rates.

2.4. CO_2 induced degradation study

The studies on CO_2 induced degradation have been divided into two parts. Section 2.4.1 presents the degradation pathways resulting in CO_2 induced degradation in MEA . Further, Section 2.4.2 and 2.4.3 give a review PEI and TEPA used as adsorbents in state of the art research. The details include information on absorption, desorption, amine loading and amine losses (CO_2 and O_2 induced degradation). Not all the information might be relevant for the current thesis study but, the information gives an overview of the state of the art.

2.4.1. CO_2 induced degradation in MEA

The reaction pathways observed in CO_2 induced degradation in MEA is shown in figure 2.10. CO_2 induced degradation occurs during the desorption phase where the partial pressure of

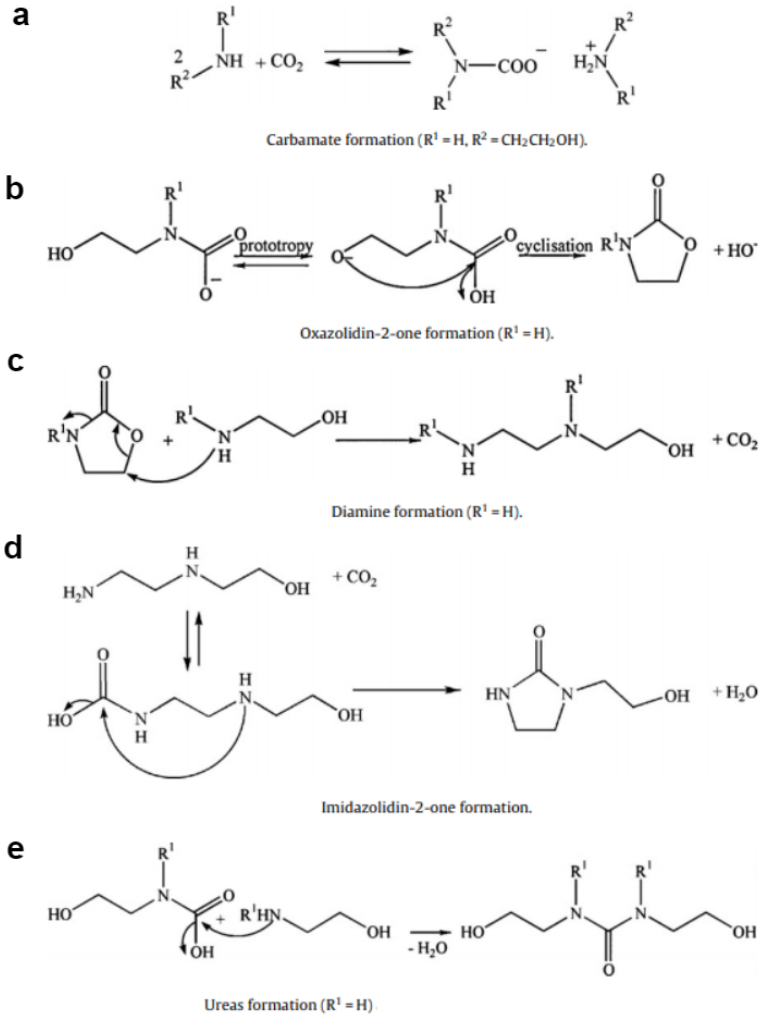

Figure 2.10: Reaction pathways of CO_2 induced degradation in MEA

CO_2 and temperature is high. In this section, the possible reaction mechanisms are presented. The influence of temperature and pressure have not been discussed.

In the absorption phase, MEA reacts with CO_2 to form carbamate. This is shown in **a** of figure 2.10. The formation of Oxazolidin-2-one from carbamates is a possible pathway [54]. Formation of Oxazolindin-2-one can be seen in **b** . Figure **c** shows that Oxazolidin-2-one can react with MEA to form HEEDA. Further, HEEDA can react with CO_2 to form carbamate which can undergo intermolecular cyclisation to form HEIA. This is shown in **d**. HEIA is a stable molecule that can accumulate in the solution. Studies conducted by Launay et al. observed that HEIA was the major degradation product [55, 56].

e of figure 2.10 shows the pathway of urea formation. Carbamates reacts with MEA to form urea. But, this degradation product is considered less favourable in comparison to formation of HEIA [54]. Similar degradation pathways are discussed for various amines such as diethanolamine (DEA), methyldiethanolamine (MDEA) and piperazine (PZ) in the review of Gouedard et.al [54].

2.4.2. Studies on polyethylenimine (PEI)

In this section, various studies on PEI performance are discussed. Factors such as CO_2 loading and different degradation mechanisms are considered to evaluate the performance. It must be noted that the PEI is conventionally being used as an adsorbent (impregnated on porous support). The studies discussed in this chapter use silica or mesoporous carbon as

a support structure on which PEI of different molecular weights is impregnated or grafted.

CO_2 absorption capacity

The absorption capacity is defined as the number of moles of CO_2 undergoing carbamate or bicarbonate reactions per unit mass of PEI. The loading capacity is expressed in terms of $mol\,kg^{-1}$ or $mmol\,g^{-1}$. The absorption capacity depends on factors such as PEI loading (quantity of PEI impregnated on unit mass of support material), temperature, the concentration of gas mixtures, material and support structure.

Dependence on PEI loading

The absorption capacity of PEI is strongly influenced by the support structure and the quantity of PEI impregnated on them. This effect was studied by Filburn et al. [57] . Increase in PEI loading enhanced the CO_2 absorption process. A mesoporous carbon support structure was used in these experiments. The highest absorption of 3.02 $mmol\,g^{-1}$ was observed with 75 wt% of PEI loading at 75°C pure CO_2 atmosphere.

Filburn et al. [57] also reported that the maximum efficiency was observed with 50 wt% PEI loading in an equimolar CO_2/N_2 conditions. Excess PEI loading decreases the accessibility of free amine groups to CO_2 molecules and thus reducing the amine efficiency. The concentration of CO_2 in the gas mixture also plays an important role. A 50 wt% PEI loading showed a reduced absorption capacity of 2.03 $mmol\,g^{-1}$ when exposed to 15:75 (% volume) of CO_2/N_2 gas stream.

Temperature

The CO_2 absorption in PEI is an exothermic reaction. Elevated temperatures are not a favorable conditions for effective absorption. But Filburn et al. observed that the absorption capacity lowered with decreased in temperature. Belmabkhout et al. explained this phenomenon based on the diffusion mechanism [58]. PEI has a higher diffusion resistance at low temperatures. Increase in temperature results in lowering the diffusion resistance and the CO_2 absorption will get enhanced. This effect of temperature on amine efficiency was also studied by Wang et al. [59] and similar observations were concluded.

Effect of moisture in CO_2 absorption

Filburn [57] studied the effect of water/moisture concentration in the gas stream on the absorption capacity for PEI impregnated on mesoporous carbon. A 50 wt% PEI loading was exposed to an anhydrous gas mixture containing 15% CO_2 and 75% N_2 (by volume). This experiment showed an absorption capacity of 2.03 $mmol\,g^{-1}$. An addition of 10% moisture to 13% CO_2 and N_2 (by volume) being the remainder resulted in an increased absorption capacity of 2.84 $mmol\,g^{-1}$. Belmabkhout et al. explained this effect in terms of carbamate and bicarbonate reaction mechanisms [60]. It must be noted that this positive effect was observed only with moisture concentrations lesser than that of CO_2.

Structure and Material

Filburn et al. reported the influence of support materials on PEI absorption capacity [57]. It was observed that porous silicate material SBA - 15 showed 1.5 times more absorption (3.18 $mmol\,g^{-1}$) than silicate material MCM - 41. Son confirmed this observation by explaining the influence of reaction kinetics on pore size and structure [61].

Evaporation and thermal degradation

Smith et al. studied the stability of silica supported PEI (MW- 1800) under nitrogen, air and CO_2 conditions within a temperature range of 25 °C to 250 °C. [40]. A brief experimental procedure followed by Smith et al. is presented below.

Experiments were carried out in a Q500 thermogravimetric analyser (TGA) by TA instruments. 10mg of adsorbent was heated upto 100 °C in a nitrogen atmosphere. A flow rate of 20 ml/min was maintained during the process and was extended to 30 min in order to remove adsorbed moisture. The system temperature was then reduced to 25 °C. The gas flow was

then switched to air or CO_2 which was maintained for a duration of 2h. The temperature was increased to 200 °C with an increment rate of 0.25 °C/min. The change in adsorbent mass was monitered. Results showed that a mass reduction took place gradually from 95 °C to 135 °C and became rapid beyond 135 °C. This rapid decrease was considered to be occurring due to volatilisation.

Varga et al. studied the interactions of PEI on silica surface and found out that PEI volatility was considerably reduced due to anchoring of PEI molecules in silca pores [62]. But, in air and CO_2 atmosphere, volatility still existed at elevated temperatures due to O_2 induced degradation.

Hydari-Gorji and Sayari carried out thermal stability studies on PEI impregnated microporous silica (SBA 15) [50]. PEI with molecular weights 400, 600 and 2500 were tested. The samples were exposed to dry nitrogen for 30 h. The losses at different temperatures determined for PEI with different molecular weights are presented in table 2.1.

Table 2.1: Loss of PEI at different temperatures observed during evaporation test conducted for 30h

%wt loss of PEI			
Temperature (^0C)	PEI 400	PEI 600	PEI 2500
75	2.6	0.3	0.0
105	n.d	1.0	n.d
120	22.5	4.0	1.3
150	n.d	10.0	5.0

PEI - 400 showed 22.5% weight loss at 120 °C. PEI - 600 showed significantly less evaporation till 120 °C, but increased drastically at 150 °C. PEI - 2500 showed only 5% loss at 150 °C. It was concluded that PEI with higher molecular weights are relatively stable at higher temperatures. The measurements of material loss at different temperatures were carried out using thermogravimetric analyzer (TGA - Q500 TA Instruments). In both the studies, the composition of evaporated or thermally degraded products were not determined.

Dubovitskh carried out thermal degradation tests on PEI with molecular weights 3000, 20000 and 40000 [63]. The results showed that PEI - 3000 underwent thermal degradation at a temperature of 250 °C. The degradation products were identified as ammonia, ethylamine, pyrrhole and C-substituted ethylpyrrholes.

CO_2 induced degradation

Sartori and Kim reported that the CO_2 induced degradation was significantly observed when PEI was exposed to temperature higher than 120°C. The degradation of PEI will reduce the CO_2 loading capacity and increases the viscosity of the absorbent [64]. Equipment such as Gas chromatograph (GC), High performance liquid chromatograph (HPLC), Fourier transform infrared spectroscopy (FTIR) can be used to identify the degradation products and possibly their concentration.

Hyedari-Gorji and Sayari extended the studies on thermal stability of BA-PEI 600 in a pure CO_2 atmosphere. CO_2 induced degradation occurs at higher temperatures or during the desorption phase where concentration of CO_2 is high in the adsorbent. In the first case, the adsorbent was exposed to pure CO_2 for 30 min at 75 °C. Desorption was carried out at 105 °C and 120 °C in N_2 atmosphere. After 66 cycles of temperature swing adsorption, the adsorbent showed 40% and 52% uptake loss at 105 °C and 120 °C respectively.

In case 2, prehumidified gas with 6% relative humidity was used which showed only 2% and 3.5% uptake loss at 105 °C and 120 °C respectively. The effect of water in reducing CO_2 induced degradation was confirmed by Sayari and Belmabkhout [60]. Studies of Li et al. [65] showed that it was not possible to completely eliminate the CO_2 induced degradation by adding moisture to the gas stream. Thus, they reported that further studies are required to understand the influence of water in amine degradation. Hyedari-Gorji Sayari suggested that CO_2 induced degradation occurs via urea formation which was drastically reduced in

the presence of water

Smith et al. [40] conducted thermogravimetric study on PEI -1800 with silica support. The sorbent was exposed to CO_2 for 16 h at 140 °C which resulted in formation of insoluble organic compound. This was also identified with change in colour of the liquid from transparent to yellow after degradation occurred. The cause of degradation was explained as formation of urea linkages and loss of water as a result of secondary reactions to carbamate foramtion. The different mechanisms of urea formation has been delineated in the work of Pierre et al. [66].

Li et al.[67] carried out cyclic adsorption-desorption experiments to study the stability of PEI at high temperatures. Adsorption of CO_2 was carried out at 75°C and the desorption was carried out at temperatures ranging from 105°C to 130°C with an interval of 1°C. The samples of the cyclic experiments were tested using FTIR to identify the urea linkages. The complete spectra of FTIR at different temperatures can be found in Appendix C. The FTIR of the samples desorbed at different temperatures were compared to the FTIR of the pure sample. Li et al. reported that FTIR of the PEI samples did not show any form of degradation or urea linkages up to 108°C. But, studies of Sayari et al[68] on amine degradation reported that urea linkages occurs in amines at lower temperature but the rate at a slow rate of formation. Further, Li et al. reported that, above 109 the FTIR spectrum showed a new peak at 1685cm^{-1} which was associated with C=O stretching vibration in urea. As the temperature increased to 111°C, a peak at 1496cm^{-1} was observed which indicated C−N stretching vibration. Also at 118°C, a peak at 1361cm^{-1} was formed which was associated with C−N stretching and N−H deformation in urea linkages. During the formation of urea, it was reported that the peaks related to amine groups (1574 and 1627cm^{-1}) and carbamates (1304 and 1410cm^{-1}) were weakened.

O_2 induced degradation

Amines undergo deactivation in the prescence of O_2 due to amine oxidation [69]. This process occurs due to the formation of free radicals by O_2 reaction at elevated temperatures [70]. The rate of oxidation is dependent on the molecular structure. Studies by Belmabkhout & Sayari show that linear PEI (consists if primary and secondary amines) is relatively stable when compared to branched PEI (consists of primary, secondary and tertiary amines) [71].

The effect of O_2 degradation on silica supported PEI-600 was studied by Hydari-Gorji Sayari. The sorbent was exposed to different concentrations of air mixture and different temperatures. The duration of sorbent exposure was 30 h and the results observed are shown in table 2.2.

Table 2.2: Uptake loss recorded at different temperatures and various air mixtures [50]

	pure CO_2 uptake loss (%) at 75 °C					
			$CO_2/O_2/N_2$			
treatment temp.	CFair	SFG	1:17:82	5:14:81	7.5:10.5:82	20:17:63
50	n.d.[b]	0.0	n.d.	n.d.	n.d.	0.0
75	6	0.1	n.d.	n.d.	0.1[c]	n.d.
90	22	1.8	n.d.	n.d.	n.d.	1.8
100	70	n.d.	70	37	3.0[d]	2.6
120	100[e]	n.d.	n.d.	n.d.	n.d.	n.d.

[a]All streams except CFair were humidified using a water saturator controlled at 20 °C. [b]n.d.: not determined [c]After 120 h exposure. [d]50% uptake loss in the presence of 10.5:89.5 O_2/N_2 stream, under otherwise the same conditions [e]After 20 h exposure.

It can be seen that complete deactivation of sorbent occurred at 120 °C when exposed to CO_2 free CF air. Further, the uptake losses decreased with increase in CO_2 or decrease in O_2 concentrations. This study suggests that deactivation is influenced by O_2 partial pressure along with temperatures. Further, the sorbent was exposed to a gas mixture of 7.5:10.5:82 $CO_2/O_2/N_2$. This test showed a limited loss of 3% after a duration of 30 h at 100 °C.Thus, Hydari-Gorgi Sayari inferred that carbamate formation kinetics is faster than oxidation process. The CO_2 concentration in in the amine reduces the oxidation degradation by undergoing rapid carbamate and bicarbonate formations.

2.4.3. Studies on tetraethylenepentamine (TEPA)

In comparison to TEPA, impregnated PEI is widely considered as an absorbent in the carbon capture process due to its thermal stability. But, studies show that TEPA has a better carbon capture capacity when compared to PEI [72]. In this section, the absorption capacity of TEPA, techniques followed to enhance the thermal stability and resistance to oxidative degradation are discussed.

CO_2 absorption capacity

Chun et al. carried out studies on TEPA impregnated on porous silica material (SBA - 15 and MCM -41) [73]. A 70% loading of TEPA on SBA -15 showed an absorption capacity of 3.93 $mmol\,g^{-1}$. Further, 60% of TEPA on MCM -41 showed higher absorption capacity of 5.39 $mmol\,g^{-1}$. Hyun et al. and Kuo et al. demonstrated a good absorption capacity (4.27 $mmol\,g^{-1}$) of TEPA impregnated in a Y-type Zeolite. But, TEPA showed a poor thermal stability beyond 80 °C [72, 74].

Further, Sun et al. carried out experiments on a mixture of TEPA and diethanolamine (DEA) impregnated on SBA - 15 silica material. A mixture of 35 wt% TEPA with 15 wt% DEA resulted in an absorption capacity of 4 $mmol\,g^{-1}$. The mixture also showed improved cyclic capacity [75].

CO_2 induced degradation

As mentioned earlier, TEPA has a weak thermal stability over 100 °C when compared to PEI. The presence of primary amines in the TEPA chain is considered to be responsible for the drawbacks of the sorbent. Conversion of primary amines to secondary amies was proposed by Zhang to overcome the stability problems [76].

The synthesis of modified TEPA was carried out preparing a mixture of TEPA with acylamide. The procedure followed can be found in the literature of Zhang [76]. The modified product could be identified by its yellow viscous appearance. This modified TEPA was impregnated on a mesoporous material. A comparison was made between 50 wt% loaded TEPA with 50 wt% loaded modified TEPA. The samples were subjected to 25 °C during absorption and 100 °C for desorption. It was observed that TEPA had higher absorption capacity (4.4$mmol\,g^{-1}$) than modified TEPA (2.9 $mmol\,g^{-1}$). But, the desorption time of modified TEPA (70 min) was shorter than TEPA (110 min). It was also observed that by increasing the modified TEPA loading to 60% resulted in an enhanced adsorption capacity of 3.6 $mmol\,g^{-1}$. Further increase in modified TEPA loading reduced the absorption capacity to 2.73$mg\,g^{-1}$. This was due to aggregation of amine in the pore which increases diffusion resistance. Thus, modified TEPA shows a balanced performance in the absorption capacity and desorption time which makes it an improvised amine for carbon capture.

With respect to thermal stability over absorption/desorption cycles, modified TEPA showed an enhanced stability characteristics. A comparison was made with TEPA over 12 cycles and the results are represented in figure 2.11.

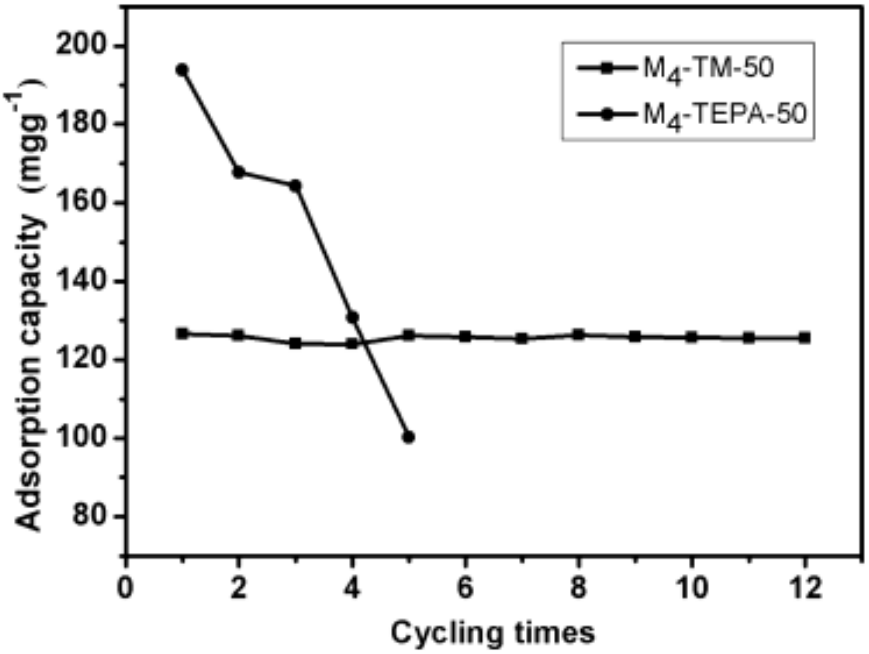

Figure 2.11: Uptake losses observed in TEPA and modified TEPA over 12 absorption/desorption cycles [76]

It can be seen that modified TEPA lost approximately 0.02 $\mathrm{mmol\,g^{-1}}$ of absorption capacity compared to its initial capacity. Whereas TEPA was completely deactivated after 5 cycles and turned yellow. This improved stability of modified TEPA was attributed to the conversion of primary to secondary amines.

Chaehoon et al. studied the effects of 1,2 epoxybutane on PEI impregnated silica adsorbents. This study showed that PEI adsorbent showed improved thermal stability in anhydrous condition as epoxybutane hinders urea foramtion at elevated temperatures [77]. Hyun Jung et al. extended the study on the effects of epoxybutane on TEPA [72]. A brief discussion on TEPA fictionalization (the process of converting primary amines of TEPA to secondary amines using different concntrations of epoxybutane) , absorption /desorption capacities and thermal stability has been made in the coming section.

Three samples were prepared by adding different molar ratios of epoxybutane to TEPA. The preparation procedure can be found in the literature [72]. The molecular structure of the three samples were identified using Flash 2000 and the results are presented in figure 2.12. TEPA and modified TEPA were loaded (70 wt%) onto silica materials and tested for absortion and thermal stability.

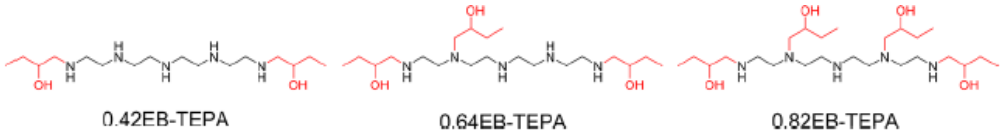

Figure 2.12: Representation of modified TEPA with different EB/TEPA molar ratios (2:1,3:1,4:1) [72]

A TGA was used to analyse the thermal stability and absorption capacity. 15:85 (% volume) CO_2/N_2 gas mixture was used in the experiment. The absortion, desorption temperature was maintained at 30 °C and 90 °C respectively. The results showed that 0.82 EB-TEPA performed stably over 10 cycles with a minimum loss of 0.001 $\mathrm{mmol\,g^{-1}}$ in absorption capacity. But, the absorption capacity was in the order TEPA>0.42 EB-TEPA >0.64 EB-TEPA > 0.82EB-TEPA.

This trade off between stability and reduction in absorption capacity was attributed to increase in molecular weight and hydrogen bonding of hydroxyl groups and amine. Thus, it was concluded that increased functionality improves stability but reduces absorption capacity.

0.64 EB-TEPA showed a balanced performance.

O_2 induced degradation

The oxidation degradation of TEPA impregnated on mesostructured cellular silica foam (MF) was investigated by Yamanda et al. [78]. FT-IR spectroscopy and gas chromatography was used to analyse the sorbent behaviour under various amine loading, temperature and gas mixture conditions.

Effects of TEPA loading

Activated carbon support structure loaded with 10,30, 50, 60 and 70 wt% TEPA were tested for CO_2 capture capacities after long term exposure to O_2 environment at 100 °C. Conventionally TEPA-n is used to represent TEPA with different loading where n is the wt%. TEPA-10 showed higher stability than rest of the loading conditions. After 5h exposure to O_2 TEPA-10 retained 95% of its initial capacity. Other loading conditions showed a reduction upto 33%. After 42h of O_2 exposure, TEPA-10 retained 65% of its capacity and the remainders showed only 8%.

Effects of temperature

To understand the effect of temperature, TEPA with different loadings as mentioned before were subjected to 18 hours of pure O_2 exposure (40 cm^3/min) at temperature range from 60 °C to 100 °C. No significant loss in adsorption capacity was observed at 60 °C. At 80 °C TEPA-10 lost 13% of it's initail capacity wherein other samples lost up to 62%. At 100 °C TEPA-10 retained 65% of its initial capacity while other samples lost more than 88%.

Effects of O_2 concentration

The concentration of O_2 was varied and the absorption capacities were measured. Air and 5:95 O_2/N_2 mixture was used in this experiment. After 18h of exposure to air, all TEPA samples showed 3 times less degradation effects. In 5% O_2 conditions TEPA-10 retained 91% of its initial adsorption capacity and other samples also showed higher retention values.

Effects of support structure

The effective performance of TEPA-10 under oxidative conditions was attributed due to formation of hydrogen bond between silica support and hydroxyl group. This provides better resistance to oxidation when compared to other samples which resulted in amine bulk formations. This effect was confirmed other studies in which polyethylglycol was added to TEPA. The results are discussed below.

A study on TEPA impregnated SiO_2 adsorbent investigated by Tanthana Chuang reported that the O_2 induced degradation correlates to the accumulation of carbamic and carboxylate species. The addition of polyethylene glycol (PEG) was proposed to suppress the carboxylate formation [79].

The FT-IR spectroscopic studies carried out by Srikanth Chuang and group reported the formation of imide species as a result of oxidative degradation [80]. The addition of PEG in order to slow down the oxidative degradation was also tested. This effect of PEG was explained with respect to the formation of hydrogen bonds between amines and hydroxyl species. The hydrogen bond formation reduces the accessibility of O_2 to TEPA and induces resistance to oxygen degradation.

2.5. Other relevant literature

The absorption and desorption charaterisitcs of PEI-600 and TEPA were studied by Sinha and B.Ovaa at ZEF. A brief review on the results are presented in this Section 2.5.1 and 2.5.2. Studies carried out by Jhon et al. [81] on PEI adsorbents showed anomalies during absorption-desorption process. The observations and the hypothesis to explain the anomalies are presented in Section 2.5.3.

2.5.1. Absorption characteristics of PEI and TEPA

Viscosity study of PEI and TEPA

Viscosity is an important parameter that influences the absorption and desoprtion characteristics of both PEI and TEPA. Sinha [27] studied the variation of viscosity as a function of temperature, concentration of water and CO_2 absorbed. The findings of the reseach are summarised below:

- Viscosity of both PEI and TEPA reduces with increase in temperature.
- At 20 °C both PEI and TEPA show an increase in viscosity with increase in concentration of water in the amine upto 20 % by weight. Further, viscosity of PEI reduces with increase in concentration but the viscosity of TEPA reduces with concentration of water above 30% by weight.

During the absorption process, the amines absorb both water and CO_2. The effect of the CO_2 and water mixture on the viscosity of the amines are shown in figures 2.13 and 2.14.

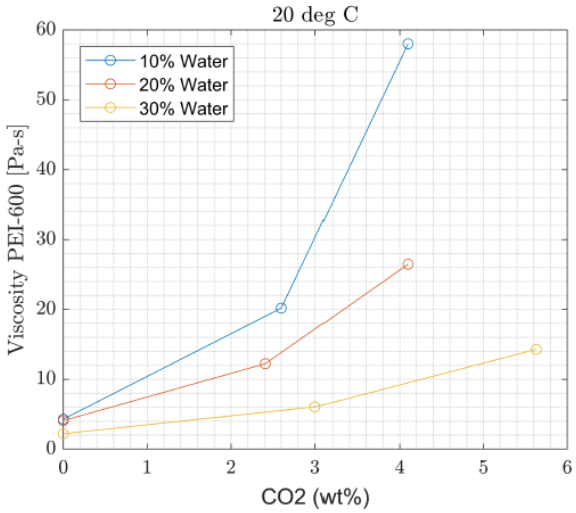

Figure 2.13: Change in viscosity of PEI in the presence of water and CO_2 [27]

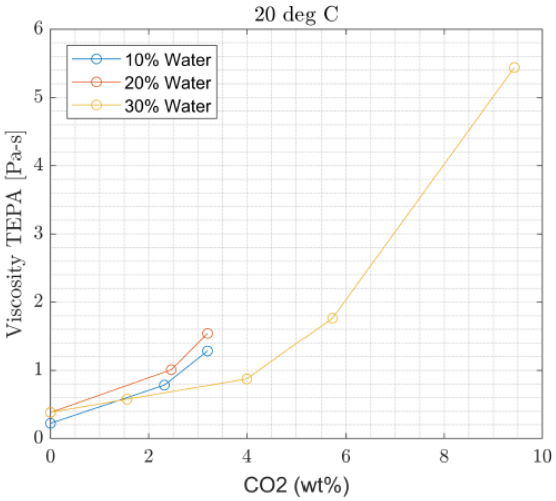

Figure 2.14: Change in viscosity of TEPA in the presence of water and CO_2 [27]

Influence of viscosity on absorption

The absorption of CO_2 and water in the amines takes place primarily on the surface. Over time, due to concentration gradient between the top surface and the pure amine, the CO_2

molecules starts to diffuse into the bulk. The studies carried out by M.Sinha shows that the absorption of water and CO_2 increases the viscosity of the amine. When the amines are exposed to air, the absorption at the top surface creates a viscous region which creates ressitance to the diffusion of molecules into the bulk. Thus it slows down the absorption process.

2.5.2. Studies on desorption

B.Ovaa [28] studied the desorption of water and CO_2 from the amines at different temperatures and pressures. The amine samples were loaded with 4.3 wt% of CO_2 and 30 wt% H_2O. The temperature range selected for the desorption test was 70, 80, 90, 100, 110, and 120^0C. The operating pressure was 50, 100 and 200 bar. Important results are presented below.

Desorption of water

It was observed that at the end of each experiment, 96% of water was removed from the amine sample. The results were verified by subjecting the tested sample to Karl-Fischer titration which showed 1-2% of water remained in the sample. This difference was attributed to experimental errors and a conclusion was drawn stating that all water was desorbed from the amine.

Desorption of CO_2

Table 2.3 and 2.4 show the trends observed during CO_2 desorption.

Table 2.3: Desorption of CO_2 from PEI at different temperatures and pressure [28]

			50 mbar	
PEI [g]	13.7			
T [°C]	CO_2 output [L]	CO_2 output %	CO_2 output [mol CO_2/ kg amine]	Ldg/ kg amine [mol CO_2 / kg amine]
80	0.01	6.9	0.04	1.20
90	0.03	19.5	0.11	1.13
100	0.07	37.6	0.22	1.02
110	0.13	71.3	0.41	0.83
120	0.18	100.0	0.58	0.66
			100 mbar	
PEI [g]	13.7			
T [°C]	CO_2 output [L]	CO_2 output %	CO_2 output [mol CO_2/ kg amine]	Loading amine [mol CO_2 / kg amine]
80	0.01	4.8	0.03	1.21
90	0.03	16.2	0.08	1.16
100	0.05	34.5	0.18	1.06
110	0.09	54.8	0.28	0.96
120	0.16	100.0	0.51	0.73
			200 mbar	
PEI [g]	13.9			
T [°C]	CO_2 output [L]	CO_2 output %	CO_2 output [mol CO_2/ kg amine]	Ldg/ kg amine mol CO_2 / kg amine
80	0.0	0.0	0.0	1.24
90	0.01	9.1	0.04	1.20
100	0.04	31.9	0.13	1.11
110	0.09	67.4	0.27	0.97
120	0.13	100.0	0.41	0.83

Table 2.4: Desorption of CO_2 from TEPA at different temperatures and pressure [28]

		50 mbar		
TEPA [g]	13.6			
T [°C]	CO2 output [L]	CO2 output %	CO2 output [mol CO2/ kg amine]	Loading amine [mol CO2 / kg amine]
80	0.015	5.7	0.051	1.151
90	0.05	17.3	0.15	1.09
100	0.20	73.9	0.66	0.54
110	0.26	94.3	0.84	0.36
120	0.27	100.0	0.89	0.31
		100 mbar		
TEPA [g]	13.8			
T[°C]	CO_2 output [L]	CO_2 output %	CO_2 output [mol CO_2/ kg amine]	Loading amine []mol CO_2 / kg amine]
80	0.02	6.4	0.05	1.15
90	0.05	19.9	0.16	1.04
100	0.14	54.6	0.44	0.76
110	0.21	86.4	0.69	0.51
120	0.25	100.0	0.80	0.40
		200mbar		
TEPA [g]	13.8			
T[°C]	CO_2 output [L]	CO_2 output %	CO_2 output [mol CO_2/ kg amine]	Loading amine []mol CO_2 / kg amine]
80	0.0	0.0	0.0	1.20
90	0.02	10.2	0.06	1.14
100	0.06	33.9	0.20	1.00
110	0.12	64.1	0.38	0.82
120	0.18	100.0	0.59	0.61

The last column of the figures 2.3 and 2.4 show the amount of CO_2 left behind in the sample after the desorption at a particular temperature and pressure. It was concluded that for a given pressure and temperature of desorption not all CO_2 can be removed.

2.5.3. Studies on PEI MCM-41 adsorbent

Jhon et al. [81] studied the characteristics of PEI supported by MCM-41. The experiment was carried out by exposing different loading of PEI to pure CO_2. The flow rate of CO_2 was maintained at 100mL/min. The absorption and desorption was carried out at the same temperatures for a duration of 150 min. During desorption, the gas flow was switched from CO_2 to pure N_2.

Figure 2.15 shows the adsorption capacity measured with different loadings.

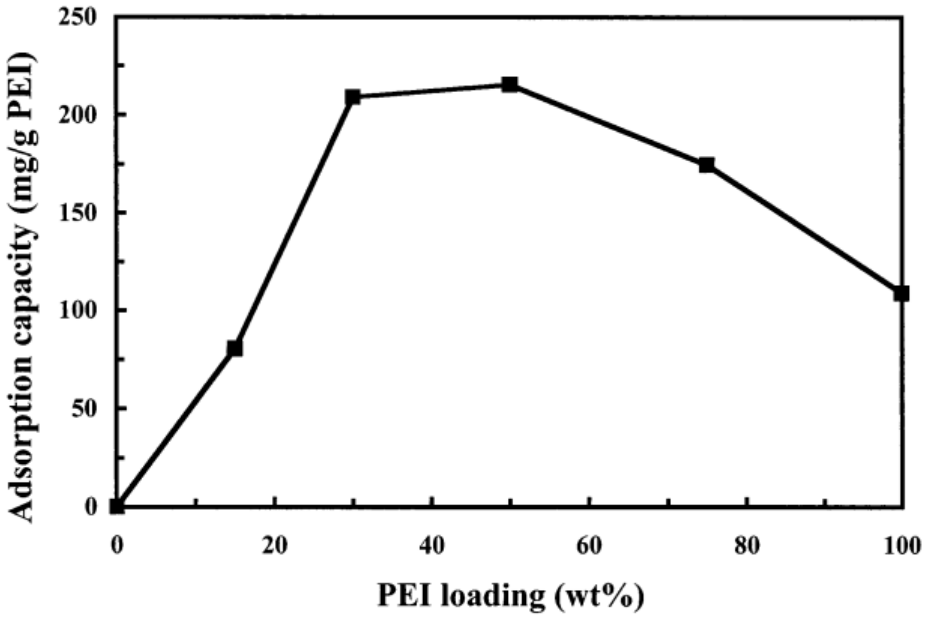

Figure 2.15: Adsorption capacity of MCM-41 with different PEI loading [81]

Jhon et al.[81] observed that the adsorption capacity lowered with the increase in PEI loading. This was associated with slow diffusion kinetcs of CO_2 molecules

Table 2.5 shows the absorption and desorption capacity of different PEI loading at different temperature observed by Jhon et al..

Table 2.5: Absorption and desorption capacity of MCM-41 with different loading and temperatures [81]

adsorbents	temper-ature (°C)	adsorption capacity (mg/g-adsorbent)	desorption capacity (%)
MCM-41 only	50	14.3	100
MCM-41 only	75	8.6	100
MCM-41 only	100	6.6	99
MCM-41-PEI-15	75	19.4	101
MCM-41-PEI-30	75	68.7	98.3
MCM-41-PEI-50	50	44	24.7
MCM-41-PEI-50	75	112	99.8
MCM-41-PEI-50	100	110	84.1
MCM-41-PEI-75	75	133	101
PEI	75	109	56.4

It was observed that maximum adsorption and desoprtion was exhibited by MCM-41 with 75 wt% PEI loading. Pure PEI showed only 56% of desorption at 75^0C. Further, comparing the desorption of MCM-41 with 50 wt% PEI loading at 75 and 100^0C, desorption at 100^0C was lower than that of 75^0C. CO_2 absorption is an exothermic process. High temperatures must favour desorption process. The results observed in this study showed that desorption capacity was lowered with increase in temperature. Jhon et al. [81] proposed an hypothesis to explain this anomaly which is presented in figure 2.16.

Figure 2.16 shows the hypothetical structure of amines at low and high temperatures.

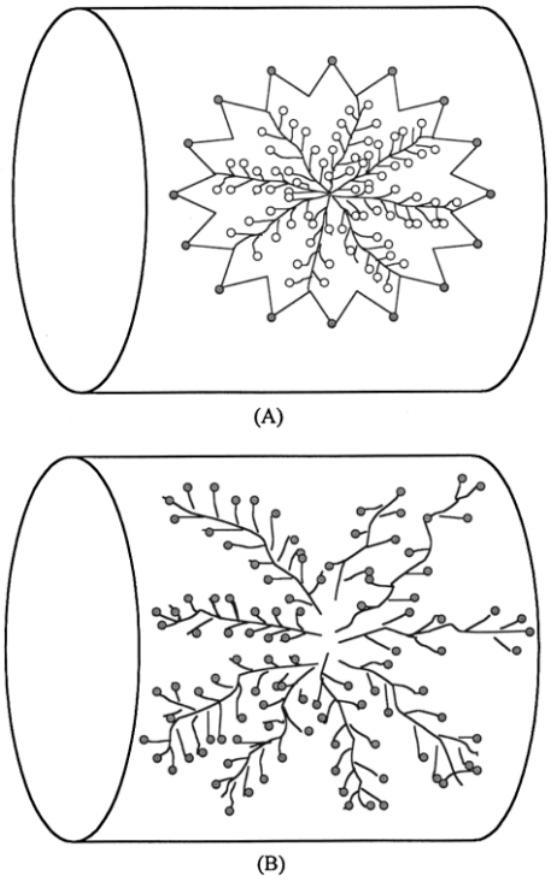

Figure 2.16: Hypothesis to explain the anomaly observed during desorption of PEI- MCM41 [81]
A. Amine structure at low temperatures
B. Amine structure at high temperatures
• Active amine sites, ∘ inactive amine sites

The hypothesis of Jhon et al. is as follows: Figure 2.16 A shows the amine structure at low temperatures. In this condition only a few amine sites are active and are present on the perimeter of the amine structure which can absorb CO_2. In order to reach the inactive sites, the CO_2 has to diffuse into the structure and this process is very slow. When temperature increases, the structure of the amine chain changes as shown in Figure 2.16 B, where more active sites are formed. In this case the CO_2 can reach the amine site in a short duration.

3
Experimental Procedures

3.1. Evaporation

As explained in section 2.3.1, evaporation of liquids is accelerated when exposed to high temperature. In DAC process, the desorption of CO_2 is carried out at elevated temperatures. Determining the evaporation rates of amines will help in choosing the amines that evaporates slower during the process or introduce mechanisms that reduces evaporation loss. The evaporation of amines were tested using a muffle furnace. The details are given in section 3.1.1. Confirmatory tests were done on evaporation rates using TGA and the procedures are given in section 3.1.2.

3.1.1. Muffle furnace Experiments

A simple layout of a muffle furnace is shown in figure 3.1. A muffle furnace is an oven that is capable of reaching very high temperatures such as 3000^0C. The temperature sensor placed inside the heating chamber helps to maintain a required isothermal temperature by regulating the heater. The required gaseous atmosphere inside the heating chamber can be achieved by continuously passing the feed gas. The excess gas in the heating chamber moves out through an exhaust.

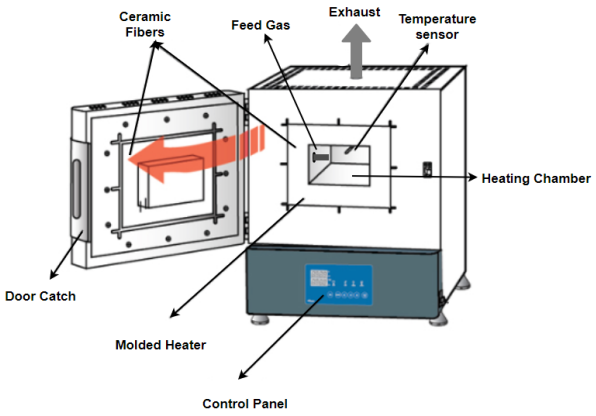

Figure 3.1: Basic Layout of a muffle furnace [82]

The operation method of the muffle furnace is shown in figure 3.2. The inputs to the muffle furnace are required isothermal temperature (T_{max}), flushing (F_t), ramping (R_t)and isothermal (I_t)duration. Initially the required gas is fed into the heating chamber. The volumetric flow rate is controlled with a rotameter. No heating takes place during flushing period. This is to make sure that the unwanted gases in the heating chamber is completely removed. During the ramping period, the temperature inside the heating chamber starts to rise at a rate of $\frac{T_{max}}{R_t}$ $^0Cs^{-1}$. On reaching T_{max}, this temperature is further maintained throughout the isothermal period.

The amine evaporation experiments were carried out in the muffle furnace as explained below:

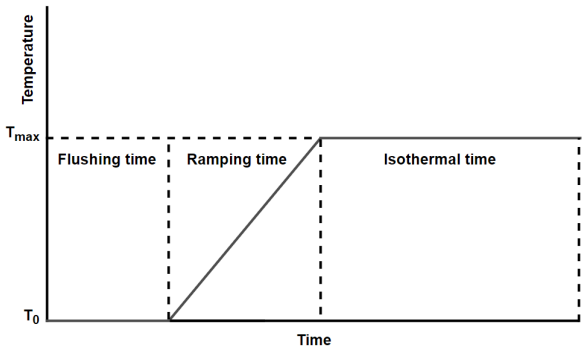

Figure 3.2: Operation of Muffle furnace

- The following masses were measured using a milligram scale - mass of the petridish, mass of pure amine samples, mass of amine sample with petridish
- The amine samples on a petridish were placed in the muffle furnace and it was flushed with nitrogen with a volumetric flow rate of 80 L/ min
- The flushing duration was set as 4h so as to completely remove CO_2 and O_2 from the heating atmosphere
- The above step was carried out to overcome the possible degradation that could occur due to the presence of CO_2 and O_2 at high temperatures and its effect on the change in amine mass
- The flushing of nitrogen is continued throughout the experiment so that the amine vapours are flushed out continuously, this step is to mimic the vacuum conditions maintained in the ZEF desorption process
- The ramping time was set to 1h (The selection of ramping duration is random. Effects of rapid heating or slow heating is not considered in this study)
- T_{max} values considered for the study was 80 °C,100^0C and 120^0C, the isothermal duration was set as 25h
- After the isothermal duration was completed, the furnace was allowed to cool down
- The heat carried away by the exhaust gases were the only means of cooling. Thus, this process took upto 6h to 8h to reach room temperature
- Once the furnace temperature reaches a value lower than 25^0C the samples were removed and the change in amine masses were measured.
- Furthermore, the amine samples subjected to high temperatures were tested on FTIR (Fourier Transform Infrared Spectroscope) to identify changes in the molecular structure of the amine

3.1.2. Thermogravimetric Analysis (TGA)

When a substance is subjected to increased temperatures, mass change occurs due to transition in phase or reaction taking place in the system. Thermogravimetric analysis is a method of determining the change in mass of a sample as a function of temperature and time [83]. The TGA is used to understand the physical and chemical phenomena of the samples under controlled temperatures and different gas environment[84]. The basic layout of a TGA is shown in figure 5.5.

The TGA consists of a furnace in which the thermal experiments are carried out. The sample to be tested is taken in a alumina crucible and is placed on a balance which is coupled to a temperature sensor. The balance has a sensitivity of 0.1 μg and a precision of $\pm$0.01%. The temperature sensors have an accuracy of $\pm 1^0C$ [86]. The required gas environment inside the furnace can be maintained by flowing the purge gases. The purge gas also helps to flush out the gaseous products formed during the experiments. There is also a reference

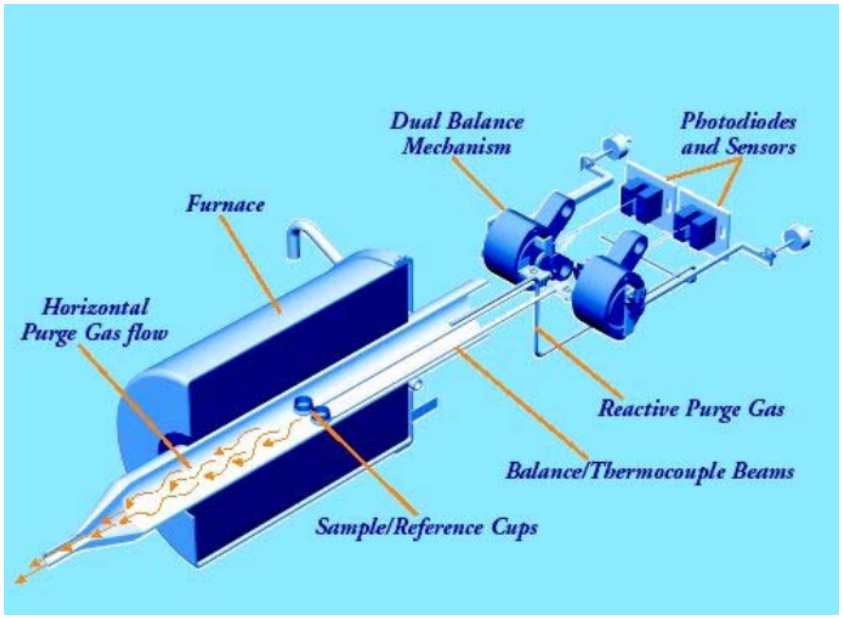

Figure 3.3: Layout of thermogravimetic analyser [85]

cup which has the exact dimension and mass of the sample cup. Every change in the mass of the sample is determined with respect to the reference cup. This negates the influence of any disturbances on sample weight measurement.

One experiment on TEPA evaporation was carried out in the TGA. The data obtained from the TGA was used to confirm the results of muffle furnace experiments. TGA from ThermoFischer Scintific (SDT Q600 V20.9 Build 20) was used for the experiments and the procedure followed is explained below:

- The ceramic crucible (surface diameter 0.0055m) was loaded with 13.64 mg of pure TEPA and was placed on the balance
- The furnace was flushed with nitrogen for 10 min at the rate of 50ml/ min before heating up the furnace, flushing of the nitrogen continued throughout the experiment
- The maximum temperature of 120°C was selected for the confirmatory test, the ramping rate was set at 10°C/ min
- The isothermal period was set as 240 min

3.2. CO_2 induced degradation

As seen in section 2.2 and 3.2, CO_2 , moisture and temperature influences the amine degradation. Generally, degradation of amine occurs at higher temperatures and results in formation of irreversible products. These products accounts for loss of amine as they cannot take part in CO_2 absorption or desorption.

3.2.1. Cyclic absorption-desorption setup

The CO_2 induced degradation testing setup is as shown in figure 3.4. The functions of the components and the experimental procedure followed are explained below.

Nitrogen gas tank - Nitrogen gas was used as a purge gas during desorption phase of the experiment. N_2 5.0 from Linde gas (99.9% pure) was used for this purpose.

Air inlet fan - ambient air was used during absorption phase. The concentration of CO_2 was assumed to be approximately 400 ppm. Minor variations in concentration levels are neglected. A pump was used to force the ambient air into the reaction chamber.

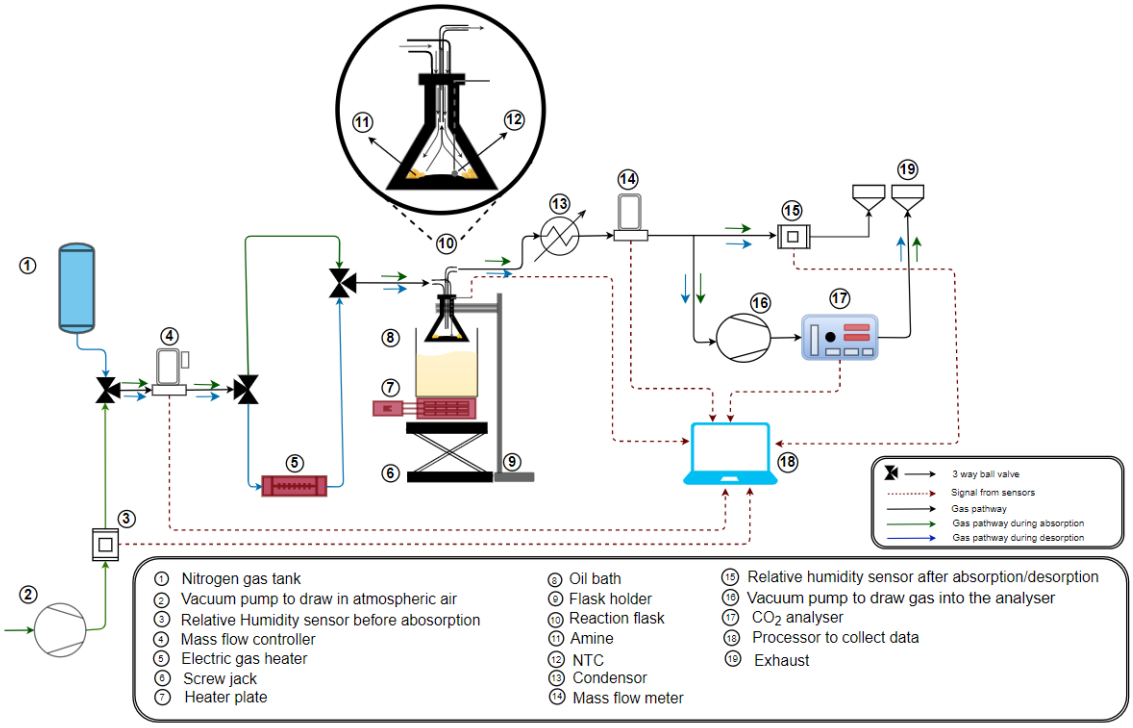

Figure 3.4: Setup to study CO_2 induced degradation via cyclic exposure

Relative humidity Sensor - An arduino compatible Si7021 relative humidity sensor was used to measure the moisture content of the gas stream. The sensor has an accurcy of ±3% RH and a response time of 17s [87]. It also has an inbuilt temperature sensor. Two such sensors were used, one to measure the RH in the inlet air stream and the other to measure the moisture in the gases coming out of the reaction flask.

Massflow Controller/Meter - The volumetric flow rate of the inlet and the outlet gas stream was measured using Bronkhorst mass flow controller/meter. The inlet gas stream was regulated using massflow controller and the volumetric flow rate was set to 300 l/h. The volumetric flow rate at the oulet was measured using a flow meter.

Gas heater - During desorption phase, the amine is heated to higher temperature and the absorbed CO_2 and moisture are released. In order to reduce the partial pressure of CO_2 in the gas phase, the reaction chamber is flushed with nitrogen gas. Due to temperature difference between the nitrogen and the desorbed gases, the moisture would condense and remain inside the reaction flask without being flushed out. This leads to error in moisture balance during desorption phase. To overcome this situation, the inlet nitrogen gas is preheated to the required desorption temperature using a simple coiled heater. As mentioned before, during the desoprtion process the reaction flask is continuously purged with heated nitrogen with a flow rate of $300 l\,h^{-1}$.

Heater plate/oil bath - The heating of the reaction flask during desorption phase is achieved by immersing the flask in an oil bath. The heating process is carried out using a heater plate. In order to maintain an isothermal state for a fixed duration after reaching the desorption temperature, the flask is constantly taken out and immersed back into the oil bath. This process is carried out by rising and lowering the oilbath using a simple lab jack. The arrangement can be clearly seen in figure 3.4.

reaction flask - A borosilicate conical flask of 250 ml capacity was used as a reaction flask.

NTC - An NTC thermistor is a temperature sensor . The temperature sensor was paced inside the reaction flask as shown in figure 3.4.

CO_2 Analyser - Binos 100-2M CO_2 analyser was used in measuring the concentration of CO_2 in the gas streams. The analyser incorporates the principles of infrared radia-

tion absorption by CO_2 gas molecules. The magnitude of IR absorbed corresponds to the concentration of CO_2 in the gas stream [88].The analyser data is produced in terms of corresponding voltage signals. The Binos 100M model consists of ppm (parts per million,range -0 to 1000) and $\%CO_2$ (range - 0 to 2) measurements. During experimentation, the ppm measurements showed large fluctuations. Thus, $\%CO_2$ measurements were recorded. The analyser requires a recommended inflow of 1l/min for accurate measurements. To achieve this an external pump was used and the arrangement is as shown in figure 3.4. The $\%CO_2$ measurement has a resolution of 0.01 %. Any concentrations falling within the resolution values creates disturbances in the voltage signals.
.

Condenser - During the desorption phase, moisture and amine vapours are released along with CO_2. The presence of condensable gases in the analyser inflow will cause error in the measurements and can also cause damage to the system. Therefore it is necessary to remove such gases from the analyser inlet flow. A condenser unit is used for this purpose.

Calibration of CO_2 analyser

The $\%CO_2$ with a range of 0 to 2% was used to measure the CO_2 content in the gas flow. Before the start of the experiments, the analyser was flushed with nitrogen gas for a duration of 2 to 3 min and the 0 value was calibrated. To calibrate the higher value on the scale, 1.62% (80% of the full range) CO_2 gas mixture was passed through the analyser. The analyser was turned off and disconnected from the setup multiple times. The process of calibration was carried out before the experiments were resumed. A drift in the measuring scale was often observed during the experiments. The reasons for the drift are unknown. The analyser was re-calibration during such situations.

Experimental procedure - Absorption Phase

- Generally in cyclic experiments or degradation studies, the experiment is carried out until the sample degrades. But in this thesis, due to lack of time the number of cycles and the duration of cycle were predetermined based on certain observations made during the experiments. The duration of the absorption phase was set as 20 min. The details on the selection of the duration is given in section 4.2.1.
- The amine sample was taken in the reaction flask and the mass was measured
- The flask was placed in the experimental setup as shown in figure 3.4
- Before the start of the experiment, the inlet to the analyser fan (16 of figure 3.4) was disconnected and the fan was turned on to flush the analyser with ambient air
- The previous step is to check if the analyser reads 0.04%
- If drifting is observed, then the scale was re-calibrated with respect to 0 using pure nitrogen
- The fan to draw in ambient air (2 in figure 3.4) was turned on and the flow rate was set to $300 l\,h^{-1}$ using a mass flow controller
- The flow rate of $300 l\,h^{-1}$ was the minimum flow required to overcome the pressure drop created by the analyser pump in the gas line connecting the mass flow meter and the exhaust
- A flow rate $<300\ l\,h^{-1}$creates a pressure drop in the line which leads to drawing in air from the exhaust which disturbs the CO_2 measurements whereas, a flow $>300 l\,h^{-1}$ would further dilute the CO_2 levels during desorption phase which would again influence the measurements
- The CO_2 and relative humidity data were recorded continuously

Desorption Phase

- During the desorption phase, the gas flow channels are shifted from air to nitrogen
- The flow of nitrogen was started and the analyser pump was turned on, in case of no drifting the analyser reads 0.00%, else the analyser is re-calibrated to 0 value
- once the analyser reads 0, the reaction flask was immersed in a hot oil bath which was maintained at 150°C
- The desorption temperature chosen in the experiments were 80°C and 120°C
- The temperature of the flask was measured using an NTC, the gas heater is also turned on and the outlet temperature is also measured using an NTC
- On reaching the required desorption temperature, the reaction flask was removed from the oil bath and the heater was turned off when the heater gas outlet NTC reads >100°C
- When the temperature of the flask or the heated nitrogen reads by 2°C below the required temperature, the heater is turned on and the flask was again immersed in the oil
- The duration of the desorption phase was considered to be 20-25 min. The details on the selection of the duration are given in section 4.4
- Completing the desorption phase, the reaction flask was taken out from the oil bath, the heater was turned off and the system was allowed to cool down until the flask temperature reached the room temperature. The duration of the cooling phase was observed to be 30-40min depending on desorption temperature (experiments with desorption temperature 120°C took longer to cool down when compared to 80°C.
- The total duration for 1 cycle (absorption+desorption+cooling) was approximately 85 - 100min. As mentioned before, due to lack of time the number of cycles for all cyclic experiments were limited to 30 which.

3.3. Confirmatory tests conducted

Confirmatory tests were carried out on amine samples subjected to evaporation and CO_2 induced degradation experiments to verify the results. Brief details on the tests are given in the upcoming sections.

3.3.1. Karl-Fischer and Phosphoric acid test

Karl-Fischer test is performed to determine the water content in the sample. Similarly, Phosphoric acid test helps to determine the CO_2 concentration. The details on the experimental set-up is given in Appendix A. A simple procedure to conduct the above tests are given below:

- A small aliquot of X g is taken from the main sample Y and mixed with methanol Z (Z ≈10*X g)
- Tests are conducted on the new amine-methanol sample.
- Methanol is just an extraction solvent that helps to release water and CO_2 faster in insoluble organic liquids. It dose not undergo any side reactions that affects the measurement.
- The results obtained from the test will be CO_2 or water in X g of amine.
- We can then calculate the gCO_2/g amine or gH_2O/g amine.
- From the ratio obtained the total concentration of CO_2 or water in main sample Y can be determined.

It is important to note that samples tested using the above mentioned procedures must be a homogeneous mixture. As mentioned in section 2.5.1, the CO_2/water absorption-desorption takes place on the surface of the amine. To measure the mass of CO_2 or water accurately, the amine sample have to be thoroughly mixed. In-case of no mixing, multiple

tests have to be conducted by taking small samples (as shown in figure 3.5) such that an approximate value can be determined.

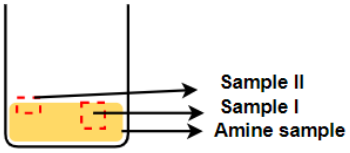

Figure 3.5: Multiple small samples collected from main sample to conduct Karl-Fischer and Phosphoric acid tests

During the CO_2 induced degradation study, the amine sample collected after the experiment could not be mixed. Thus, two aliquots (Sample I and II) were taken as shown in figure 3.5 so as to determine an average value of CO_2 and water in the sample after 30 cycles.

3.3.2. Fourier transform infrared spectroscopy (FTIR)

The basic application of the FTIR is to identify the different molecular species that are present in the sample. The chemical bonds between different elements absorbs different frequencies of IR. Thus, each frequency is a fingerprint of a specific bond between specific elements.

FTIR was conducted on the amine samples to check if any new species of molecules are formed during the process of absorption-desorption or evaporation.

4

Analysis of Experiments

4.1. Data conversion - % CO_2 to grams of CO_2

The procedure to analyse CO_2 induced degradation was explained in section 3.2. It was seen that the data set obtained during the experiments were volumetric flow rate, %CO_2. To analyse the data quantitatively, the obtained data set must be converted into mass of CO_2. The details on the conversion are presented in this chapter.

The volumetric flow rate (l/h) and the CO_2 concentration (%CO_2) if gas stream are the data set obtained during experiments.The equations used to convert these data into grams of CO_2 in the gas stream are shown below. For conventions, volumetric flow rate of gas is considered as F_{gas} and concentration of CO_2 as $C_{\%}$.

Total flow of CO_2 in the gas stream

$$F_{CO_2} = \frac{C_{\%} * F_{gas}}{100} \qquad (\frac{l}{h}) \tag{4.1}$$

Total flow of CO_2 in terms of m^3/h

$$F_{CO_2,m^3} = \frac{C_{\%} * F_{gas}}{100 * 1000} \quad (\frac{m^3}{h}) \tag{4.2}$$

The density of CO_2 (ρ_{CO_2}) at experimental conditions (25^0C and 1 bar pressure) is approximately 1.98 Kg/m^3. Therefore, the volume to mass conversion is as shown below:

$$M_{CO_2,Kg} = \frac{C_{\%} * F_{gas} * \rho_{CO_2}}{100 * 1000} \quad (\frac{Kg}{h}) \tag{4.3}$$

In the equation 4.4, the mass of CO_2 has been converted from Kg/h to g/s

$$M_{CO_2,g} = \frac{C_{\%} * F_{gas} * \rho_{CO_2} * 1000}{100 * 1000 * 3600} \quad (\frac{g}{s}) \tag{4.4}$$

Solving the constant values in equation 4.4, we arrive at a value of $5.5 * 10^{-6}$. This value is multiplied with the raw volumetric flow and %CO_2 data to obtain the mass of CO_2 measured in each second. Finally, the data set is integrated as shown in equation 4.5 to obtain the total CO_2 measured during the experiment. The integration procedure was carried out in MATLAB 2019 version using *trapz* function.

$$M_{CO_2,g,total} = \int_0^t C_{\%} * F_{gas} * 5.5 * 10^{-6} dt \quad (g) \tag{4.5}$$

4.2. Analysis of plots

4.2.1. CO_2 analyser - absorption

The graphical representation of an example data set obtained from the CO_2 analyser during absorption phase is shown in figure 4.1. Four important regions are marked on the plot and their significance is explained below.

As explained in section 3.2, the analyser was first flushed with ambient air to check if there are any shifts in the measuring scale. In case of no shift, the analyser reads 0.04%. It

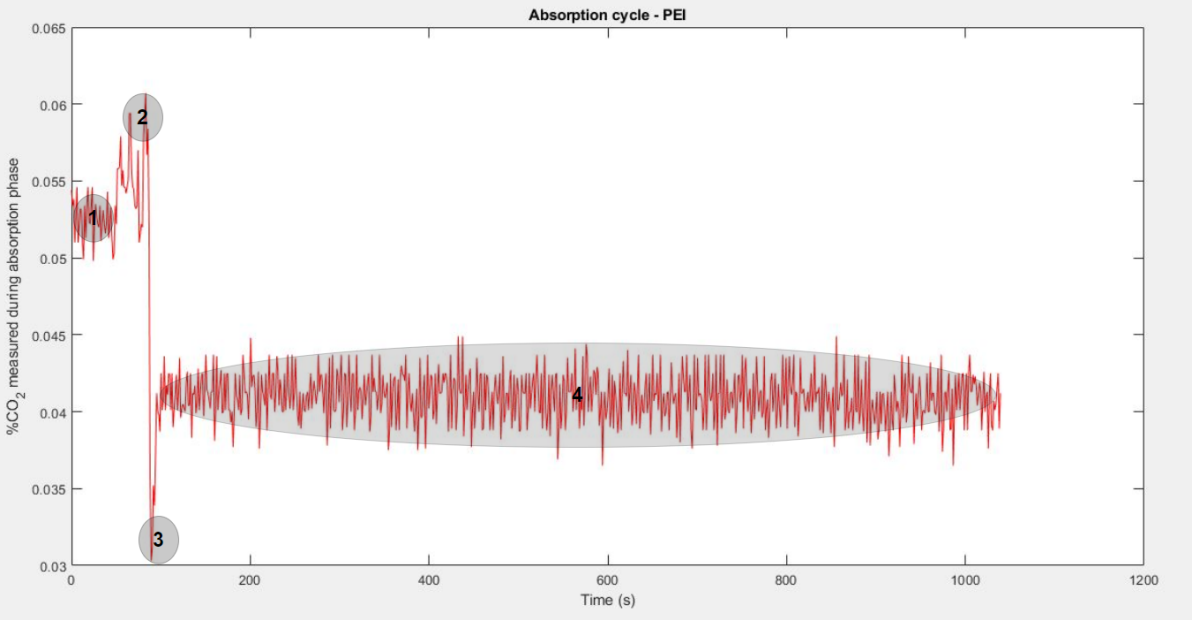

Figure 4.1: Example plot of % CO_2 measurements during absorption using PEI

can be seen in the **1st region** of the figure 4.1, that the initial readings of the analyser before the start of the experiment was approximately 0.053%. During the course of the experiment, it was made sure that no additional CO_2 was added externally by any means. Thus, the region 1 indicates that there was a shift in the scale. This behaviour was observed frequently during the experiments and reasons were not investigated.

It was frequently observed that, when the analyser fan was turned off or when there was a delay in the gas flow reaching the analyser, a disturbance was created in the output voltage signal. This resulted in a measurement error which showed an increased CO_2%. This can be seen in **region 2** of the plot where the measured values shits higher than the initial reading .

As the ambient air passes over the amine in the reaction flask, CO_2 and moisture is absorbed. Initially, the CO_2 is absorbed in the top surface of the amine which can be seen in **region 3**. Further, the CO_2 molecules diffuse through the liquid amine creating free absorption sites on the top layer of the amine. As the diffusion process is slow, a large number of CO_2 molecules do not get absorbed and flow out with the remainder gas. This results in a sharp increase in CO_2 concentration which can be observed in **region 4**. Since the mass of amine taken in the reaction flask during the experiments was much higher than the surface area exposed to air, a small quantity of CO_2 molecules continues to get absorbed slowly due to diffusion. Therefore, the region 4 does not reach the initial levels of CO_2% until all the absorption sites in the bulk amine are taken up by CO_2 molecules.

As seen in figure 4.1, after 200s the absorption curve dose not show any change. That is the absorption of CO_2 becomes slower as mentioned above. As mentioned in section 3.2.1, due to limited time, the duration of absorption was set as 20min.

Plot offsetting

As seen in figure 4.1, the initial measurements of CO_2 concentrations were higher than 0.04%. This error was observed in multiple absorption cycles. In order to maintain a standard initial condition, an offset value was added or subtracted form all the data points of the cycle such that the region 1 was shifted to approximately 0.04%. This can be seen in figure 4.2. This helps in easy calculations of mass of CO_2.

The increased values (>0.04%) measured during the start of the absorption experiment could also be due to increased CO_2 concentration in the ambient air. But, when the analyser was flushed with pure nitrogen after the absorption cycle (or before the desorption cycle), the

analyser did not read 0.0%. Thus, an assumption was made that the initial concentration during the experiments was 0.04%.

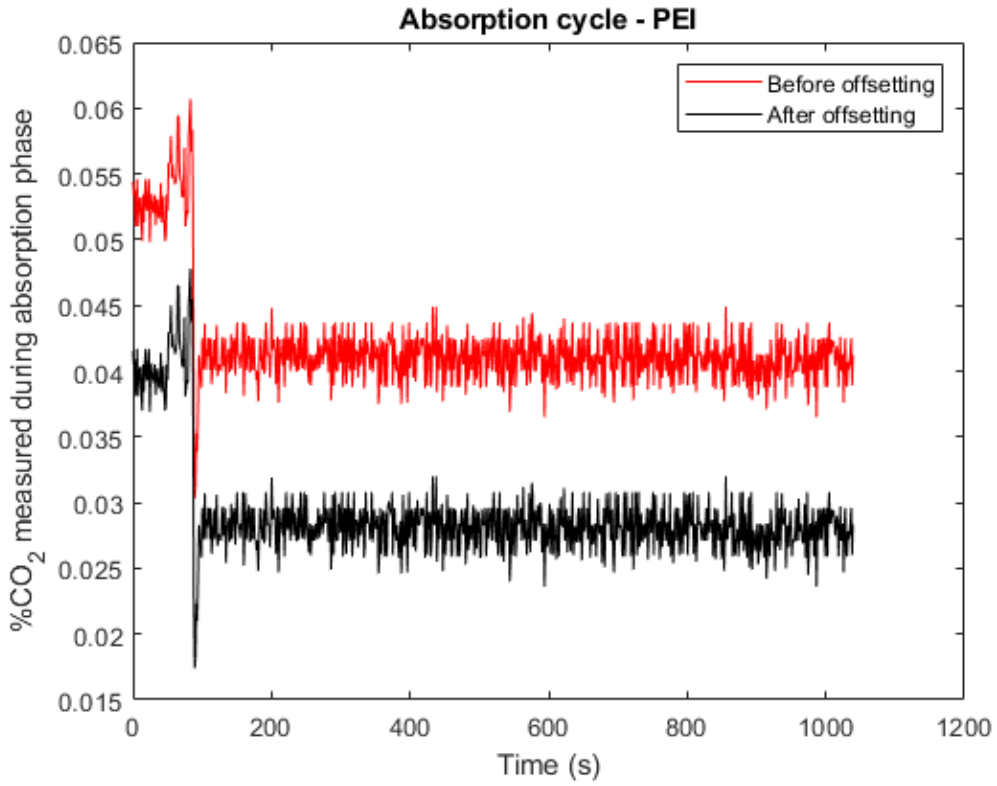

Figure 4.2: Example plot of % CO_2 measurements during absorption - with and without offsetting

Conversion

After offsetting the CO_2 analyser data plots, the conversion of $\%CO_2$ to mass of CO_2 was carried out using the equations explained in section 4.1. The graphical representation of the converted data points are shown in figure 4.3.

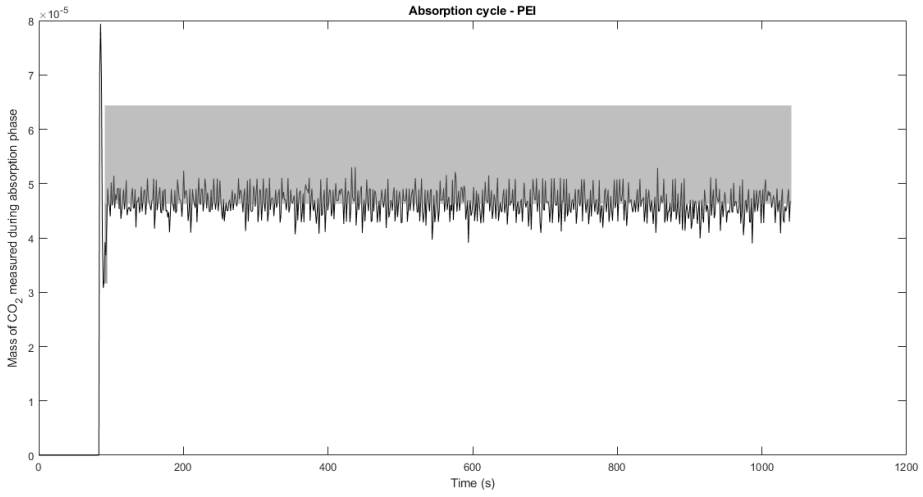

Figure 4.3: Example plot to determine the mass of CO_2 during absorption

The shaded region of figure 4.3 represents the total mass of CO_2 absorbed during the absorption cycle by the bulk amine. The area of the shaded region was determined using ”trapz” function in MATLAB 2019. All the data obtained during the absorption phase was subjected to similar analysis to determine the mass of CO_2 absorbed.

4.2.2. CO_2 analyser - Desorption

The graphical representation of the CO_2 analyser data set during desorption cycle is as shown in figure 4.4. The red , black and blue plots represents the raw data, corrected values and the temperature respectively. The issue of scale shifting (explained in section 3.2) was observed in the desorption phase as well. The process of evaluating the errors, corrections made and determination of the total CO_2 mass are explained below.

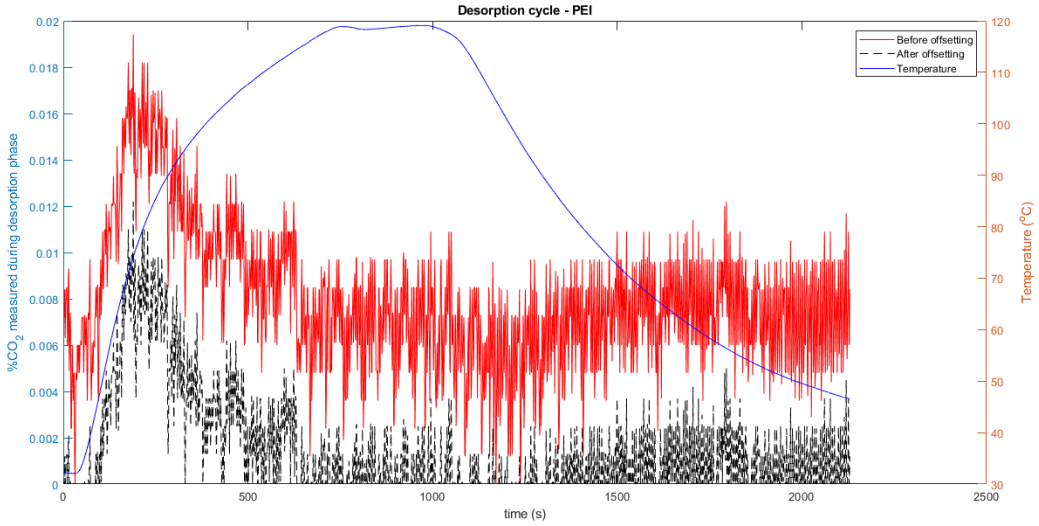

Figure 4.4: Example plot of $\%CO_2$ measurement during desorption cycle - before and after offsetting v/s temperature

During the desorption phase, the reaction flask was purged with N_2 gas to continuously remove the desorbed products. At low temperatures, the absorbed CO_2 in the bulk amine will not be released into the N_2 atmosphere. Thus, the $\%CO_2$ during the initial stage (before applying heat to the reaction flask) must be 0.00%. Comparing the CO_2 concentration (red plot) with the temperature (blue) in figure 4.4, the initial CO_2 measurement shows 0.008% when the temperature is below 35^0C. Similar behaviour is seen towards the end of the experiment where the temperature falls below 50^0C whereas the CO_2 analyser reads an average value of 0.08%. This indicates that the error due to shifting in the scale exists. Thus, an offset value was introduced (added or subtracted) to the data set such that the initial values are maintained at 0.0%. This can be seen in the black plot of figure 4.4.

It can be seen in figure 4.2.2 that the desorption activity slows down or becomes 0 after 500s. With respect to the temperature of the amine, the desorption process stops even before the rection flask (or amine) reaches the required desorption temperature. This behaviour was observed in all the experiments. As mentioned in section 3.2.1, due to lack of time, the desorption duration was set as approximately 20-25min. This time includes ramping time and 10 min of isothermal state.

The conversion procedure explained in section 4.1 was followed after correcting the data set. The figure 4.5 shows the corrected graph and the shaded region represents the total mass of CO_2 desorbed. The area of the shaded region was determined using ”trapz” function in MATLAB.

4.3. Analysis of Moisture Data

The sensitivity of the RH sensor used was tested by exposing it to pure nitrogen. The results are shown in figure 4.7.

It can be seen from figure 4.7 that the sensor requires 3-4 min to read 0% relative humidity when exposed to pure nitrogen. Almost same duration is required to read the relative humidity of air when the gas flow is switched. This shows that the response time of the sensor is high and time constant τ was calculated to be 1.3min. Further, the response time increases when the sensor reads below 20% RH. This behaviour is usually attributed to aging of the sensor or deposition of particles on sensing units [87]. Thus, the data obtained

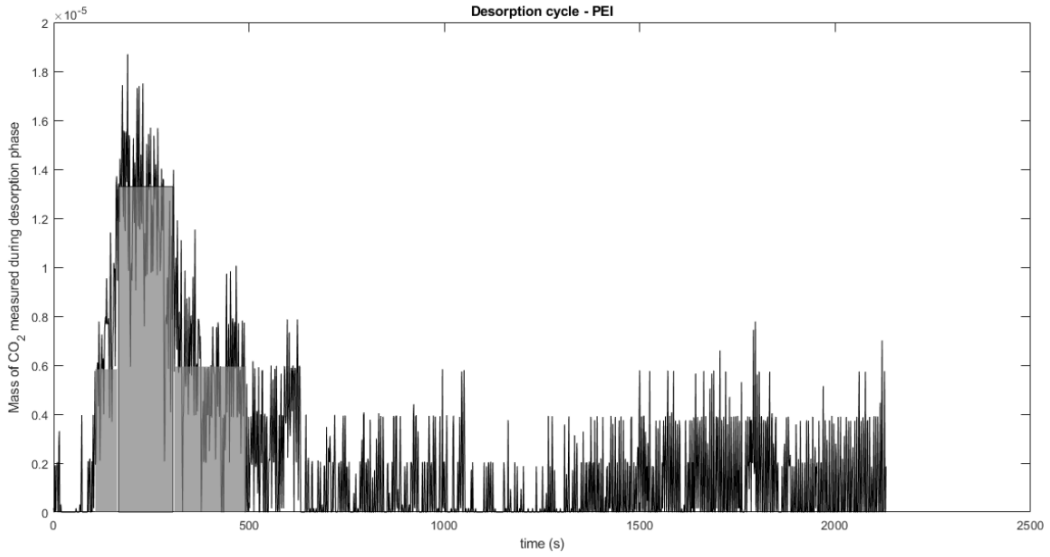

Figure 4.5: Example plot of CO_2 mass measurement during desorption cycle

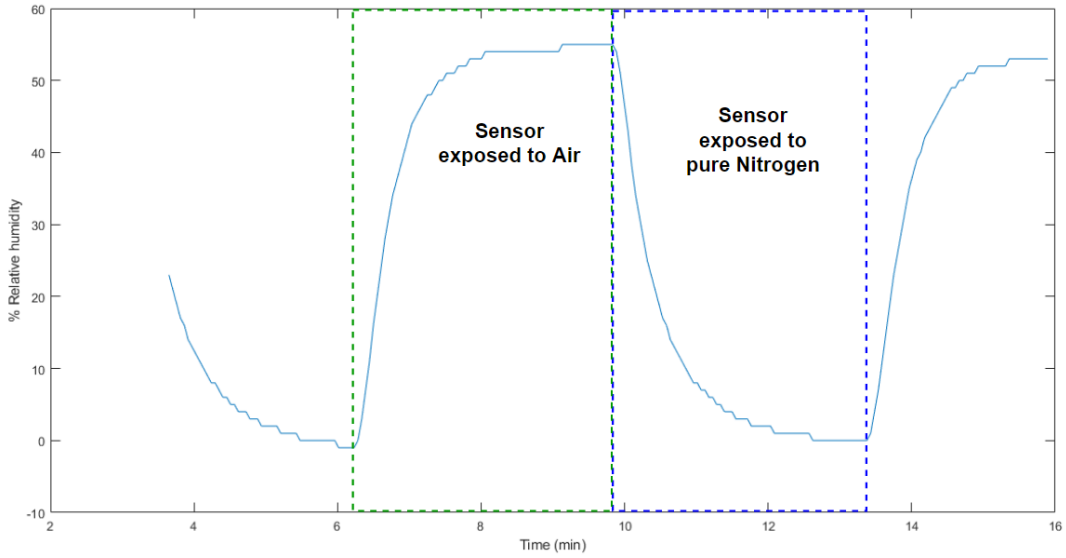

Figure 4.6: Behaviour of RH sensor when exposed to air and pure nitrogen

from the sensor cannot be used for quantifying the results as it might show high degree of inaccuracies.

The relative humidity data obtained form the sensor during the cyclic experiments were analysed and the observations are shown in section 4.3.1 and 4.3.2.

4.3.1. Absorption

The relative humidity measurements obtained during the absorption phase is as shown in figure 4.7.

Comparing the flow (black) and the RH (red) plot, we can see that the relative humidity starts to decrease sharply when air is made to flow over the amine. This indicates surface absorption of moisture in amines. Further, the value of RH increases but do not reach the initial value during the course of the experiment due to diffusion process taking place within the liquid. This trend is similar to the CO_2 absorption seen in section 4.2.1. Similar observations made during desorption phase is given in section 4.3.2.

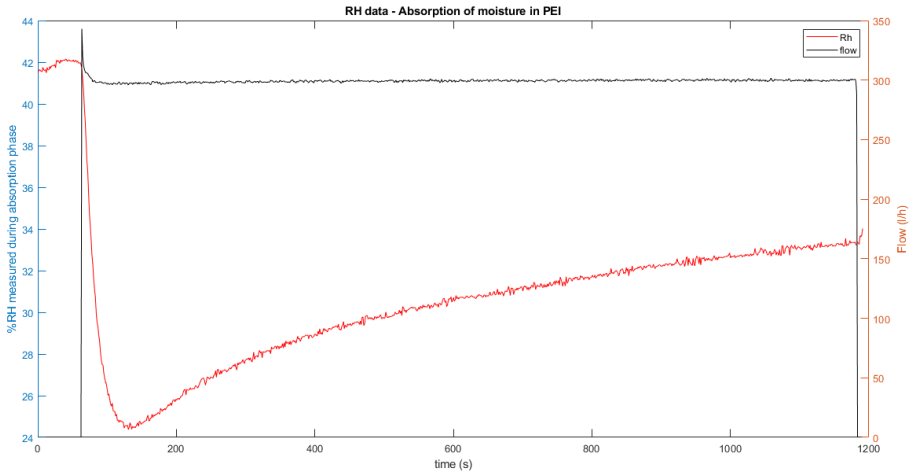

Figure 4.7: Example plot of RH measurement

4.3.2. Desorption

The RH measurements (red) obtained during the desorption process is shown in figure 4.8. The corresponding flask temperature (black) is used to validate the response of the RH sensor.

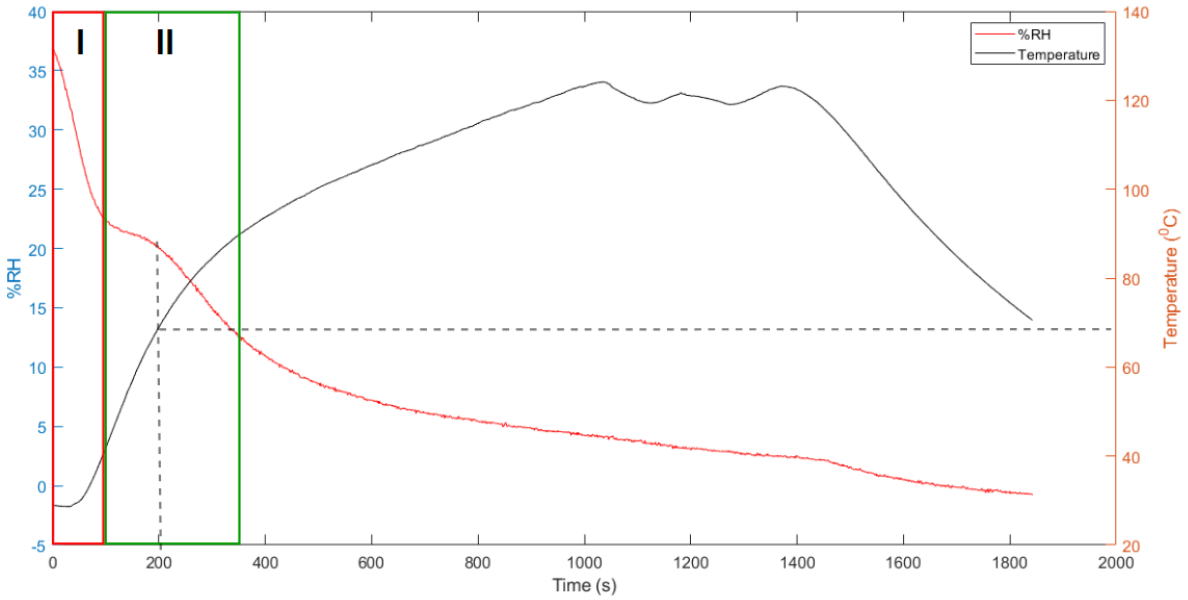

Figure 4.8: Example plot %RH measurement and temperature variance during desorption

During the desorption process, the reaction flask is purged with N_2 gas. It can be seen in **region I**, the relative humidity starts to decrease at the beginning of the experiment. Ideally, if no water is present in the gas stream then the sensor must read 0% RH. But, the sensor dose not reach 0. This could be due to the following reasons:

- The slow response from the sensor which was explained in section 4.3.
- The air from the absorption cycle being slowly purged by N_2 at the beginning of the desorption cycle.
- During the desorption cycle, the reaction flask is purged with pure nitrogen. This reduces the partial pressure of moisture is the gas stream. This might causes the equilibrium of moisture between amine and the gas stream to shift resulting in desorption of water even before the amine is heated.

Considering the possibilities mentioned above, no conclusions can be drawn to explain the behaviour in region I.

At **II**, the temperature of the flask increases and a slight increase of moisture in the gas stream was sensed. This shows that a significant moisture content was sensed and could be due to desorption of water from the amine. Beyond region II, the plot gradually tends to 0. Thus, it is not possible to argue about the end point of moisture desorption.

It is clear that the relative humidity data cannot be used for quantitative analysis. But, the observation in the region II can help to analyse the process qualitatively. The end samples of the cyclic experiments were subjected to Karl-Fischer experiment explained in section 3.3.1 to determine the water concentration. The results are discussed in chapter 5.

4.4. Calculation of theoretical evaporation rates

The theoretcial evaporation rates of TEPA were calculated using the equations mentioned in section section 2.3.1(page 15). The important parameters and constant values used to determine the evaporation rate of TEPA are listed in table 4.1

Table 4.1: Parameters and constant values used to determine the theoretical evaporation rate of TEPA

Parameter	Constant value
Heat of vaporization H_{vap}	71300J mol^{-1}
Vapour pressure	less than 1.3Pa at 20°C $1.06e^{-4}$Pa at 20°C 1.3Pa at 20°C

The heat of vaporization value was taken from NIST webbook [89] and the vapor pressures were taken from the archive of U.S national library [90].

It can be seen in table 4.1 that the vapour pressure vary from one source to another within a range of 10^{-}4Pa. The reason for the discrepancies between the vapour pressure values obtained from sources are not studied in this thesis. The theoretical evaporation rate of TEAP at 120 °C was calculated using the vapor pressure value as 1.3Pa and $1.06e^{-4}$Pa. The calculated evaporation rates were compared with the evaporation rate obtained for TEPA at 120°C via TGA to verify as to which numerical value of the vapor pressure presented in table 4.1 is acceptable . The result of the TGA experiment is given in section 5.1.2 and the evaporation rate was found to be 16.9$mg\,m^{-2}\,s^{-1}$. The procedures followed to calculate the theoretical evaporation rate at 120°C and the comparison between the TGA experimental value are explained below:

- Using the numerical values given in table 4.1 and the Clausius-Clapeyron equation shown in equation 2.18 (page 16), we can calculate the vapour pressure of TEPA at 120°C.
- With the new vapour pressure at 120°C, we can calculate the evaporation rate of the amine using equation 2.11 shown in page 15.
- In equation 2.11, we can see that the mass transfer coefficient k_m depends on the factors such as velocity of gas flowing over the amine, the kinematic viscosity of nitrogen and the molecular diffusivity of the amine vapor.
- The numerical values of the above mentioned factors must be similar to that of the TGA experimental conditions in order to make a comparison between experimental and theoretical evaporation rates. The numerical values considered are given in tabel 4.2.

The comparison between theoretical evaporation rate calculated using vapor pressure 1.3Pa , $1.06e^{-4}$Pa and the evaporation rate obtained from TGA are shown in figure 4.9

It can be seen in figure 4.9 that the experimental evaporation rate shows a large deviation form both the theoretical evaporation rates. This suggests that the vapor pressure of TEPA at 20°C might not be exactly 1.3Pa or $1.06e^{-}$4Pa but within the range $1.06e^{-4}$Pa<P_{vap}<1.3Pa

Table 4.2: Parameters considered during the TGA experiment to determine the evaporation of TEPA at 120°C

Parameter	Constant value
Diameter of the alumina crucible	5.5 mm
Diameter of TGA heating chamber	20mm
Velocity of nitrogen flow	0.0027 $m\,s^{-1}$
Volumetric flow of nitrogen	50ml/ min
Kinematic viscosity of nitrogen at 120 °C	$2.5e^{-5} m^2\,s^{-1}$
Molecular diffusivity of water vapour at 100°C	$3.9e^{-5} m\,s^{-1}$

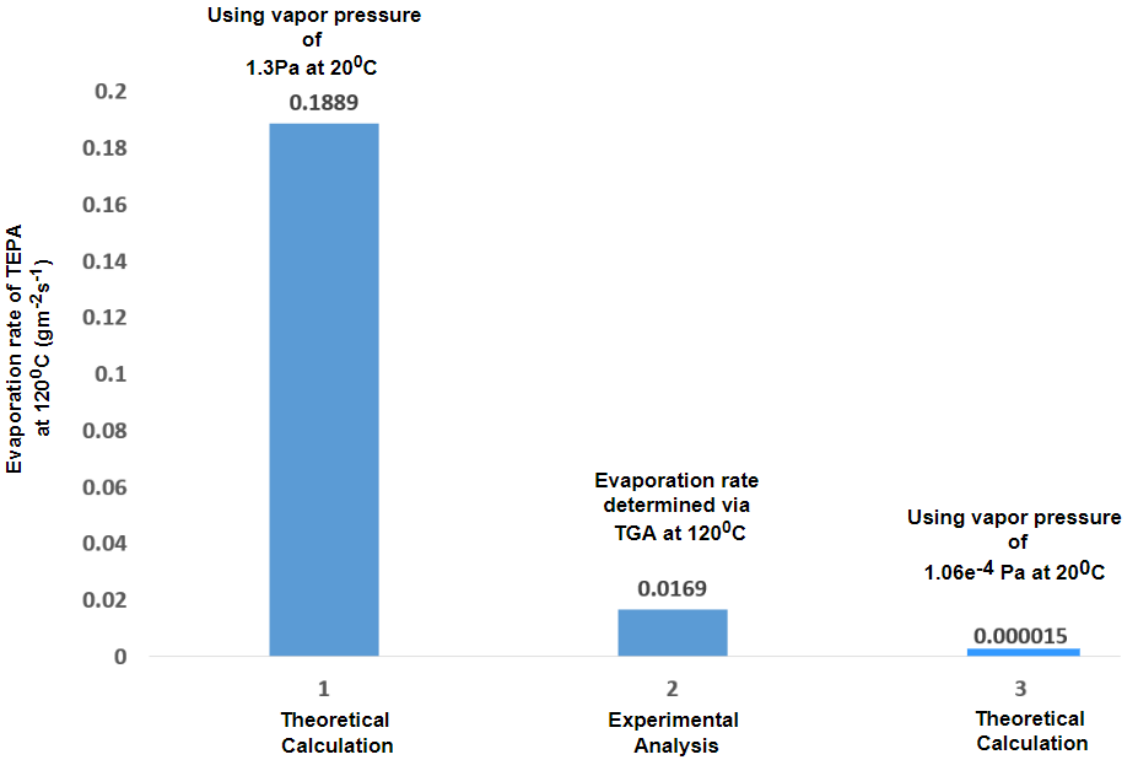

Figure 4.9: Comparison of theoretical evaporation rates of TEPA at 120°C

at 20°C. Further, using the evaporation rate obtained from TGA (16.9$mg\,m^{-2}\,s^{-1}$), the vapour pressure of TEPA at 20°C was calculated and the result was found to be **0.1213Pa**.

The calculated vapour pressure was used to determine the theoretical evaporation rate of TEPA under muffle furnace conditions. A comparison was made between theoretical and experimental evaporation rates under muffle furnace conditions. The results are presented in section. A discussion on the calculated vapor pressure of TEPA can also be found in section 5.1.2.

The important information such as vapor pressure and heat of vaporization could not be found for PEI - 600. Depending on the application, PEI is modified into various chain lengths and molecular masses. Thus, the simplest form of PEI is aziridine which has a molecular formula of CH_2NHCH_2. In general, all the physical properties of PEI with different molar masses were associated with aziridine. The properties of Aziridine are given in tabel 4.3.

It can be seen in table 4.3 that the vapor pressure of aziridine is very much higher when compared to that of TEPA shown in table 4.1. This suggests that aziridine evaporates faster than TEPA. But, this cannot be true as the results of the evaporation experiments given in section 5.1.2 shows that PEI-600 evaporates slower than TEPA. Therefore, the physical properties of aziridine cannot be used to calculate theoretical evaporation rate of PEI-600.

Table 4.3: Physical properties of aziridine

Property	Constant value
Molecular mass	43.07 $g\,mol^{-1}$
Vapour pressure	21.3kPa at 20°C
Heat of Vaporization	$7.75e^5$ $J\,kg^{-1}$

4.5. Assumptions

The assumptions made during the analysis of the results are given below:

4.5.1. Moisture in methanol

The procedure of Karl-Fleischer and phosphoric acid testing includes the addition of methanol. Sinha[27] carried out three tests on methanol and the water concentrations were found to be 0.067, 0.063 and 0.058%wt. The water concentration found in amine samples through Karl-Fischer must be corrected with water in methanol to determine the accurate value. In this thesis the average of the three values mentioned, that **0.062%wt** of water in methanol, is considered. This value was used to correct the water concentrations determined during this research.

4.5.2. Duration considered for calculating evaporation rates in cyclic experiments

The time duration considered for evaporation rates for cyclic experiments are shown in figure 4.10.

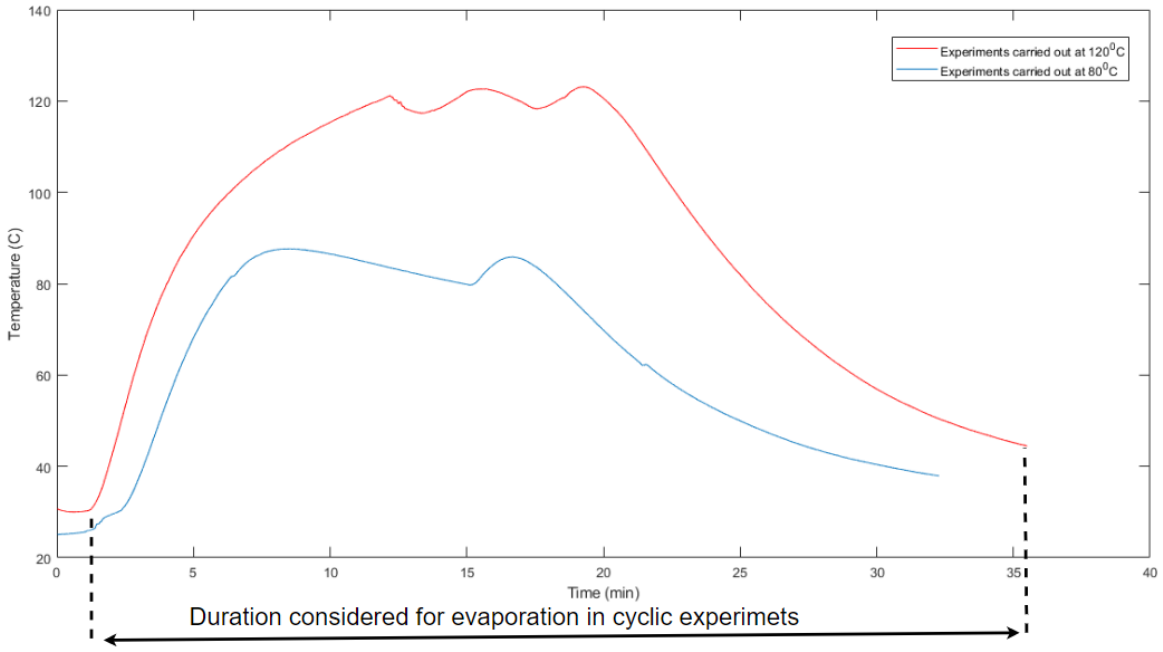

Figure 4.10: Temperature curves for 80^0C and 120^0C cyclic experiments
Duration considered for evaporation

For both PEI and TEPA cyclic experiments at desorption temperatures 80^0C and 120^0C, the duration of desorption is considered to be approximately 40 minutes. For 30 desorption cycles, the total duration is 20 hours.

4.5.3. Surface area of amine samples during cyclic experiments

The surface area of amine samples taken in the reaction flask was not measured during each experiment. The base diameter of the flask was 8cm and had a curved bottom of 4cm

diameter as shown in figure 4.11. Thus, the amine would have occupied between 2-4cm from the walls of the flask. The actual conical flask used during the experiments is also shown in figure 4.12.

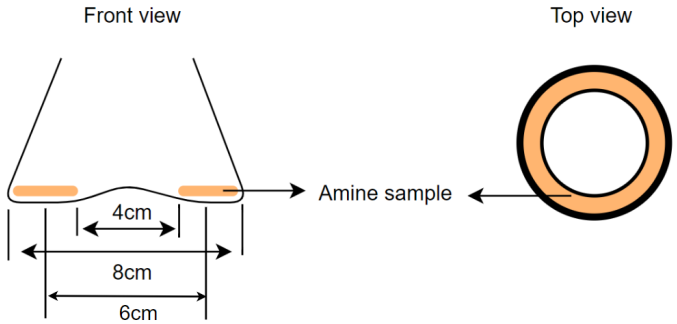

Figure 4.11: Assumption of amine surface area during cyclic experiments

Figure 4.12: A conical flask used during cyclic absorption-desorption test

The surface area of the amine during cyclic experiments was assumed to be between 22.03cm^2 (minimum) and 37.7cm^2 (maximum). Evaporation rate of the amine during the cyclic experiment was calculated using both the minimum and the maximum surface area that the amine would have possibly covered. A vernier caliper used to measure the dimensions of the flask has an error of 0.05mm. Thus, the calculated surface area might have an error of ±0.8cm^2. It must be noted that the surface area of amine sample during the experiment could be lower

4.5.4. Direction of nitrogen flow in muffle furnace experiment

The mass transfer coefficient used in equation 2.11 is a function of the velocity of the gas flowing over the liquid. In a muffle furnace, the nitrogen enters a cuboidal heating chamber from a 6mm tube. The dimensions of the muffle furnace is shown in figure 4.13. As the inlet of the nitrogen is very much smaller than the heating chamber, determining the actual velocity of the nitrogen over the petridish becomes a complex procedure. But, an approximate velocity can be calculated by assuming that the nitrogen flows either in direction D1 or D2 as shown in figure 4.13. In this thesis, theoretical evaporation rate for TEPA was calculated considering both direction D1 and D2. The results were also compared with the experimental data which is presented in section

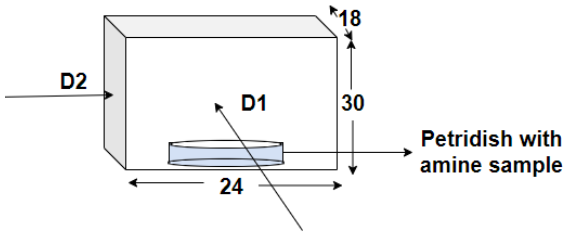

Figure 4.13: Layout of muffle furnace and the nitrogen flow directions

5
Results and Discussion

5.1. Evaporation

The evaporation studies were carried out during the absorption and desorption processes. The results are presented in section 5.1.1 and 5.1.2.

5.1.1. Evaporation during absorption

Figure 5.1 shows the change in mass of PEI when exposed to atmospheric air for a duration of 6 days.

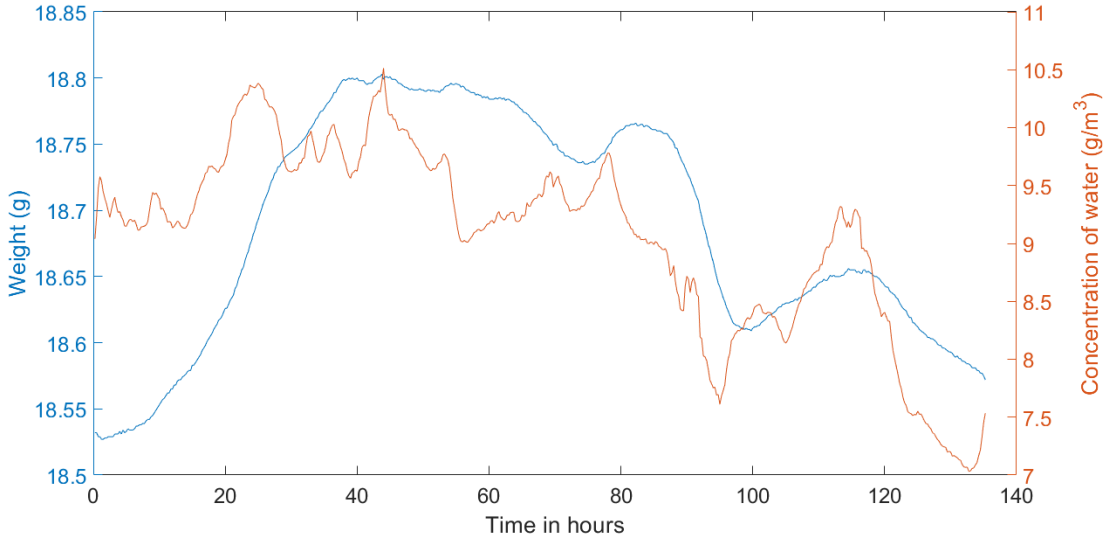

Figure 5.1: Change in mass of PEI during long term exposure to atmospheric air
and
Change in water concentration during the experiment

It can be seen in figure 5.2 that the mass of PEI (blue) increases by approximately 0.004g after exposing it to air for six days. When exposed to air, PEI absorbs water and CO_2. It can be seen that the variation of PEI mass is influenced by the concentration of water in the ambient air. The increase in mass seen after the experiment could be due to absorption of water and CO_2. Similar trends were seen during the experiments of TEPA. The results are shown in figure 5.2

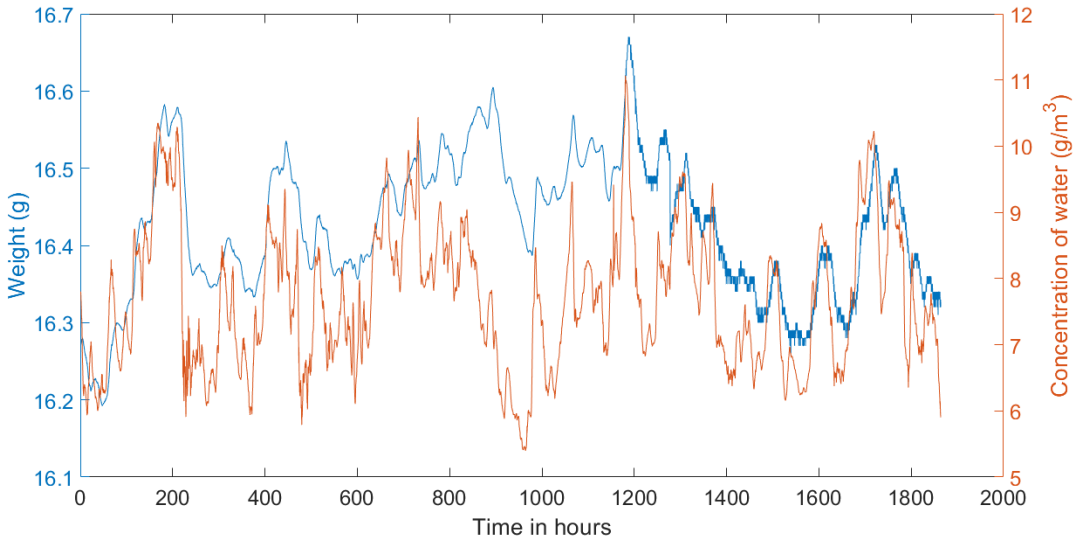

Figure 5.2: Change in mass of TEPA during long term exposure to atmospheric air
and
Change in water concentration during the experiment

It can be seen that the mass of TEPA also increased by 0.02g at the end of the experiment which could be due to water and CO_2 absorption. The mass of CO_2 and water were not measured at the end of the experiment. Therefore the actual loss of mass occurring in the amines could not be calculated. As mentioned in section 4.4, the theoretical evaporation rate of TEPA was calculated considering the ambient temperature of 20°C, air flow of $0.02 m s^{-1}$ and a liquid surface diameter of 5.5cm exposed to air. Here, the kinematic viscosity of air was considered to be $1.51e^{-5}$ $m^2 s^{-1}$ (at 20°C) and the molecular diffusivity of water vapor at 20°C was taken as $2.4e^{-5} m^2 s^{-1}$.

The theoretical evaporation rate of TEPA at the ambient condition was found to be $9.06e^{-6}$g. Considering the duration of the experiment to be 1800h, the loss in mass of TEPA was calculated to be 0.14g. But, the theoretical calculation of evaporation rate neglects the effect of partial pressure of CO_2 and water. As explained in section 2.3.1, the molecules of water and CO_2 absorbed reduces the vapour pressure of the amine. This further reduces the evaporation rate.

Also mentioned in section 4.4, the physical properties of PEI were not available to calculate the theoretical evaporation rate of PEI. But, based on the results of the evaporation rates determined at high temperatures (given in section 5.1.2), it can be assumed that the vapor pressure of PEI is lower than TEPA and thus, the evaporation rate will also be lower than that of TEPA at all temperatures.

5.1.2. Evaporation of amines during desorption

As explained in section 2.3.1, evaporation rates accelerates with increase in temperature. The evaporation rates of the amines were determined by muffle furnace experiments and a confirmatory test was done using TGA. The results are presented in section 5.1.2 and 5.1.2.

Results of muffle furncae experiments

Table 5.1 shows the evaporation rates observed during the muffle furnace experiments. The mass measurements during the experiments are given in table B.1 of Appendix B.

Table 5.1: Evaporation rates determined from Muffle furnace experiments

Temperature °C	Loss of PEI $mg\,m^{-2}\,s^{-1}$	Loss of TEPA $mg\,m^{-2}\,s^{-1}$
120	0.985	12.988
100	0.545	7.28
80	0.169	1.07

An observation made after treating TEPA at 120 °C is that the remaining sample had formed a dry layer. Figure 5.3 and 5.4 shows the condition of TEPA before and after the experiment respectively. The formation of the dry layer was not found in any other experiment. Thus, to verify the evaporation rate of TEPA at 120°C and to investigate the formation of dry layer, TGA was carried out on pure TEPA.

Figure 5.3: Before 120^0C experiment

Figure 5.4: After 120^0C experiment

TGA analysis of TEPA at 120°C

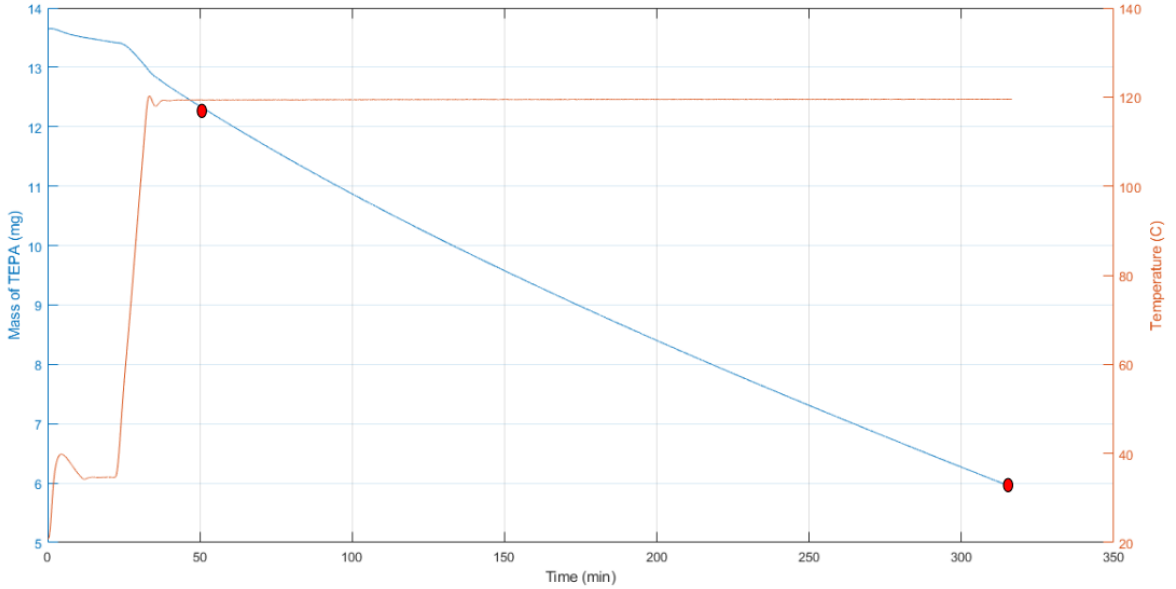

Figure 5.5: Change in mass of TEPA at 120 °C

Figure 5.5 shows the decrease in mass of TEPA over time. To determine the evaporation rates, the slope of the plot and the surface area of the amine sample has to be considered. The diameter of the TGA crucible was measured to be **5.5mm**. Considering the points marked on the plot, the slope was calculated to determine the approximate evaporation rate of TEPA at 120 °C . The value was found to be $16.9\,\mathrm{mg\,m^{-2}\,s^{-1}}$**.**

The results of the TGA show that the evaporation rate of TEPA at 120^0C is higher than that of the muffle furnace experiments. This suggests that the TEPA sample size in the muffle furnace experiment was small and all the TEPA would have been evaporated during the time of the experiment leaving behind a dry layer.

As explained in section 4.4, the vapor pressure of TEPA was determined to be 0.121Pa. This vapor pressure was used to theoretically calculate the evaporation rate of TEPA in muffle furnace conditions. The procedure followed to determine the evaporation rate was explained in section 4.13. The results were compared with the experimental values and are shown in figure 5.6.

The analysis of the results shown in figure 5.6 is given below:

- Evaporation rates at 100°C - The experimental value is higher than the theoretical values. This is because, during the experiment, the muffle furnace takes 1h to ramp up to 100°C from room temperature. Similarly it takes upto 5h-6h to cool down. The experimental evaporation rate calculated will be inclusive of evaporation taking place during ramping up and cooling down. This factor is not considered during the theoretical calculation as it is assumed that temperature remains constant throughout. This leads to higher error between theoretical and experimental calculation
- Evaporation rates at 120°C - It is important to note that the experimental value presented here is determined via TGA experiment. The procedure to determine the evaporation rate via TGA was explained in section 5.1.2. The error between the theoretical and experimental values are lower when compared to that of 100°C because the experimental results of the TGA was calculated by excluding the evaporation during ramping and cooling process.
- Evaporation rate at 80°C - The experimental result was determined through muffle furnace experiment. Unlike 100°C experiment, this result is lower than the theoretical evaporation rate. This could be due to errors in measuring mass of the sample before and after the experiment. Or, the amine sample must have been exposed to air

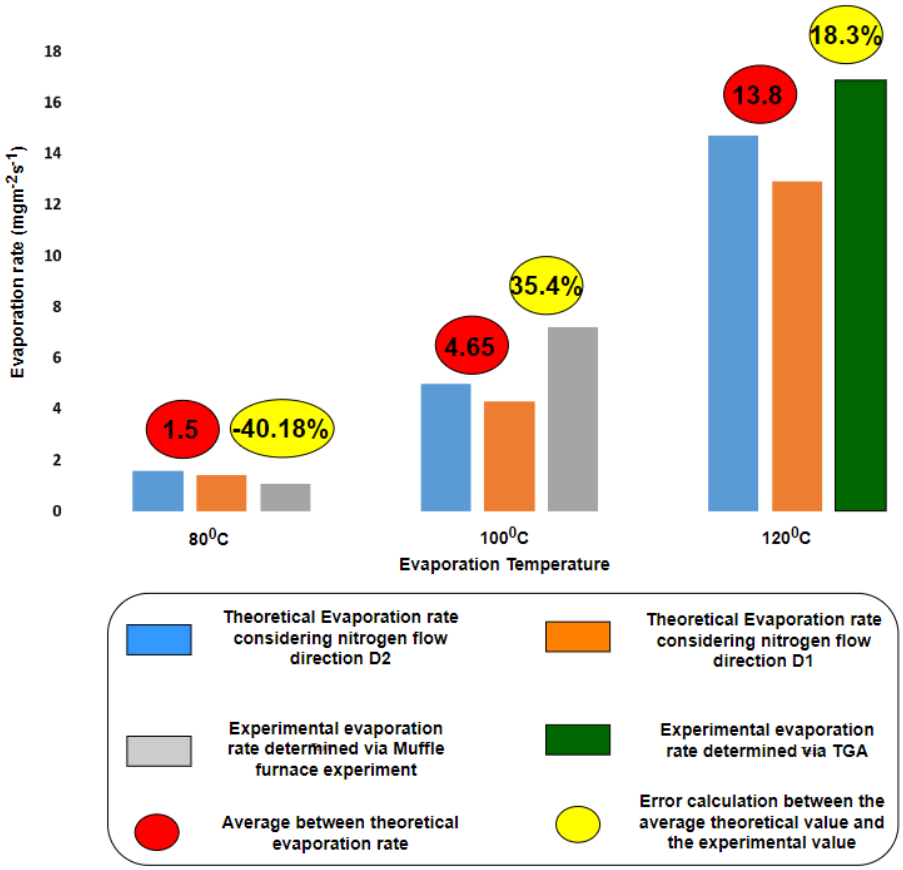

Figure 5.6: Comparison of theoretical and experimental evaporation rate of TEPA at different temperatures

for a longer duration after the experiment. This results in absorption of moisture which increases the mass of amine during weight measurement. Thus, the experimental evaporation rate is found to be lower than the theoretical value with high error.

Although the equation 2.11 includes various assumptions, the comparison between the theoretical and the experimental evaporation rates of TEPA suggests that the vapor pressure of 0.1212Pa at 20°C can be used to determine an approximate evaporation rate of TEPA at different temperatures.

Evaporation rates during desortion process

As discussed in section 2.3.1, the evaporation rate is lowered when CO_2 and water is present in the amine. This behaviour was studied through cyclic experiments. The amine samples showed decrease in mass after 30 cycles of desorption. This measurement was used to calculate the evaporation rates.In Section 5.2.1, it can be seen that after 30 cycles, the amine sample had accumulated CO_2. Also, it is assumed that after each desorption cycle, all the water was taken out of the amine. Thus only the mass of CO_2 was subtracted from the final mass measured to determine the change in amine mass. Further, the surface area and duration considered for the calculations were explained in section 4.5.

Figure 5.7 shows a comparison of evaporation rates between cyclic experiments (CO_2 loaded) and muffle furnace (pure amines) samples.

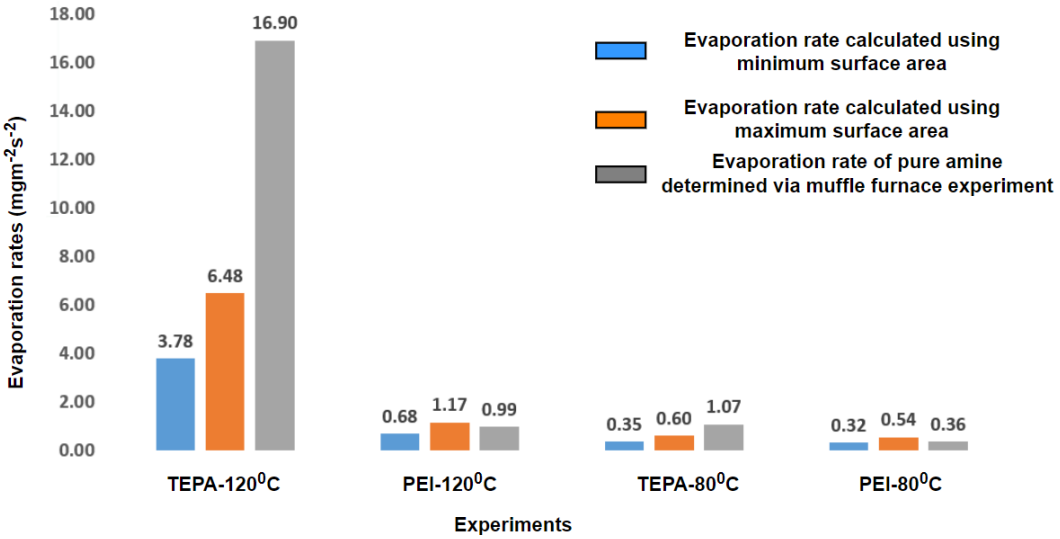

Figure 5.7: Comparison of evaporation rates between CO_2 loaded sample and pure amine samples

It can be seen in figure 5.7 that PEI - 120, TEPA - 80 and PEI - 80 experiments did not show lowered evaporation rates when compared to that of pure amines. This suggests that the partial pressure of CO_2 and water was very low during the desorption phase of the cyclic experiments resulting in the evaporation rates shown in the figure. Further, TEPA - 120 experiment shows 61% reduction in the evaporation rate when compared to that of pure amine. This indicates that the partial pressure of CO_2 & water was high during the TEPA -120 experiments when compared to the other experiments. This cannot be true as TEPA desorbed at 120°C should show better desorption characteristics which should result in low partial pressure of CO_2 and water when compared to desorption of both PEI or TEPA at 80°C [28]. It could be possible that the TEPA -120 sample, after the cyclic experiment must have been exposed to air for a longer duration due to which CO_2 and water absorption could have taken place resulting mass measurement error. It must also be noted that the weighing scale used to measure the mass has an error of ±0.005g.

5.2. Cyclic absorption and desorption test

5.2.1. Analysis of CO_2 absoption and desorption

As explained in section 4.1, each data set obtained from the CO_2 analyser was converted into mass of CO_2 absorbed and desorbed. Figure 5.8 shows the absorption and desorption trends of PEI 120 °C experiments.

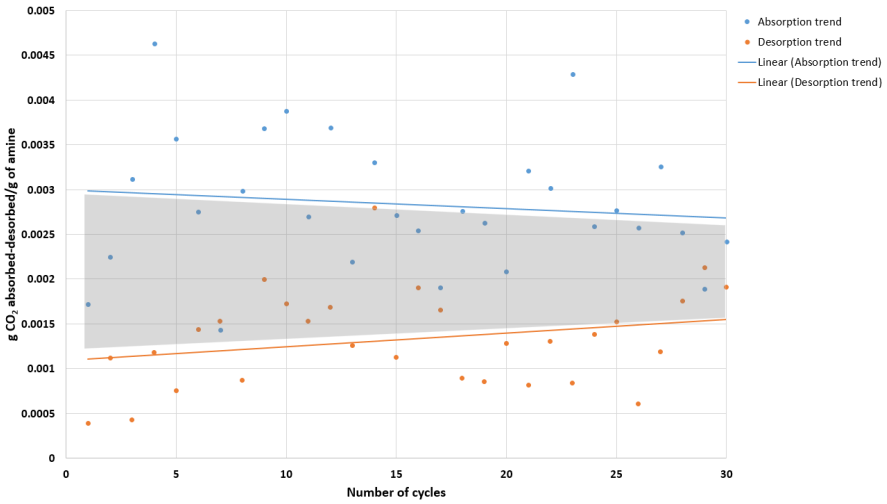

Figure 5.8: Absorption and desorption trends observed during cyclic experiments of PEI (desorption temperature - 120^0C)

As explained in section 3.2, the data set consists of noise which makes it difficult to quantitatively analyse the behaviour. But, we can observe that the difference between absorption and desorption trend line (shaded area) shows that CO_2 was accumulated during the experiment.

Similar trends were observed in other cyclic experiments. Figure 5.9 shows the trend of PEI 80 °C experiments and figure 5.10 and 5.11 shows the results of TEPA 120 °C and 80 C experiments respectively.

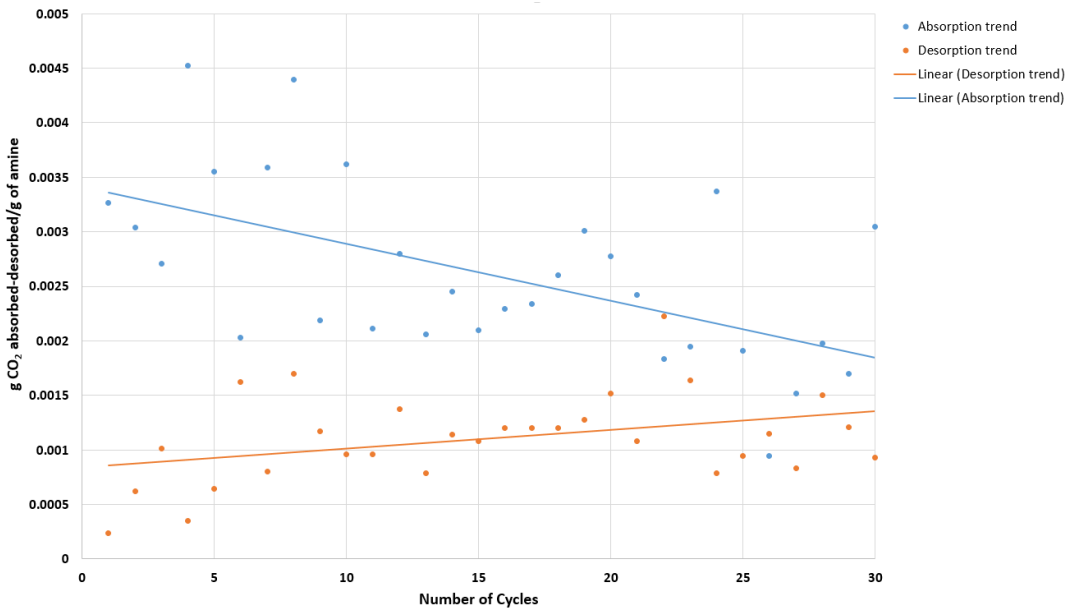

Figure 5.9: Absorption and desorption trends observed during cyclic experiments of PEI (desorption temperature - 80^0C)

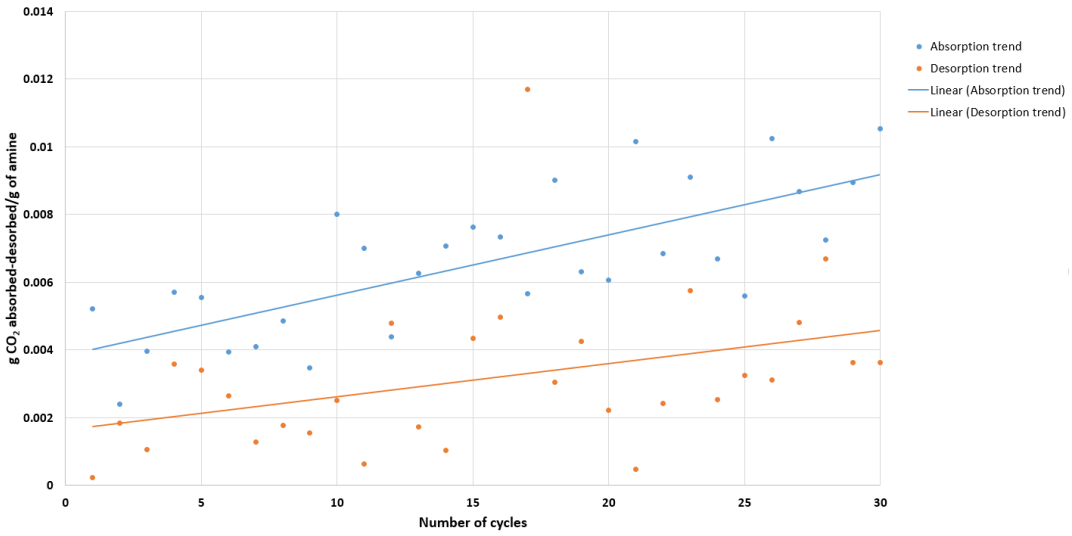

Figure 5.10: Absorption and desorption trends observed during cyclic experiments of TEPA (desorption temperature - 120 °C)

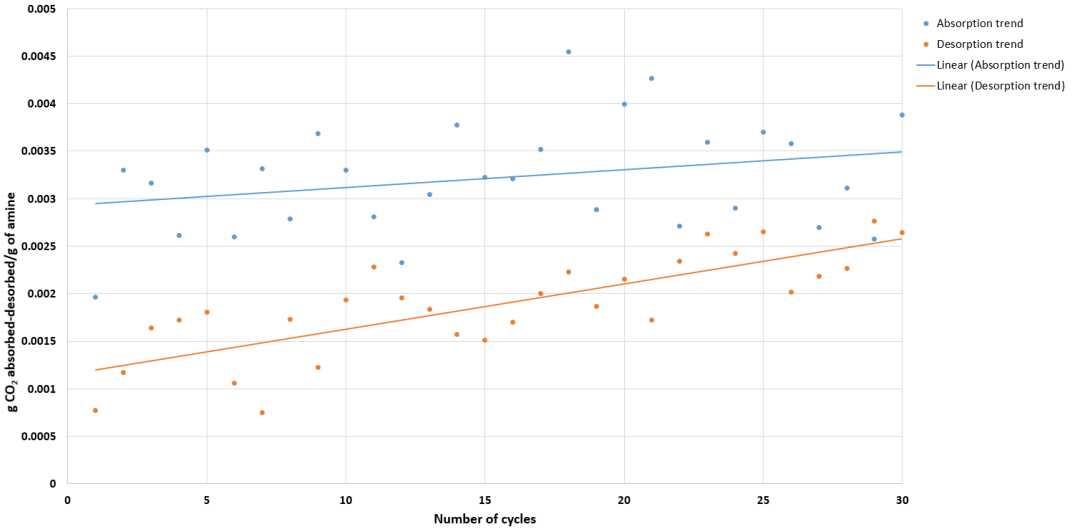

Figure 5.11: Absorption and desorption trends observed during cyclic experiments of TEPA (desorption temperature - 80 C)

Figure 5.12 shows the accumulation of CO_2 in PEI over 30 cycles. The accumulation value is represented as $gCO_2/gAmine$. After each desorption cycle, some amine was lost due to evaporation. The evaporation loss was corrected during the calculation of the CO_2 accumulation. The correction procedure is given below:

- The overall mass of amine evaporated was calculated by subtracting the mass of CO_2 accumulated. This gives the mass of pure amine that was evaporated during the desorption process. It must be noted that for this purpose, the accumulated mass of CO_2 was determined from the experimental data obtained from the CO_2 analyser.
- The mass of amine evaporated was divided by 30 as 30 desorption cycles were carried out during the experiment. This gives an approximate mass of amine evaporated during each cycle.
- Consider the mass of amine evaporated during each cycle is X, then after the 1^{st} cycle X was subtracted from the initial amine mass. After the 2^{nd} cycle, 2X was subtracted from the initial mass and so on.

Further, a sensitivity analysis was carried out by assuming no evaporation. The trends show that PEI accumulates more CO_2 when desorbed at 80 °C. This is because higher temperature increases the desorption kinetics [28] of the amine. It can also be seen that the trends of both PEI - 80 and PEI - 120°C tends to converge after 25 cycles. This indicates that the PEI - 80 sample could have reached the accumulation capacity and on conducting more absorption-desorption cycles might show a constant accumulation of approximately 0.045gCO_2/gAmine.

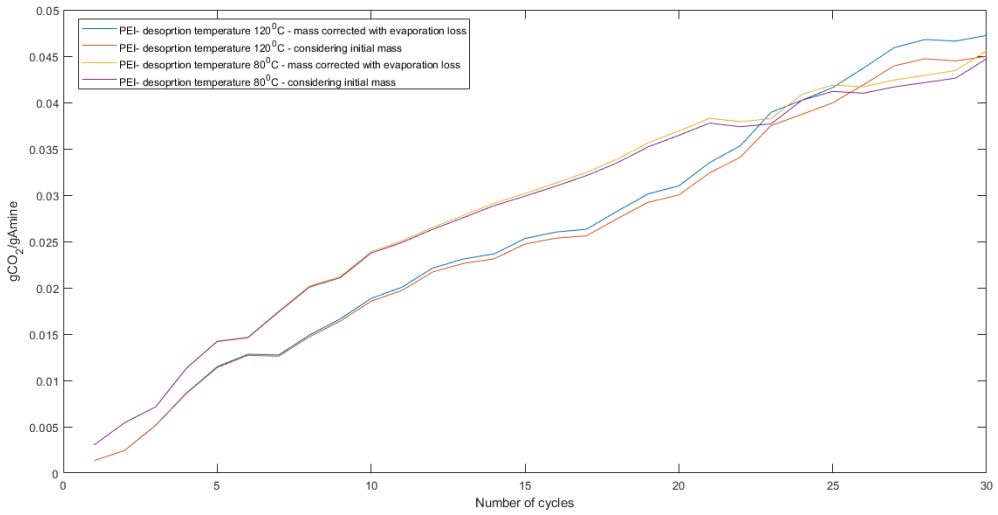

Figure 5.12: Mass of CO_2 accumulated in PEI over 30 cycles

Similar accumulation trends are shown for TEPA in Figure 5.13. It can be seen that TEPA accumulated more CO_2 when desorbed at 120 °C. As mentioned earlier, high temperatures induces better desorption kinetics. Thus, this result is an anomaly or an experimental error.

During the desorption of TEPA at 120 °C, thick fumes were observed at the outlet of the system. Considering the results of TEPA evaporation at 120°C given in section 5.1.2, the fumes can be associated with TEPA vapors. As the gas stream entering the CO_2 analyser had TEPA vapours, the measurement of CO_2 could have been disturbed resulting in errors.

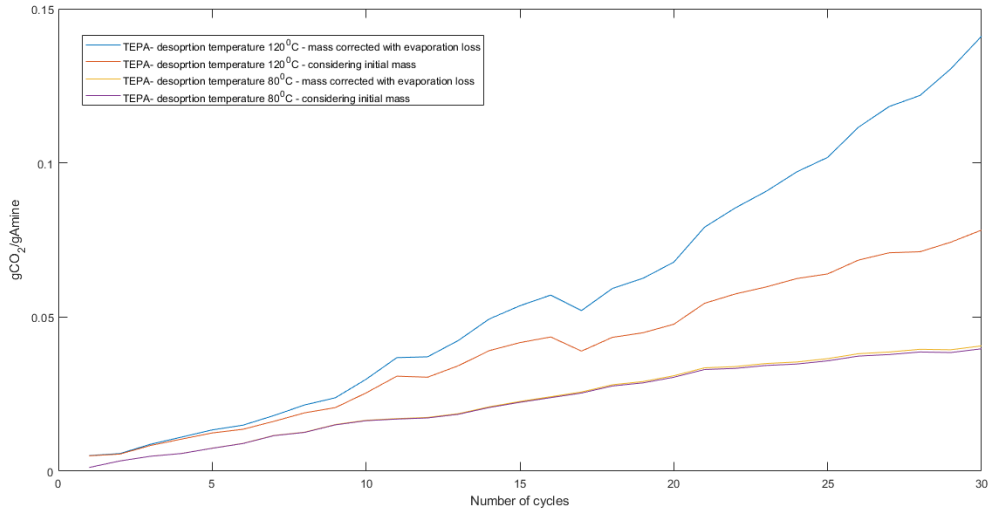

Figure 5.13: Mass of CO_2 accumulated in TEPA over 30 cycles

To verify the results of the experiments, the mass of CO_2 present in the amine samples after 30 cycles was determined via phosphoric acid testing. The sample preparation was explained in Section 3.3.1. The results are given in the table 5.2.

Table 5.2: Phosphoric acid test results of PEI/TEPA samples subjected to 30 cycles of absorption and desorption

Amine	Desorption temperature	Sample I (gCO_2/g of Amine)	Sample II (gCO_2/g of Amine)	Different in measurement (%)
PEI	120 °C	0.03454	0.03390	1.85
PEI	80 °C	0.04059	0.04134	1.81
TEPA	120 °C	0.01468	0.014426	1.77
TEPA	80 °C	0.03511	0.03588	2.14

From the table 5.2 we can see that there was a significant amount of CO_2 present in the amine sample after 30 cycles. Also, the difference in measurements between the two samples is close to 2%. It is to be noted that to achieve repeatable results in phosphoric acid testing, the sample mixture must be homogeneously mixed. But, no external mixing was done after the cyclic experiment. Thus, the result indicates that there could be mixing of bulk amine and CO_2 taking place during the desorption process. The mass measurements of the phosporic acid tests are given in table B.3 of Appendix B.

Studies of Ovaa [28] showed that during the CO_2 desorption process, some CO_2 remained in the sample. The concentration of CO_2 in the sample varied when desorption temperature and the pressure were changed. The results are given in section 2.5.2. Ovaa inferred that for a given temperature and pressure, there could be a desorption limit beyond which CO_2 could not be desorbed. The results of Ovaa are given in table 5.3.

Although the desorption pressure was not measured during the experiments of this thesis, a comparison can be made between the results presented in table 5.3 and 5.2. It can be seen that the accumulation observed after 30 cycles of absorption and desorption is still lower than the accumulation observed by Ovaa.

According to the inferences of Ovaa, the CO_2 desorption should not occur if the concentration of CO_2 is below the limit mentioned in table 5.3. In this study, it was observed that the

Table 5.3: Accumulation of CO_2 observed by Ovaa during desorption of PEI and TEPA at 200mbar [28]

Amine Desorption temperature	Desorption Accumulation observed gCO_2/g of amine
PEI - 120°C	0.036
PEI - 80°C	0.054
TEPA - 120°C	0.026
TEPA - 80°C	0.052

concentration of CO_2 in amine after 30 cycles was still lower than the threshold suggested by Ovaa. However, in contrast, CO_2 was desorbed in all the desorption cycles. A possible explanation for this behaviour is given in section 5.3.

5.2.2. Moisture data - Results of Karl-Fischer experiments

Table 5.4 shows the concentration of water in amine samples after the cyclic experiments. The methanol sample preparation and calculations are given in table B.2 of Appendix B.

Table 5.4: Karl-Fischer experiment results

Amine	Desorption temperature (C)	Sample I %wt H_2O in amine	Sample II %wt H_2O in amine	% Difference between Sample I II measurements
PEI	120 °C	3.0	6.2	51.6
PEI	80 °C	4.7	10.3	54.3
TEPA	120 °C	4.9	3.0	38.7
TEPA	80 °C	3.3	4.0	17.5

The absorption of water in the amine takes place by hydrogen bonding [30] or by forming bicarbonates [36]. Sinha [27] reported that, carbamates are dominant species formed during the absorption process. Thus, during the absorption process, it can be assumed that the water molecules are absorbed by forming hydrogen bonds with the amine molecules. During the desorption process, water molecules are desorbed faster than CO_2. Ovaa [28] studied the desorption process of water in PEI/TEPA and inferred that during the process, complete desorption of water takes place and it is faster than that of CO_2. However, as per the results displayed in table 5.4, a significant amount of water can be observed to be remained in the sample after the desorption process. A possible explanation for this accumulation of water could be as follows:

- If water had accumulated in the amine sample after each desorption cycle then, like CO_2 accumulation and mixing explained in section 5.2.1, the water molecules should have also undergone mixing. This should have resulted in equal concentrations of water in Sample I and Sample II.
- But, between the 2 sample tested, the results of Karl-Fischer experiment shows that the measured concentration of water vary up to 50%. This suggests that the absorption of water could have been taken place after the desorption process. This could be a reason why no mixing of water was observed.
- Ovaa [28] reported that the desorbed samples showed 1-2% water in the amine after his desorption experiment. The results observed in this thesis (table 5.4 are much higher than that of Ovaa.
- As explained in section 3.3.1, two aliquots were taken from the main amine sample to conduct the Karl-Fischer test. There could be a possibility that the moisture was absorbed after the cyclic experiment (mostly on the top surface of the amine) and the aliquots collected for the tests were also from the top surface. In this case, the Karl-Fischer would indicate high concentration of water.

Based on this discussions, it can be assumed that all the water was desorbed during the desorption process.

5.3. Hypothesis to explain the CO_2 accumulation and mixing of amine during desorption process

Based on the previous studies of absorption, desorption characteristics of amine (Section 2.5.2 and 2.5.3) and the results obtained through cyclic experiments, an attempt was made to explain the behaviour of CO_2 accumulation that was observed during cyclic experiments. Figure 5.14 shows individual absorption and desorption process that illustrates the hypothesis.

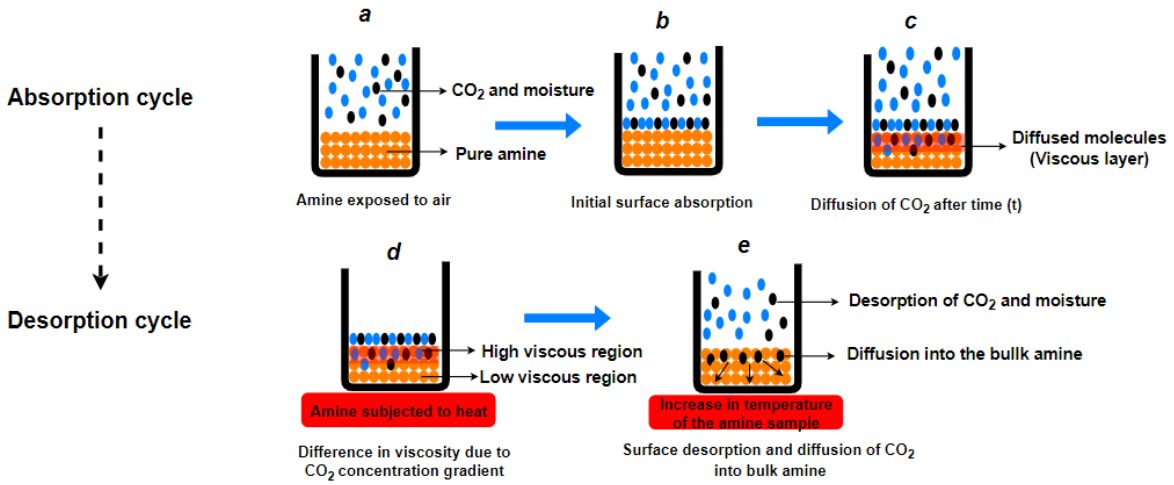

Figure 5.14: Process of absorption and desorption explained

Absorption cycle

When pure amine (PEI/TEPA) is exposed to air, initially surface absoprtion takes place (figure 5.14 **b**). Later, the top surface which is now a mixture of amine, water and CO_2 becomes more viscous. This adds resistance to the process of CO_2 and moisture diffusion. Thus, after a certain duration of time (t), the molecules slowly diffuse into fresh amine layer due to concentration gradient of CO_2 and moisture (figure 5.14 **c**)

Desorption cycle

During desorption phase, the bulk amine can be distinguished into different layers based on the viscosity. The bottom most layer is the one with fresh amine (without CO_2 and water). Whereas, the topmost layer is highly viscous containing CO_2 and water (figure 5.14**d**). As temperature rises, the viscosity of the bottom layer reduces. This allows more CO_2 to easily diffuse from high viscous region into the bulk (figure 5.14**e**). Additionally, some CO_2 in top layer escapes into the gas phase. The diffused molecules might accumulate until certain limit is reached and will be constantly mixed within the bulk due to temperature and concentration gradients.

The process of desorption explained in figure 5.14 can be observed in experimental data obtained during the desorption cycle. Figure 5.15 shows an individual desorption cycle of TEPA. The experiment was performed at desorption temperature of 80°C. The scale of the CO_2 analyser data has been set to RH data to analyse the desorption trend.

It can be seen in figure 5.15 that, during the maximum desorption of CO_2 a significant amount of moisture reading was recorded from the gas stream by the sensor. After 10 minutes the CO_2 concentration in the gas stream dropped to the initial value. This might suggest that some of the CO_2 and all the water molecules from the surface was desorbed and the remainder CO_2 was released in very low concentrations such that the CO_2 analyser failed to

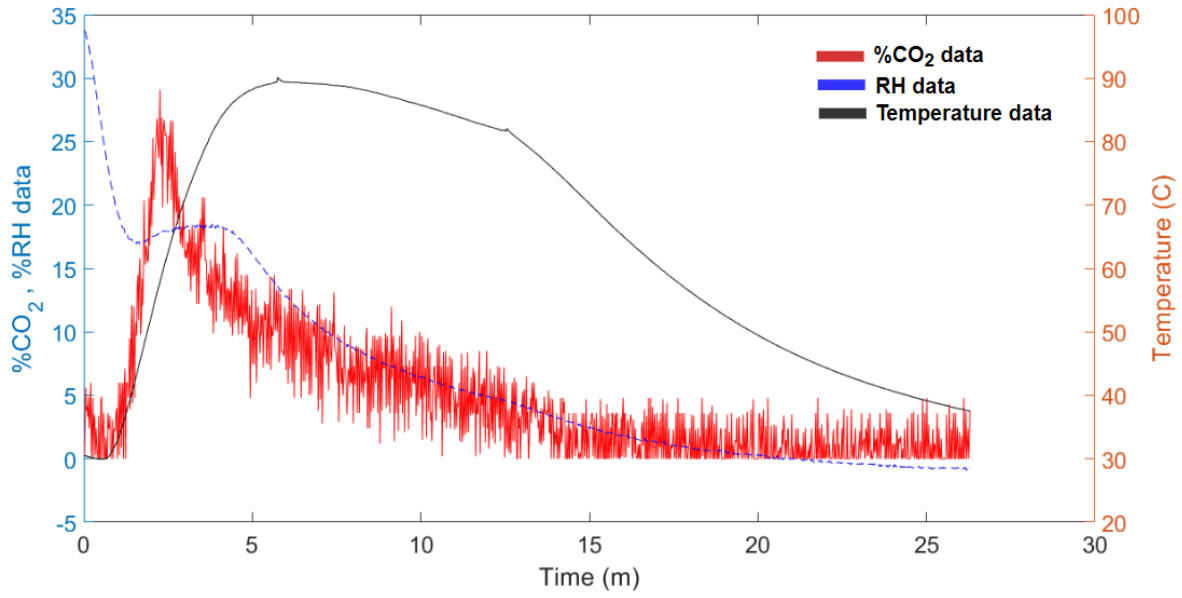

Figure 5.15: Desoprtion cycle of TEPA at 80^0C

measure. Similar trends were observed during PEI 80, 120 and TEPA-120°C experiments and the relevant plots are given in Appendix C.

5.4. FTIR results

The samples subjected to evaporation and cyclic experiments were analysed using FTIR to determine if any new molecular groups were formed during the experimental process. The spectra between 900cm^{-1} to 1800cm^{-1} has been presented in this section as it contains the important observations. The full spectra of all the results are given in Appendix C. During the analysis, the results are compared with that of pure amine (PEI/TEPA) to identify changes. The FTIR results of pure samples and their characterization can also be found in Appendix C.

5.4.1. Analysis of samples from muffle furnace experiments

Figure 5.16 shows the FTIR analysis of PEI subjected to evaporation testing via muffle furnace. When compared to the FTIR spectra of pure amine 3 important changes can be observed (shaded region).

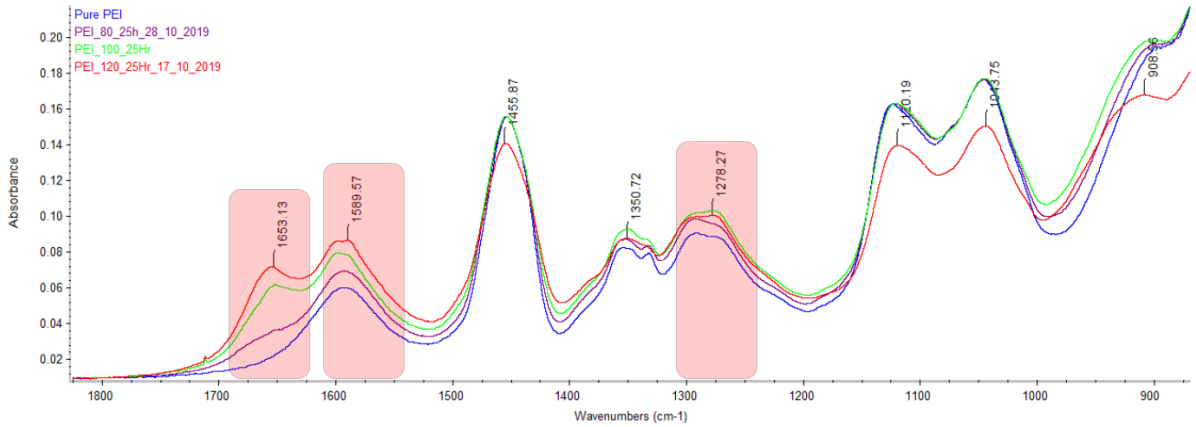

Figure 5.16: FTIR results of PEI subjected to evaporation test and comparison with pure amine

At 1653.13cm^{-1} PEI treated at 120°C and 100°C shows a distinct peak when compared to

that of pure PEI. PEI treated at 80°C shows transformation in those region. Similar changes can be observed at 1589.57cm^{-1} and 1278.27cm^{-1}. According to Li et al. [67], the formation of urea linkages in amines results in peaks at 1685, 1562, 1496, 1258, 1276cm^{-1}. The most important identification of urea linkage is the C=O stretching as the formation of urea takes place in the presence of CO_2. According to the spectral characterization chart [91] given in Appendix C ,the peak at 1653.13cm^{-1} observed in figure 5.16 also belongs to the band that signifies C=O stretching. It must be noted that the samples subjected to evaporation testing in the muffle furnace was pure, i.e the amine must be free of CO_2 molecules or in small quantities. But, the C=O stretching indicates that CO_2 might have been present in the amine sample that could have induced degradation. Before discussing further, it is important to analyse the FTIR results of TEPA samples subjected to evaporation testing as both TEPA and PEI reacts in similar pathways when exposed to CO_2. The FTIR results of TEPA samples are shown in figure 5.17.

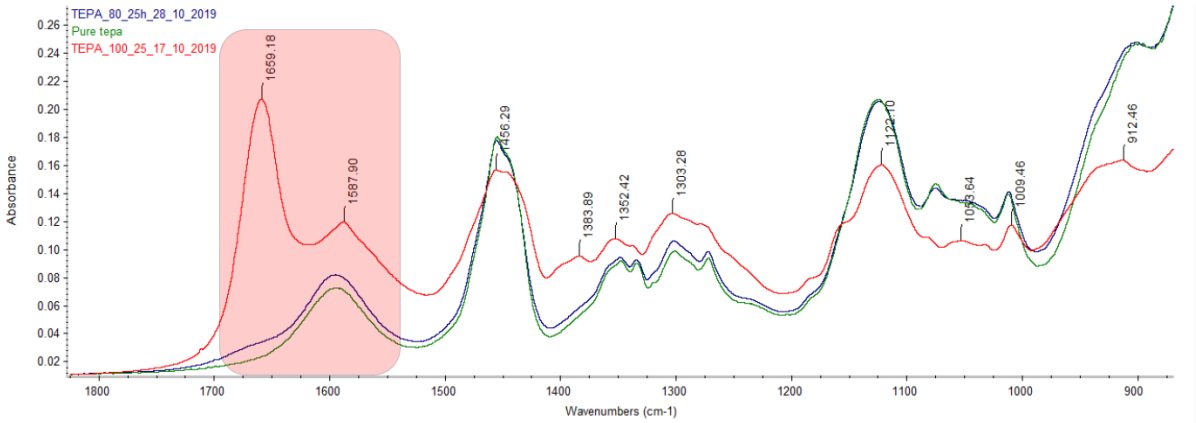

Figure 5.17: FTIR results of PEI subjected to evaporation test and comparison with pure amine

It can be seen that TEPA samples heated at 100°C also shows a peak at 1659.18cm^{-1} and 1587.90cm^{-1} which is similar to that of PEI seen in figure 5.16. A discussion on the degradation indicating peaks observed in both PEI and TEPA are given belwo:

- Although pure amine is assumed to have no CO_2, some CO_2 could have been absorbed during the sample preparation for the muffle furnace experiment.
- Studies of Ovaa [28] showed that the removal of CO_2 becomes difficult as the concentration of CO_2 in the amine reduces. Thus, a small quantity of CO_2 absorbed before the start of the experiment will remain the sample during evaporation test.
- The CO_2 could have reacted with the amine at higher temperatures (>100°C) resulting in urea formation [67].
- As TEPA is less stable than PEI [76], more urea linkages might have formed in TEPA. This could be the reason for a large peak in the C=O stretching band of TEPA seen in figure 5.17.
- As reported by Sayari [68], degradation of amines can also take place below 100°C but cannot be observed via FTIR as the formation rate is very slow. In such cases the peaks indicating the urea linkages will be masked by the amine and carbamate groups.

5.4.2. Analysis of samples from cyclic experiments

Figure 5.18 shows the FTIR of PEI samples subjected to cyclic absorption and desorption. The results are compared with the FTIR of pure PEI to identify the degradation products. It can be seen that both PEI samples (desorption temperature 120°C and 80°C) shows a peak at 1296.33cm^{-1}. Barthe [92] reported that this peak signifies carbamates and carbonates (i.e, the CO_2 absobeded by the amines will form carbamtes or carbonates). It was also mentioned in section 5.2.1 that the amine samples subjected to cyclic experiments showed accumulation of CO_2 after 30 cycles. This accumulation of CO_2 in the form of carbamates can be seen in

figure 5.18 at 1296.33cm^{-1}. Other than the peak at 1296.33cm^{-1}, there is no significant change in other parts of the spectra when compared with pure amine. This indicates that no degradation was observed during the 30 cycles of absorption and desorption (at desorption temperatures 120°C and 80°C)

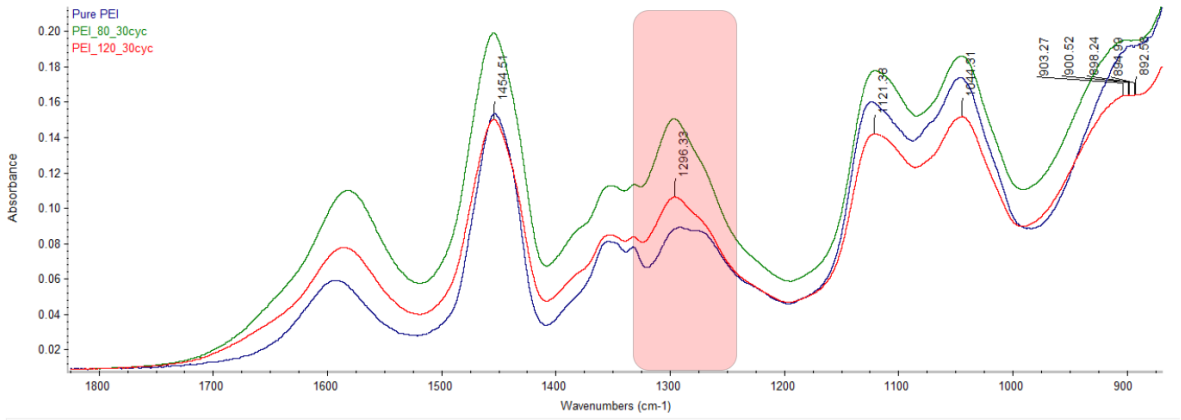

Figure 5.18: FTIR results of PEI subjected to cyclic absorption-desorption

Figure 5.19 shows the FTIR of TEPA samples subjected to cyclic absorption-desorption test. As seen in figure 5.18 and reported by Barthe[92], the peak at 1301.83cm^{-1} signifies carbamates. But it can be seen in figure 5.19 that pure TEPA also shows a peak at 1301.83cm^{-1} which indicates that the TEPA samples had absorbed CO_2 before the start of the experiments. Further, comparing the peaks of TEPA samples, TEPA desorbed at 80°C shows higher peak than TEPA desorbed at 120°C. This indicates that more carbamates were present in the sample that was desorbed at 80°C after 30 cycles. This result was confirmed by phosphoric acid testing and was presented in section 5.2.1.

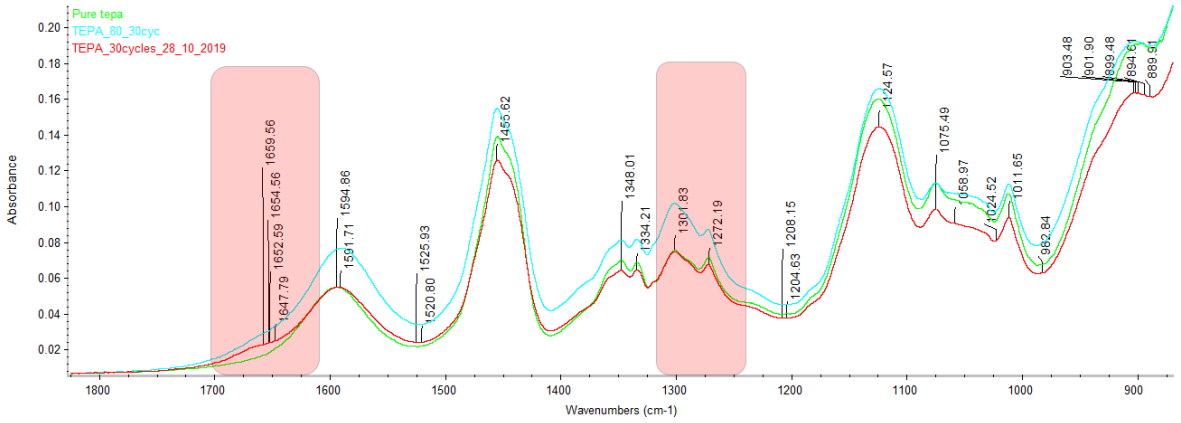

Figure 5.19: FTIR results of TEPA subjected to cyclic absorption-desorption

An important observation in figure 5.19 is that the TEPA sample desorbed at 120°C shows a peak at 1659.56cm^{-1}. As discussed in section 5.4.1, this peak indicates C=O stretching which is associated with urea linkages. It can be seen that no other significant peaks reported by Li [67] can be observed other than the peak at 1659.56cm^{-1}. The total duration of desorption during the 30 cycle experiment was approximately 20h. Considering the intensity of the peak at 1659.56cm^{-1} in figure 5.17 (TEPA sample subjected to evaporation at 120°C for 25h) , the TEPA sample subjected to cyclic test at 120°C for 20h shows a peak of low intensity. This could be due to the moisture absorbed during absorption. phase [50].

6

Conclusions and Recommendations

This thesis was focused on studying the evaporation and CO_2 induced degradation occurring in PEI and TEPA during the DAC process. The procedures of the experiments carried out were explained in Chapter 3. From the analysis made on the experimental data, few results and their implications in ZEF DAC system are discussed in Section 6.1. Further, few observations were made which could not be explained in this report as it lacks substantial experimental or theoretical evidence. Recommendations on such cases are presented in Section 6.2.

6.1. Conclusions

- Evaporation during absorption: The evaporation tests conducted on PEI and TEPA showed increase in mass. This could be due to absorption of CO_2 and moisture. As explained in section 2.3.1, the evaporation of amine reduces as the partial pressure of CO_2 and water increases with absorption. Thus, it can be concluded both PEI and TEPA do not experience evaporation losses during absorption phase.
- Vapor pressure of TEPA : The vapor pressure of TEPA was calculated from the evaporation results of TGA experiments. The value was found to be 0.1231Pa at 20°C. This value was used to theoretically estimate the evaporation losses under muffle furnace conditions. The results were compared with the experimental evaporation rates obtained from the muffle furnace experiments. The results were comparable and therefore, the calculated vapor pressure, 0.1231Pa at 20°C can be used to calculate approximate evaporation rates of TEPA at different temperatures.
- Evaporation of pure amine samples : The results of muffle furnace and TGA experiments showed that both PEI and TEPA experience significant evaporation losses (80, 100 and 120°C were selected temperatures for testing). As mentioned, the samples were pure or had very less concentration of CO_2 and water during the start of the experiment. The amines are subjected to high temperatures, i.e, >80°C during the desorption process. During the desorption process, the amines will contain significant concentration of CO_2 and water. But, as desorption progresses, the partial pressure of CO_2 and water reduces which will increase the evaporation rates of the amines. Thus, the results of this study can be considered as the maximum evaporation rates that the amines (PEI/TEPA) might experience during the desorption process.
- Evaporation during cyclic experiments: PEI and TEPA subjected to cyclic absorption and desorption showed that the evaporation during cyclic operation were comparable to that of the pure amine evaporation (i.e, the losses were significant). As mentioned earlier, the presence of CO_2 and water must reduce the evaporation of amines. But, based on the results of this study, it can be inferred that the during the desorption process, the amines might have been subjected to heat when the concentration of CO_2 and water was less. This condition might also take place during the actual DAC process. Thus, during long term operation, both PEI and TEPA will experience evaporation losses. This might increase the operation cost of DAC as new amine has to be frequently added. Adding a condenser block to collect the evaporated amine would be beneficial.
- CO_2 accumulation: The cyclic experiments showed accumulation of CO_2 in both PEI and TEPA after 30 cycles. The results were confirmed via phosphoric acid testing. The results also suggests that the CO_2 was constantly mixed within the amine bulk. As the presence of CO_2 increases the viscosity of the amine, the accumulation would cause flow related problems in the DAC system.

- CO_2 induced degradation: The amine samples (both PEI and TEPA) form the evaporation tests (muffle furnace experiment) showed new peaks which when compared to literature suggests that the amines might have undergone CO_2 induced degradation and degradation product could be urea. The new peaks were significant in TEPA when compared to PEI indicating that TEPA was less resistant to CO_2 induced degradation.

  Furthermore, for cyclic experiments after 30 cycles, the FTIR of PEI samples did not show any changes in the spectra when compared to that of pure PEI for both 80°C and 120°C. But, for TEPA desorbed at 120°C a new peak was observed (when compared to spectra of pure TEPA). The intensity of the peak was low and no other peak which are associated with urea was observed. This suggests that TEPA might have undergone degradation when desorbed at 120°C producing very low concentrations of urea.

6.2. Recommendations

- The concentration of moisture and CO_2 influence amine degradation. In this research, ambient air was used during absorption phase. As the concentrations of CO_2 and moisture in air varied due to various reasons, the effects of moisture and CO_2 concentrations with respect to degradation could not be observed. Thus, a regulated flow of CO_2 and moisture might help to analyse the behaviour better. This can be achieved by using gas bottles of required gas concentrations. The required humidity can also be achieved by adding water to the gas stream externally.
- During the cyclic experiments (CO_2 induced degradation study), the concentration of CO_2 absorbed and desorbed was within the range 0% to 0.02%. Measuring these low concentration resulted in errors. To obtain accurate and consistent data, the concentration of CO_2 absorption and desorption should be at least over 20% of the full scale (i.e, 0.4% CO_2 in the gas stream).
- In this research, the experimental set up constructed to carry out the cyclic absorption and desorption process was completely manual. The operation must be automated so that higher number of cyclic experiments can be conducted and human errors can be avoided.
- studies on absorption of O_2 in amines has to be carried out. This can be done by conducting vapor liquid equilibrium (VLE) experiment. A known mass of amine (PEI/TEPA) sample must be exposed to a known quantity of air in a closed system. The absorption of O_2 can be studied by observing the change in partial pressure of O_2. Furthermore, the O_2 induced degradation tests must be carried out.
- Influence of water in amine degradation must be studied. An accelerated degradation study can be carried by loading a known mass of amine sample with a know mass of CO_2. Different aliquots from the main sample should be prepared by adding different masses of water. The aliquots must be sealed in high pressure tubes and must be heated to required temperature and an extended duration of time. After the heat treatment, the samples must be removed FTIR should be conducted to identify the degradation. The degraded products can be quantified by carrying out potentiometric titration. The experiment can be conducted changing the water, CO_2 concentration and the heating temperature. This helps to understand the influence of water, CO_2 and temperature.
- The effect of amine thickness on desorption capacity should be studied. This can be done by loading a large sample of PEI/TEPA with a know mass of CO_2 and water. The sample must be well mixed to ensure homogeneous mixture is formed. The sample must be distributed into petridishes (same surface area) such that each aliquot has a different thickness. All aliqouts must be subjected to desorption at same temperature and same duration. After the experiment, the mass of CO_2 in the sample must be measured. This helps us to understand if desorption capacity depends on the thickness of the amine bulk.

- Pure TEPA and PEI were tested for impurities via Inductively coupled plasma atomic emission spectroscopy (ICPAE). The results are given in table 6.1. The effects of these impurities on the absorption, desorption and degradation of characteristics of amines have to be studied.

Table 6.1: Impurities (in ppm) found in PEI and TEPA via ICPAE

Amine	B	Ca	Mg	Zn	Cl	SO_4
PEI	0.1	0.0	0.0	0.0	4164.0	25.2
TEPA	0.3	1.2	0.1	0.0	0.0	26.0

- As seen in figure 5.11 and 5.10, the absorption capacity of TEPA appears to be increasing with the increase in number of cycles. This phenomena was observed in both 80°C and 120°C. Although this could be a measurement error, this is in contrast to the PEI experiments (where absorption trend decreases). This anomaly must be studied further. This can be carried out by exposing the amine to a set duration of time and measuring the mass of CO_2 and water absorbed. The loaded sample should be desorbed at a set temperature and duration. After the desorption process, the CO_2 and water in the lean mixture must be measured. The absorption process must be carried out again on the lean amine sample and the newly absorbed CO_2 and water must be measured. In case of expressing the mass of CO_2 and water per gram of amine, then the mass of amine sample taken to measure the CO_2 and water and the evaporated amine mass must be corrected during the final calculation of amine mass

Bibliography

[1] H.Shaftel. "Global Climate Change NASA"March 2019. Retrieved from *https://climate.nasa.gov/causes/*.

[2] H.Liu, R.Idem, P.Tontiwachwuthiklu. *"Post-Combustion CO_2 capture technology: By using amine based solvents "*. Springer Nature Switzerland, 2019.

[3] A.E Creamer , B.Gao. *"Carbon Dioxide Capture: An Effective way to combat Global Warmin "*. Springer Cham Heidelberg New York Dordrecht London, 2015.

[4] Church JA, White NJ. "a 20th century acceleration in global sea-level rise ". *Geophys Res Lett 33(1): L01602*, 2006.

[5] Parmesan C, Yohe G. "a globally coherent fingerprint of climate change impacts across natural systems ". In *Nature 421(6918):37–42*, 2003.

[6] Jos G.J, Olivier Jeroen, A.H.W.Peters. *"Trends in global CO_2 and total greenhouse gas emission "*. PBL Netherlands Environmental Assessment Agency, The Hague, December 2018.

[7] Cheng-Hsiu Yu, Chih-Hung Huang, Chung-Sung Tan. "a review of CO_2 capture by absorption and adsorption ". In *Aerosol and Air Quality Research, 12: 745–769*, 2012. doi: doi:10.4209/aaqr.2012.05.0132.

[8] Oh T.H. "carbon capture and storage potential in coal-fired plant in malaysia-a review ". In *Sustainable Energy Rev. 14: 2697–2709.*, 2010.

[9] Miller D.C, Litynski J.T, Brickett L.A., Morreale B. D. "toward transformational carbon capture systems". In *AIChE J, 62, 2–10.*, 2016.

[10] *BP Statistical Review of World Energy*. Retrived from: *https://www.bp.com/content/dam/bp/business-sites/en/global/corporate/pdfs/energy-economics/statistical-review/bp-stats-review-2018-primary-energy.pdf*, June 2018.

[11] Bryce Dutcher, Maohong Fan, Armistead G. Russell. "amine-based co2 capture technology development from the beginning of 2013-a review ". *ACS Appl. Mater. Interfaces 2137−2148*, 2015.

[12] Chen Chen, Massimo Tavoni. "direct air capture of co2 and climate stabilization: A model based assessment". *Climatic Change 118:59–72*, 2013.

[13] Eloy S. Sanz-Perez, Christopher R. Murdock, Stephanie A. Didas, and Christopher W. Jones. "direct capture of co2 from ambient air". *Chemical reviews*, 2016.

[14] D'allesandro DM, Smith B, Long JR. "carbon dioxide capture: prospects of new material". *Angew Chem Int Ed 49(35):6058 - 6082*, 2010.

[15] Tzimas E,Peteves.S. "controlling carbon emissions: The option of carbon sequestration". *office for Official Publications of the European Communities: Luxembourg*, 2003.

[16] Prachi Singh. *"Amine based solvents for CO2 absorption: from molecular structure to process"(PhD Thesis)*. PhD thesis, University of Twente, The Netherlands, 2011.

[17] Young Gun Ko, Seung Su Shin, Ung Su Choi. "primary, secondary, and tertiary amines for CO_2 capture: Designing for mesoporous CO_2 adsorbents ". *Journal of Colloid and Interface Science 361 (2011) 594–602*, .

[18] M. Wanga, A. Lawala, P. Stephensonb, J. Siddersb, C. Ramshawa. "post-combustion CO_2 capture with chemical absorption:a state-of-the-art review". *chemical engineering research and design 89 (2011) 1609–1624*.

[19] Parliamentary office of science and technology. "CO_2 capture, transport and storage". 2009.

[20] Keith WD, Ha-Duong M, Stolaroff KJ. "climate strategy with co2 capture from the air". *Climate Change 74:17–45*, 2005.

[21] House KZ, Baclig AC, Ranjan M, van Nierop EA, Wilcox J, Herzog HJ. "economic and energetic analysis of capturing co2 from ambient air". In *Proc Natl Acad Sci U S A 108(51):20428-33. doi: 10.1073/pnas.1012253108*, 2011 Dec 20.

[22] K.S Lackner, H Ziock, P Grimes. "24th international conference on coal utilization and fuel systems clearwater, fl ". 1999.

[23] S.A Didas, A.R. Kulkarni, D.S Sholl, C.W Jones. "role of amine structure on carbon dioxide adsorption from ultradilute gas streams susch as amibient air". In *ChemSusChem*, volume 5, pages 2058–2064, 2012. doi: 10.1002/cssc.201200196.

[24] George A. Olah, Alain Goeppert, and G. K. Surya Prakash. "chemical recycling of carbon dioxide to methanol and dimethyl ether: From greenhouse gas to renewable, environmentally carbon neutral fuels and synthetic hydrocarbons". *Loker Hydrocarbon Research Institute and Department of Chemistry, UniVersity of Southern California, UniVersity Park, Los Angeles, California 90089-1661*, 2008.

[25] *"Zero Emission Fuels - Zero emission methanol from sunlight and air."http://www.zeroemissionfuels.com/.*

[26] Poort Jonah. "solving vapor-liquid flash problems using artificial neural networks (master thesis).". Master's thesis, Retrived from TU delft education repository., 2018-10-30.

[27] M.Sinha. "characterization and design of novel absorption process". In *Master's thesis dissertation, TU/Delft*, 2019.

[28] B. Ovaa. "direct air capture: An experimental approach on the desorption of CO_2 and H_2O from pei and tepa". In *Master's thesis dissertation, TU/Delft*, 2019.

[29] *McMurry, John E. (1992), "Organic Chemistry (3rd ed.)", Belmont: Wadsworth, ISBN 0-534-16218-5.*

[30] Caplow M. "kinetics of carbamate formation and breakdown". *American Chemical Society, Vol. 90, pp 6795–6803*, 1968.

[31] Dankwerts P. V. "the reaction of co2 with ethanolamines.". *Chemical Engineering Science, Vol. 34, pp 443*, 1979.

[32] Ohno K., Inoue Y., Yoshida H., Matsuura E. "reaction of aqueous 2-(nmethylamino) ethanol solutions with carbon dioxide chemical species and their conformations studied by vibrational spectroscopy and ab initio theories.". *Physical Chemistry A, Vol. 103, pp 4283–4292*, 1999.

[33] da Silva E. F., Svendsen H. F. "ab initio study of the reaction of carbamate formation from co2 and alkanolamine". In *Industrial Engineering Chemical Research, Vol. 43, pp 3413-3418*, 2004.

[34] Crooks J. E., Donnellan J. P. "kinetics and mechanism of the reaction between carbon dioxide and amines in aqueous solution". *Chemical Society, Perkins Trans., Vol. II, pp 331*, 1989.

[35] Blauwhoff P. M. M., Versteeg G. F., van Swaaij W. P. M. "a study on the reaction between co2 and alkanolamines in aqueous solutions ". *Chemical Engineering Science, Vol. 39, pp 207*, 1984.

[36] Donaldsen T. L., Nguyen Y. N. "carbon dioxide reaction kinetics and transport in aqueous amine membranes". *Industrial Engineering Chemical Fundamental, Vol. 19, pp 260–266*, 1980.

[37] Hikita H., Asai S., Ishikawa H., Honda M. “the kinetics of reactions of carbon dioxide with monoethanolamine, diethanolamine and triethanolamine by a rapid mixing method”. *Chemical Engineering Journal, Vol. 13, pp 7*, 1977.

[38] Lin S. H., Shyu C. T. “carbon dioxide absorption by amines: system performance predictions and regeneration of exhausted amine solution.”. *Environmental Technology, Vol. 21 (11), pp 1245*, 2000.

[39] Young Gun Ko, Seung Su Shin , Ung Su Choi. “primary, secondary, and tertiary amines for CO_2 capture: Designing for mesoporous co2 adsorbents”. *Journal of Colloid and Interface Science 361 (2011) 594–602*, .

[40] Drage T C , Arenillas A , Smith K, M Snape. “thermal stability of polyethylenimine based carbon dioxide adsorbents and its influence on selection of regeneration strategies”. *Microporous Mesoporous Mater. 2008, 116, 504−512.*

[41] Liu H, Liang. Z, Sema T, Rongwong W, Li C, Na Y. “kinetics of co2 absorption into a novel 1-diethylamino-2-propanol solvent using stopped-flow technique”. In *AIChE Journal, 60, 3502–3510.*, 2014.

[42] Kohl A. L, Nielsen R. “gas purification”. *Gulf Publishing Company, Houston, Texas*, 1997.

[43] 325 1652–1654. Rochelle, G. T. (2009).“Amine scrubbing for CO2 capture”. Science.

[44] K.P. Resnik. “aqua ammonia process for simultaneous removal of co2, so2 and no”. *Int. J.Environ. Technol. Manage. 4: 89–104.*, 2004.

[45] R.S Haszeldine. “carbon capture and storage: How green can black be?”. *Science 325: 1647–1651.*, 2009.

[46] Didas. S. A. “structural properties of aminosilica materials for CO_2 capture”. *Georgia Institute of Technology*, 2014.

[47] Sjostorm.S, Krutka.H. “evaluation of solid sorbents as a retrofit tecnology for CO_2 capture.”. *Fuel: 89, 1298-1306*, 2010.

[48] Duke.M.C, Ladewig.B, Smart.S, Rudolph.V, Diniz da Costa .J.C. “assessment of post-combustion carbon capture technologies for power generation”. *Front.Chem.Eng China, 4(2),184-195*, 2010.

[49] Xiaoyun Zhang, Xiuxin Zheng, Sisi Zhang, Bei Zhao, and Wei Wu. “am-tepa impregnated disordered mesoporous silica as co2 capture adsorbent for balanced adsorption−desorption properties ”. *Eng. Chem. Res. , 51, 15163−15169*, 2012.

[50] Aliakbar Heydari-Gorji, Abdelhamid Sayari. “thermal, oxidative, and co2-induced degradation of supported polyethylenimine adsorbents”. *Ind. Eng. Chem. Res. , 51, 6887−6894*, 2012.

[51] R.Bubicco, Barbara Mazzarotta. “predicting evaporation rates from pools”. *Department of Chemical Engineering Materials Environment, Sapienza University of Rome, Via Eudossiana 18, 00184, Rome, Italy.*, 2016.

[52] L. G Thibodeaux. “chemodynamics: environmental movement of chemicals in air, water, and soil”. *New York, John Wiley and Sons*, 1979.

[53] C. O, Myers J. E. Bennett. “momentum, heat and mass transfer”. *New York, McGraw-Hill*, 1974.

[54] C. Gouedard, D.Picq, F.Launay, P.L Carrette. “amine degradation in CO_2 capture: A review ”. *International Journal of green house gas control 10- 244 - 270*, 2012.

[55] Svendsen-H.F. Lepaumier H, da Silva E.F, Einbu A, Grimstvedt A, Knudsen, J.N, Zahlsen K.R. “comparison of mea degradation in pilot-scale with labscale experiments”. *Energy Procedia 4, 1652–1659*, 2011a.

[56] Fazio M.J. “nucleophilic ring-opening of 2-oxazolines with amines – a convenient synthesis for unsymmetrically substituted ethylenediamines”. *Journal of Organic Chemistry 49, 4889–4893*, 1984.

[57] Lee S, Filburn T.P, Gray M., Park J.W, Song H.J. “screeening test of solid amine sorbents for CO_2 capture”. *Ind. Eng. Chem. Res. 47: 7419–742*, 2008.

[58] Sayari A., Belmabkhout Y, Serna-Guerrero R. “flue gas treatment via CO_2 adsorption”. *Chem. Eng. J. 171: 760–774.*, 2011.

[59] W., Jones C.W , Giannelis E.P. Qi G., Wang Y., Estevez L., Duan X., Anako N., Park A.H.A., Li. “high efficiency nanocomposite sorbents for CO_2 capture based on amine-functionalized mesoporous capsules.”. *Energy Environ. Sci. 4: 444–452.*, 2011.

[60] Abdelhamid Sayari and Youssef Belmabkhout. “stabilization of amine-containing co2 adsorbents: Dramatic effect of water vapor”. *J. AM. CHEM. SOC. 2010, 132, 6312–6314*.

[61] Chen C, Son W.J, You K.S, Ahn J.W, Ahn W.S. “carbon dioxide capture using amine-impregnated hms having textural mesoporosity”. *Chem. Eng. J. 161: 46–52*, 2010.

[62] Ro´bert Me´sza´ros, Laurie Thompson, Imre Varga, and Tibor Gila´nyi. “adsorption properties of polyethyleneimine on silica surfaces in the presence of sodium dodecyl sulfate”. *Langmuir 2003, 19, 9977-9980*.

[63] V. V. NEDEL’KO, B. L. KORSUNSK, F. I. DUBOVITSKH , G L GROMOVA. “the thwermal degradation of branced pei ”. *Chemical Physics Institute, USSR Academy of Sciences*, 1974.

[64] Kim C, Sartor G. “kinetics and mechanism of diethanolamine degradation in aqueous solutions containing carbon dioxide”. *International Journal of Chemical Kinetics, 16, 1257–1266.*, 1984.

[65] X Li K, Jiang J, Yan F, Tian S, Chen. “the influence of polyethyleneimine type and molecular weight on the CO_2 capture performance of pei-nano silica adsorbents ”. *Appl. Energy, 136, 750−755*, 2014.

[66] Jean Fournier, Christian Bruneau, Pierre H. Dixneuf, and Serge Lécolier1. “ruthenium-catalyzed synthesis of symmetrical n,n’-dialkylureas directly from carbon dioxide and amines”. *J. Org. Chem. 1991, 56, 4456-4458*.

[67] K.Li, J.Jiang, X.Chen, Y.Gao,F.Yan, S.Tian. “research on urea linkages formation of amine functional adsorbents during co2 capture process: Two key factors analysis, temperature and moisture”. The Journal of Physical chemistry, 120(45), 25892-25902, 2016.

[68] Sayari A, Belmabkhout Y, Serna-Guerrero R. “flue gas treatment via CO_2 adsorption ”. *Chem. Eng. J. , 171, 760−774.*, 2011.

[69] Bollini P, Choi S, Drese JH, Jones C. W. “oxidative degradation of aminosilica adsorbents relevant to postcombustion co2 capture.”. *Energy Fuels. 25, 2416–2425 (2011).*

[70] J. C Hicks. “designing adsorbents for co2 capture from flue gashyperbranched aminosilicas capable of capturing CO_2 reversibly”. *J. Am. Chem. Soc. 130, 2902–2903 (2008).*

[71] Heydari-Gorji A, Belmabkhout.Y, Sayari. A. “a. degradation of amine supported CO_2 adsorbents in the presence of oxygen-containing gases”. *Microporous Mesoporous Mater. 145, 146–149 (2011).*

[72] Sunghyun Park, Keunsu Choi, Hyun Jung Yu, Young-June Won, Chaehoon Kim, Minkee Choi, So-Hye Cho, Jung-Hyun Lee, Seung Yong Lee,and Jong Suk Lee. “thermal stability enhanced tetraethylenepentamine/silica adsorbents for high performance CO_2 capture”. *Ind. Eng. Chem. Res. 2018, 57, 4632−4639*, 2018.

[73] Yue M.B, Chun Y, Cao Y, Dong X and Zhu J.H. “CO_2 capture by as-prepared sba-15 with an occluded organic template”. *Adv. Funct. Mater. 16: 1717–1722.*, 2006.

[74] W. Su F, Lu C, Kuo S C, Zeng. "adsorption of CO_2 on amine-functionalized y-type zeolites". *Energy Fuels 2010, 24(2), 1441*, 2010.

[75] Yue M.B, Sun L.B, Cao Y, Wang Z.J, Wang Y, Yu Q, Zhu J.H. "promoting the co2 adsorption in the amine-containing sba-15 by hydroxyl group.". *Microporous Mesoporous Mater. 114: 74–81.*, 2008.

[76] X, Zhang S, Zhao B, Wu W. AM-TEPA Zhang, X, Zheng. "tepa impregnated disordered mesoporous silica as co2 capture adsorbent for balanced adsorption-desorption properties". *Chem. Res. 2012, 51 (46), 15163*, 2012.

[77] Woosung Choi, Kyungmin Min1,Chaehoon Ki, Young Soo Ko, Jae Wan Jeon, Hwimin Seo, Yong-Ki Park , Minkee Choi. "epoxide-functionalization of polyethyleneimine for synthesis of stable carbon dioxide adsorbent in temperature swing adsorption". *NATURE COMMUNICATIONS | DOI: 10.1038/ncomms12640*, 2016.

[78] Quyen Thi Vu, Hidetaka Yamada, and Katsunori Yogo. "oxidative degradation of tetraethylenepentamine- impregnated silica sorbents for CO_2 capture". *published by the American Chemical Society. 1155 Sixteenth Street N.W., Washington, DC 20036*, 2019.

[79] Tanthana J. and Chuang S.S.C. "in situ infrared study of the role of peg in stabilizing silica-supported amines for co2 capture". *ChemSusChem 3: 957–964*, 2010.

[80] Chakravartula S. Srikanth , Steven S. C. Chuang. "spectroscopic investigation into oxidative degradation of silica-supported amine sorbents for CO_2 capture". *ChemSusChem 2012, 5, 1435 – 1442*, 2012.

[81] Xiaochun Xu, Chunshan Song, John M. Andresen, Bruce G. Miller, and Alan W. Scaroni. "novel polyethylenimine-modified mesoporous molecular sieve of mcm-41 type as high-capacity adsorbent for CO_2 captur". *Energy Fuels 2002, 16, 1463-1469*, 2002.

[82] `http://hyscien.cafe24.com/wp/wp-content/uploads/2014/06/Structure_MF.jpg`.

[83] PerkinElmer. "beginner's guide to thermogravimetric analyser".

[84] A.W.Coats, J.P.Redrern. "thermogravimetric analysis - a review". *Royal Society of Chemistry,doi:10.1039/AN9638800906*, 1963.

[85] Linda Froberg. "thermal analysis tga/dta". *http://web.abo.fi/instut/biofuelsGS-2/kursen/C5A/lectures/Lectrure$_T$hermal20Analysis.pdf*.

[86] TA instruments. "thermal analysis". 2014.

[87] Silicon Labs. i^2c humidity and temperature sensor - manual.

[88] Binos 100M. "operation manual - ndir - analyzer".

[89] Stephenson.R, Malanowski.S. Handbook of the thermodynamics of organic compounds. 1987 ,doi.org/10.1007/978-94-009-3173-2, `https:webbook.nist.gov/cgi/cbook.cgi?ID=C112572&Mask=7FF,Thermo-Phase`.

[90] Physical properties of TEPA. `https://pubchem.ncbi.nlm.nih.gov/compound/tetraethylenepentamine`.

[91] Colthup N.B. "characteristic infrared group frequencies". In *Stamford Research Laboratories, American Cyanamid and the editor of Journal of the optical society*.

[92] Nuria Serrano Barthe. "absorption of CO_2 from air using polyamines:experiments, modellinig and design". *Master Thesis dessertation*, 2019.

[93] M.Toledo. 'karl-fischer coulometers - operating instructions".

[94] A. Adeosun, N. El Hadri, E. L. Goetheer,, and M. R. AbuZahra. "absorption of co2 by amine blends solution: An experimental evaluation ". *International Journal Of Engineering and Science 3, 12*, 2013.

A

CO_2 and water measuring devices

A.1. Karl-Fischer titration

During this thesis, the concentration of water in the amine samples were determined using a coulometric Karl-Fischer device. The basic design of the equipment is shown in figure A.1.

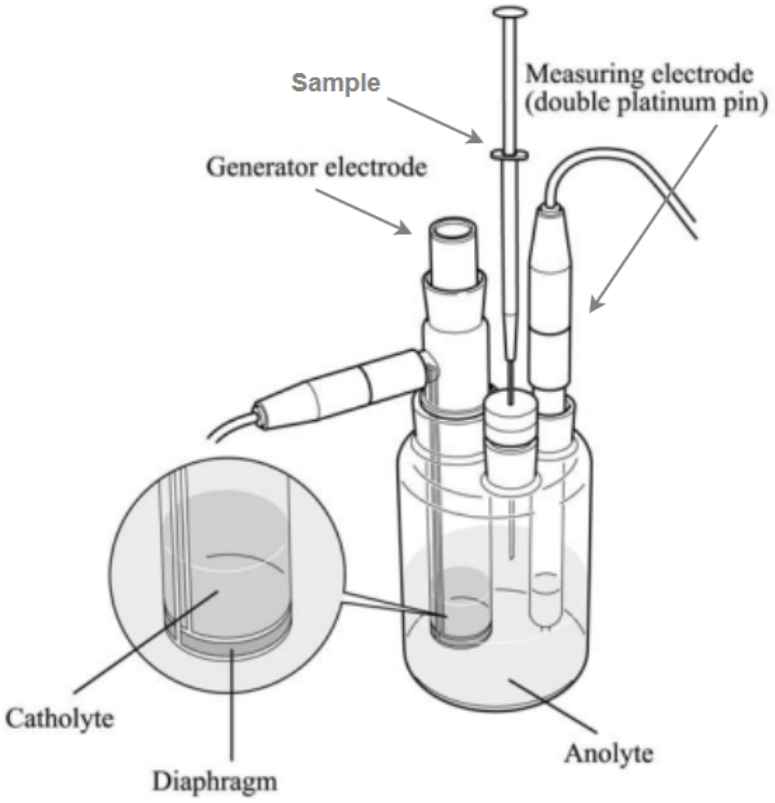

Figure A.1: Coulometric Karl-Fischer titration equipment [93]

The Karl-Fischer titrator consists of an iodine generator and a detector electrode. when a sample containing water is added to the solution, the iodine reacts with water in 1:1 ratio that results in depletion of iodine in the solution. The depleted iodine is replenished by the generator. This process continues until all the water is reacted with iodine. As per Faraday's law, the moles of iodine and the electrical charge produced are proportional. Thus, the device is calibrated such that the $1\mu H_2O$ = 10.712mC [27]. This relation helps to determine the concentration of water in the amine sample. A test sample with low pH results in faster and accurate results. This condition is maintained by diluting the test sample with methanol. The water detection limit is between $0.1\mu g$ to $10\mu g$ [93].

A.2. Phosporic acid testing

The layout of the phosphoric acid test set-up used during the thesis is shown in the figure A.2.

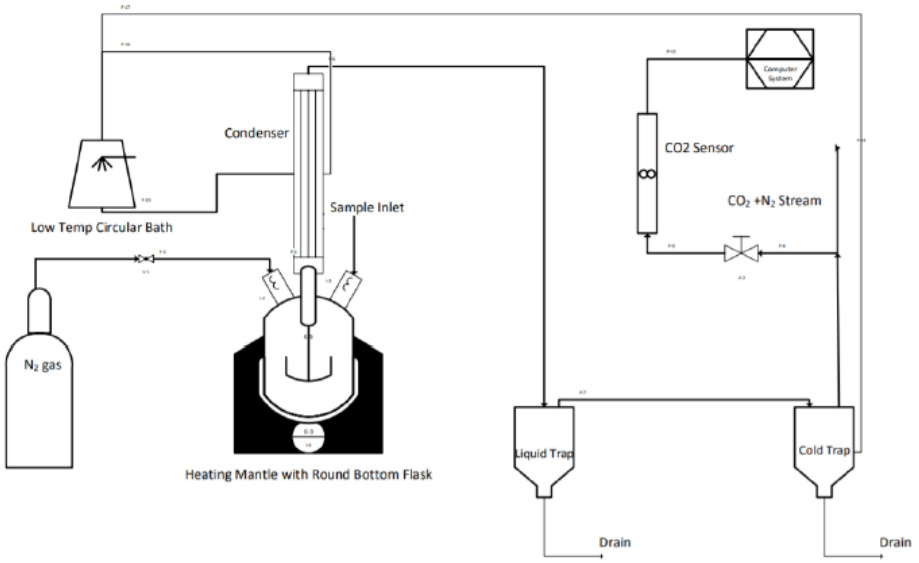

Figure A.2: Coulometric Karl-Fischer titration equipment [94]

The setup consists of a round bottom flask filled with phosphoric acid. During the experiment the flask is maintained at around 150°C [27]. when the amine loaded with cO_2 is added to the acid, the CO_2 and water is stripped out of the amine due to esterification between amine and hot acid. The gases are then passed through a condenser where water vapour is condensed. The gas stream with only CO_2 is passed through a CO_2 analyses where concentration of CO_2 is determined [94].

B

Experimental data and Calculations

B.1. Evaporation testing - Muffle furnace and cyclic experiments

Table B.1: Mass measurements of amine samples during muffle furnace experiments

Amine-Desorption temperature (Celsius)	Surface Diameter of petridish (cm)	Initial mass of sample (g)	Final mass of sample (g)	Evaporation loss ($mg\,m^{-2}\,s$)
PEI-120	6.5	5.1168	4.8162	0.985
TEPA-120	6.5	3.9626	0.1231	12.988
PEI-100	6.5	4.3395	4.1732	0.545
TEPA-100	6.5	2.5181	0.2969	7.28
PEI-80	5.5	3.9457	3.9088	0.0169
TEPA-80	5.5	5.7767	5.5428	0.1074

The evaporation results of cyclic experiments can be found in table B.3 page 78.

B.2. Methanol sample preparation

Table B.2: Mass of amine and methanol used for preparing samples for Karl-Fischer and Phosphoric acid testing (A - mass of Amine sample, M - mass of methanol)

Amine-Desorption temperature (Celsius) Sample Number	A (g)	M (g)	A + M (g)	A in M (g)
PEI - 80 - I	0.065	10.2252	10.2902	0.006317
PEI - 80 - II	0.0255	7.578	7.6035	0.003354
PEI - 120 - I	0.0803	11.2658	11.3461	0.007077
PEI - 120 - II	0.0646	10.71069	10.77529	0.005995
TEPA - 80 - I	0.1296	9.9601	10.0897	0.012845
TEPA - 80 - II	0.0852	10.2186	10.3038	0.008269
TEPA - 120 - I	0.1153	13.3461	13.4614	0.008565
TEPA - 120 - II	0.086	7.8296	7.9156	0.010865

Table B.3: Mass measurement and evaporation rate ($\mathrm{g\,m^{-2}\,s^{-1}}$) calculation during cyclic experiments

Amine-Desorption temperature (Celsius)	Initial mass of sample (g)	Final mass of sample (g)	Mass of CO_2 measured $gramCO_2/gramAmine$	Mass of CO_2 in amine after 30 cycles	Mass of amine without CO_2 after 30 cycles	Mass of amine evaporated after 30 cycles	amine loss when surface area assumed to be $0.0037\mathrm{m^2}$	amine loss when surface area assumed to be $0.0022\mathrm{m^2}$
TEPA - 120	3.59	2.6	0.0144	0.03	2.56	1.02	3.7	6.4
PEI - 120	5.17	5.16	0.0339	0.17	4.98	0.18	0.68	1.16
TEPA - 80	4.94	5.02	0.035	0.17	4.84	0.09	0.35	0.60
PEI -80	5.14	5.27	0.041	0.21	5.05	0.08	0.31	0.54

B.3. Karl- Fischer Experiment result

The results of Karl-Fischer experiment can be found in table B.4 page 80 and table B.5 page 81

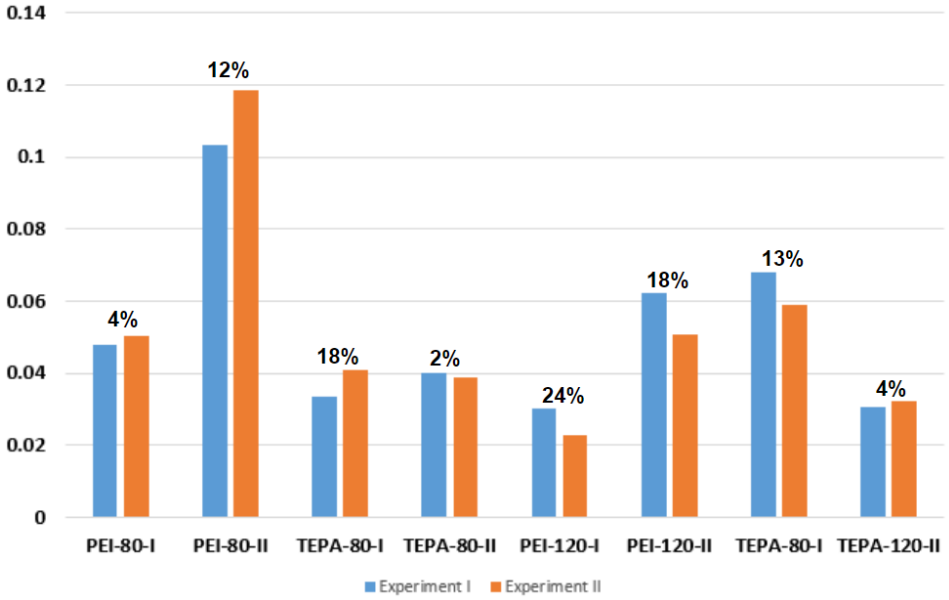

Figure B.1: Difference in results obtained during karl - Fischer experiments

Table B.4: Mass of mixture (amine+methanol) sample used to determine the water/gram of amine via Karl-Fischer experiment

Amine-T (Celsius) SN	Amine in Methanol (g)	Sample size added to KF exp (g)	Mass of water determined in the experiment (g)	water in methanol (g)	Amine in Sample (g)	Methanol in Sample (g)	Water in Methanol (g)	Water determined after correction (g)	Mass of water in amine sample
PEI - 80 - I	0.006317	0.1021	0.0000937	0.00062	0.000644934	0.101455	6.29021E-05	3.07979E-05	0.047754
PEI - 80 - II	0.003354	0.0812	0.0000783	0.00062	0.000272322	0.080928	5.01752E-05	2.81248E-05	0.103278
TEPA - 80 - I	0.012845	0.0622	0.0000647	0.00062	0.000798945	0.061401	3.80687E-05	2.66313E-05	0.033333
TEPA - 80 - II	0.008269	0.0774	0.0000732	0.00062	0.000640005	0.07676	4.75912E-05	2.56088E-05	0.040013
PEI - 120 - I	0.007077	0.0902	0.0000747	0.00062	0.000638374	0.089562	5.55282E-05	1.91718E-05	0.030032
PEI - 120 - II	0.005995	0.0459	0.0000454	0.00062	0.00027518	0.045625	2.82874E-05	1.71126E-05	0.062187
TEPA - 120 - I	0.008565	0.0635	0.000076	0.00062	0.000543892	0.062956	3.90328E-05	3.69672E-05	0.067968
TEPA - 120 - II	0.010865	0.0805	0.0000763	0.00062	0.000874602	0.079625	4.93677E-05	2.69323E-05	0.030794

Table B.5: Mass of mixture (amine+methanol) sample used to determine the water/gram of amine via Karl-Fischer experiment
Duplicate experiment

Amine- T (Celsius) SN	Amine in Methanol (g)	Sample size added to KF exp (g)	Mass of water determined in the experiment (g)	water in methanol (g)	Amine in Sample (g)	Methanol in Sample (g)	Water in Methanol (g)	Water determined after correction (g)	Mass of water in amine sample
PEI - 80 -I	0.006317	0.0569	0.0000531	0.00062	0.00035942	0.056541	3.50552E-05	1.80448E-05	0.050205
PEI - 80 - II	0.003354	0.077	0.0000782	0.00062	0.000258236	0.076742	4.75799E-05	3.06201E-05	0.118574
TEPA - 80 -I	0.012845	0.0719	0.0000819	0.00062	0.00092354	0.070976	4.40054E-05	3.78946E-05	0.041032
TEPA- 80 - I	0.008269	0.1003	0.0000939	0.00062	0.00082936	0.099471	6.16718E-05	3.22282E-05	0.038859
PEI - 120 - I	0.007077	0.1017	0.000079	0.00062	0.000719764	0.10098	6.26077E-05	1.63923E-05	0.022774
PEI - 120 - II	0.005995	0.0983	0.0000904	0.00062	0.000589328	0.097711	6.05806E-05	2.98194E-05	0.050599
TEPA - 120 - I	0.008565	0.0699	0.0000783	0.00062	0.00059871	0.069301	4.29668E-05	3.53332E-05	0.059016
TEPA - 120 - II	0.010865	0.0643	0.000062	0.00062	0.000698595	0.063601	3.94329E-05	2.25671E-05	0.032304

B.4. Phosphoric acid test results

Table B.6: Experimental values and results of phosphoric acid test

Amine- Desorb temperature (Celsius) Sample Number	Sample added to test (g)	Mass of CO_2 in sample (g)	Amine in Methanol sample (g)	Amine in Sample added to test (g)	gram CO_2 in gram Amine
TEPA - 120 - I	3.784	0.000476	0.008565	0.03241	0.014687
TEPA- 120- II	3.415	0.0005353	0.010865	0.037104	0.014426
PEI-80-I	3.9	0.001	0.006317	0.024632	0.040597
PEI-80-II	2.8	0.0003883	0.003354	0.009391	0.041347
TEPA-80-I	3.326	0.0015	0.012845	0.042722	0.03511
TEPA-80-II	3.708	0.0011	0.008269	0.030658	0.03588
PEI-120-I	3.775	0.0009236	0.007077	0.026717	0.034569
PEI-120-II	3.839	0.0007802	0.005995	0.023015	0.0339

C

Relevent plots and FTIR spectral chart

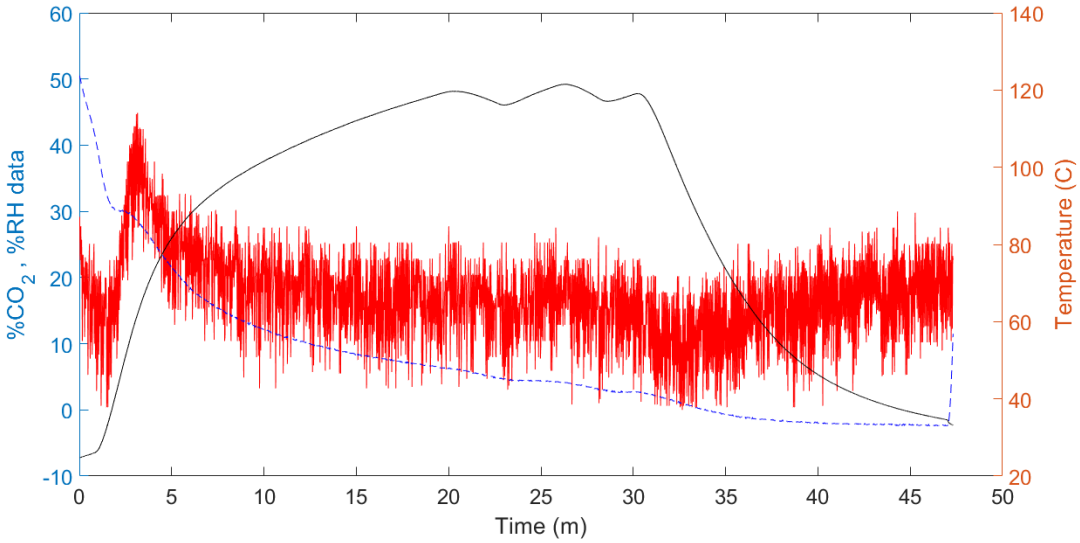

Figure C.1: Desoprtion cycle of TEPA at 120^0C
black - Temperature
blue - Relative humidity (%)
red - Concentration of CO_2 (%)

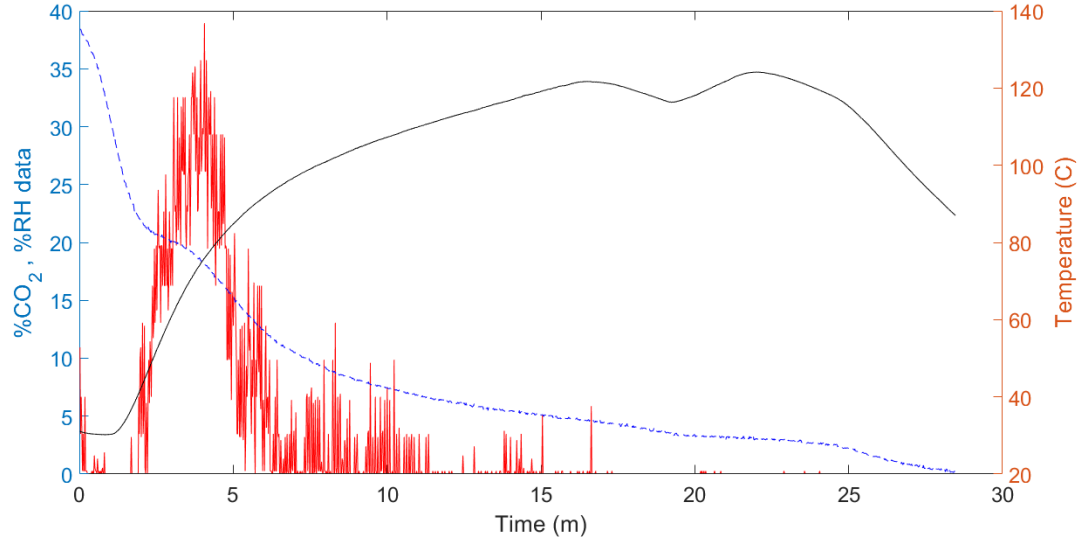

Figure C.2: Desoprtion cycle of PEI at 80^0C
black - Temperature
blue - Relative humidity (%)
red - Concentration of CO_2 (%)

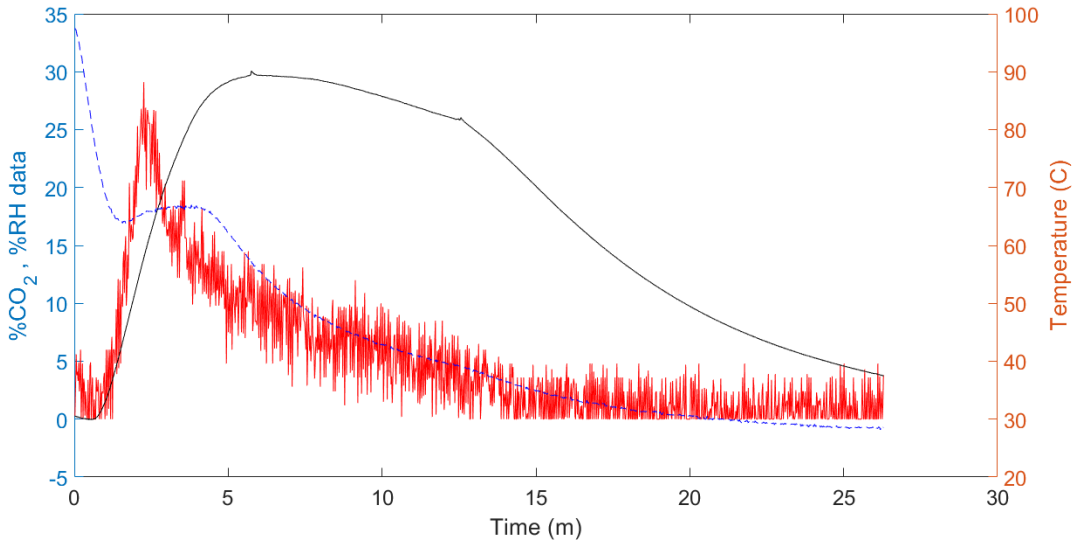

Figure C.3: Desoprtion cycle of PEI at 80^0C
black - Temperature
blue - Relative humidity (%)
red - Concentration of CO_2 (%)

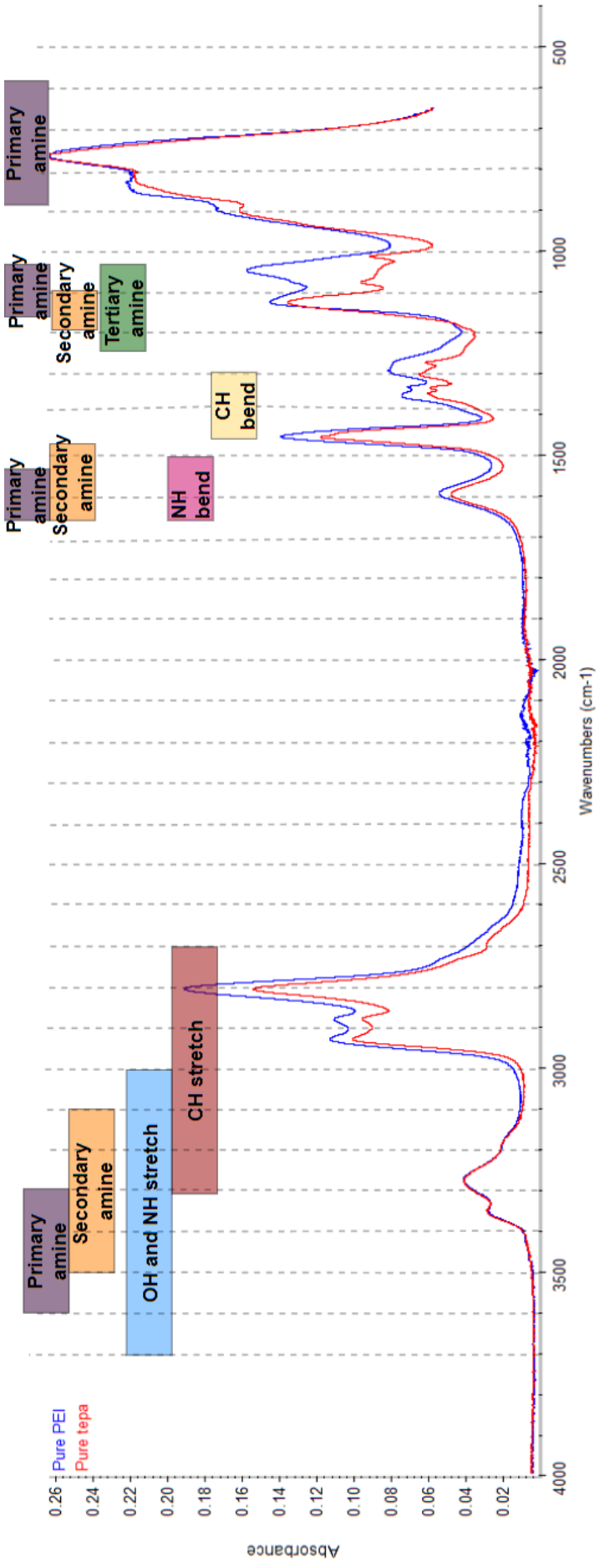

Figure C.4: FTIR results of pure PEI and TEPA // The characterization of the peaks observed in both the samples with respect to literature [91]

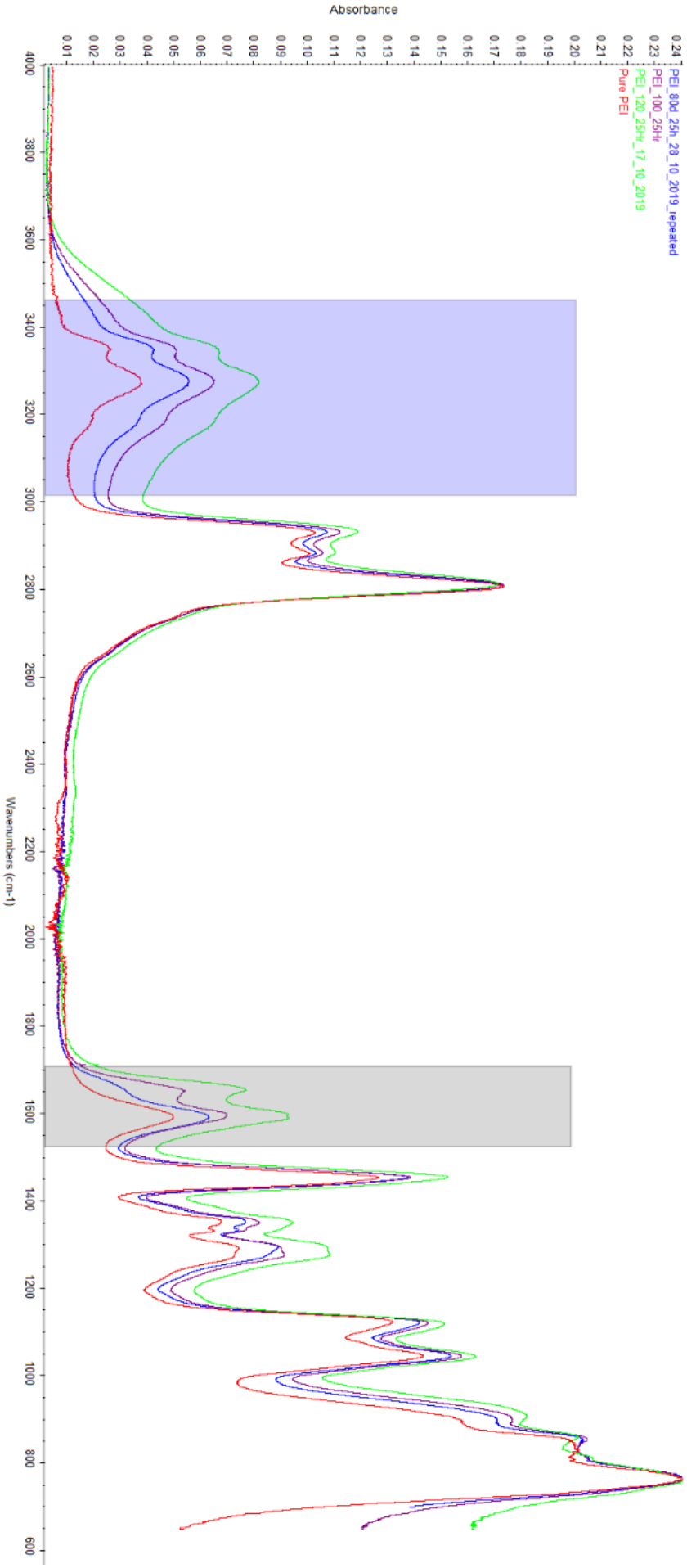

Figure C.5: FTIR results of PEI - Muffle furnace experiments
Blue - indicates presence of water
Grey - indicates change of peaks in amine region

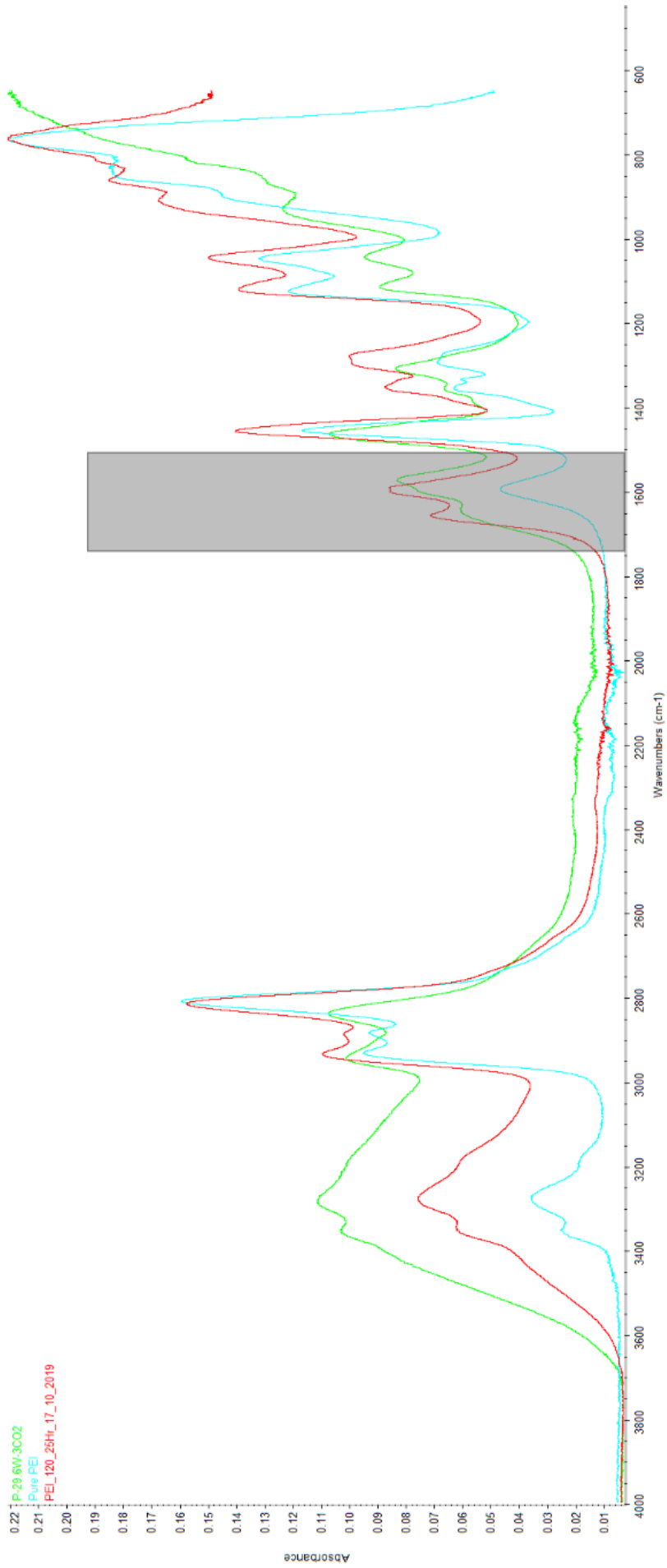

Figure C.6: Comparison of PEI results with CO_2 loaded samples
Blue - indicates presence of water
Grey - indicates change of peaks in amine region

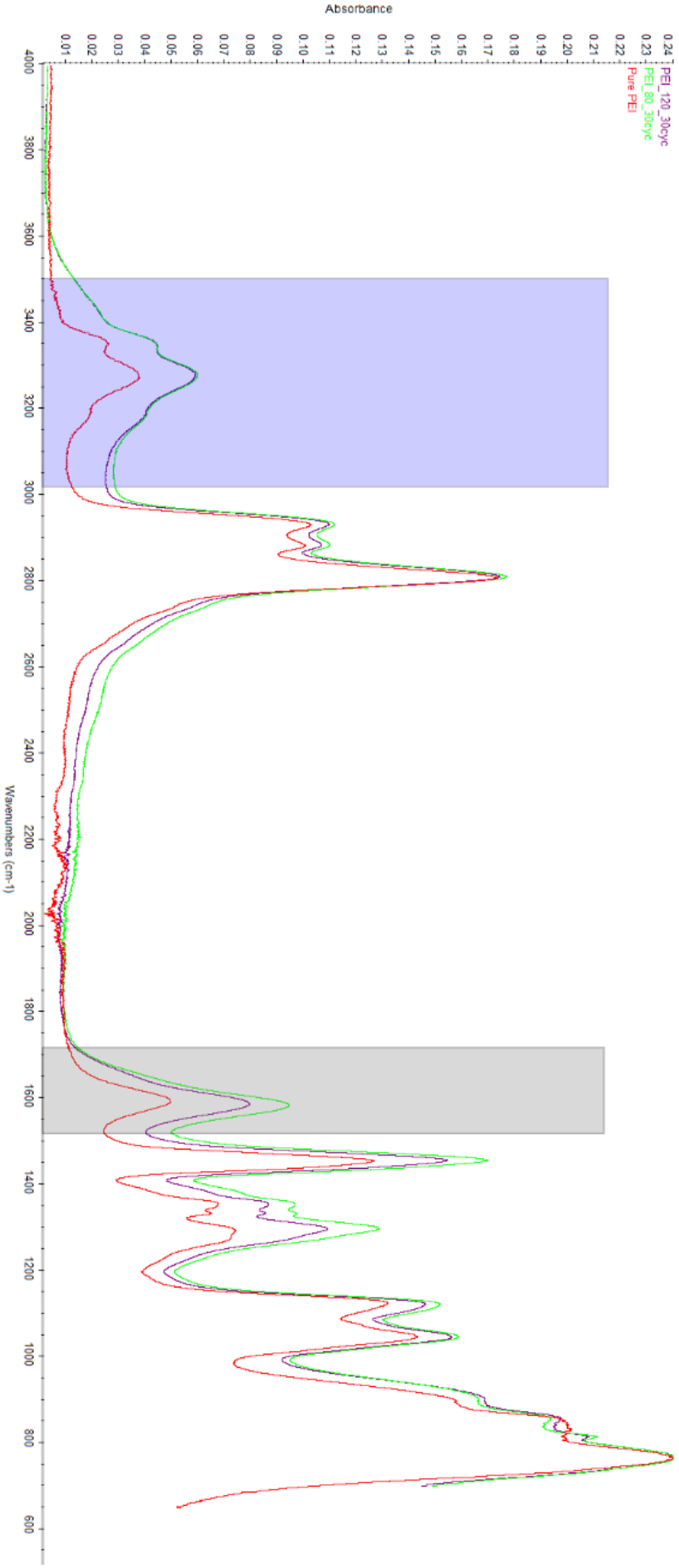

Figure C.7: FTIR results - PEI cyclic experiments
Blue - indicates presence of water
Grey - indicates change of peaks in amine region

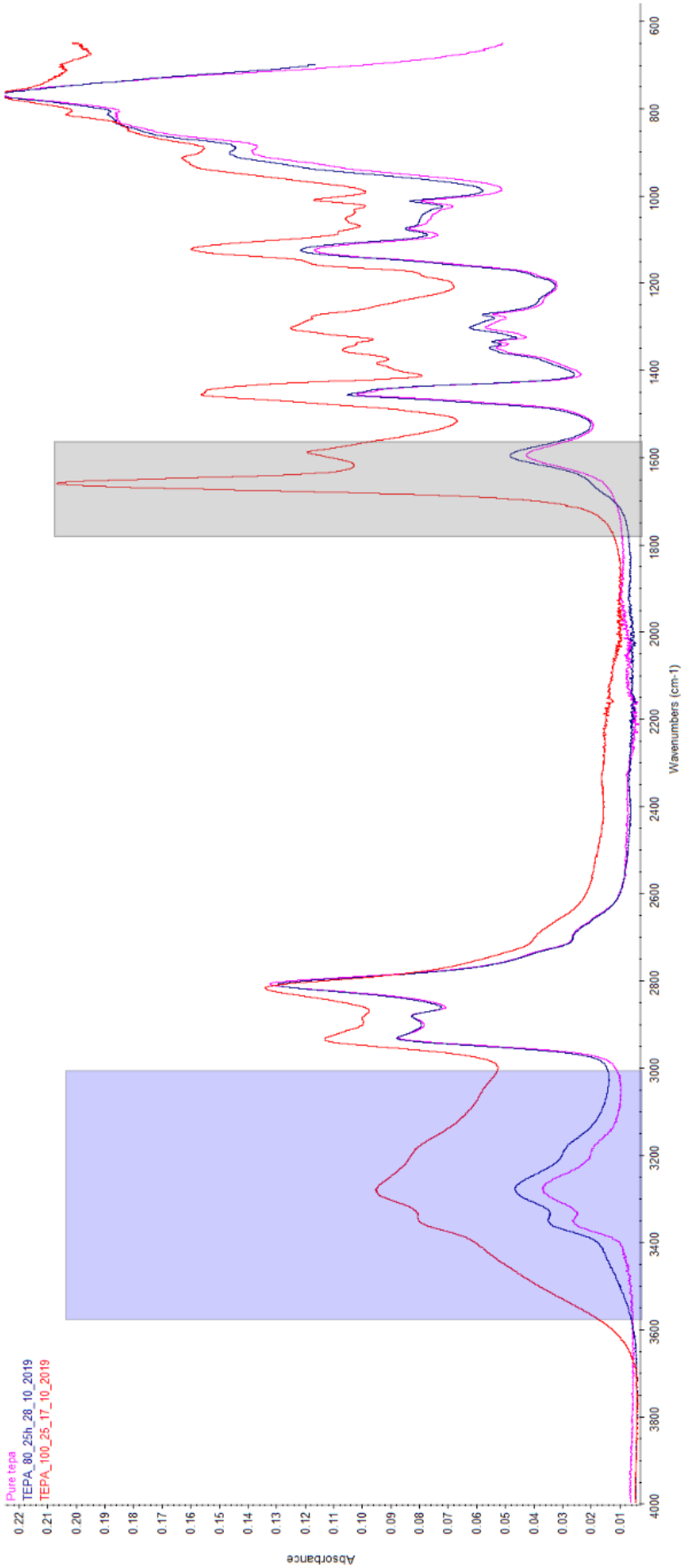

Figure C.8: FTIR results of TEPA - Muffle furnace experiments
Blue - indicates presence of water
Grey - indicates change of peaks in amine region

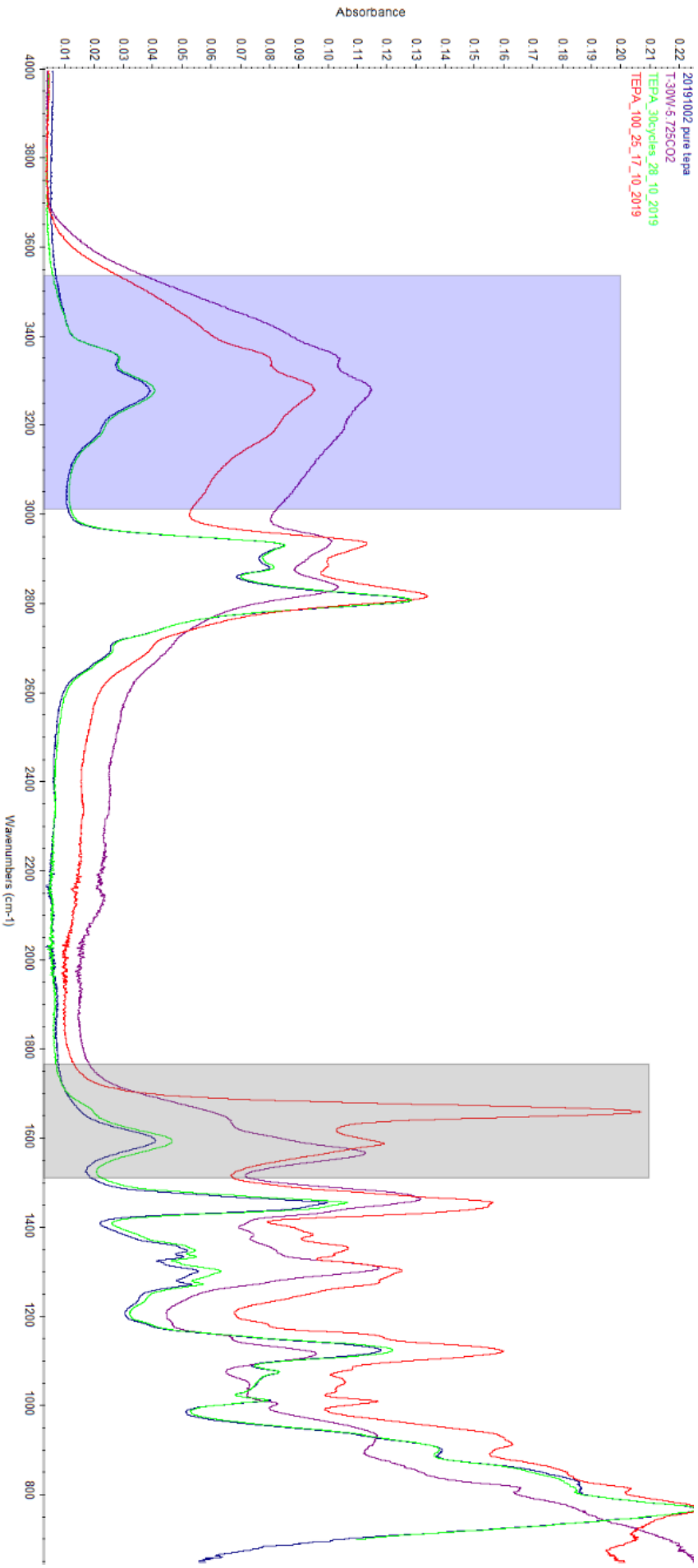

Figure C.9: Comparison of TEPA results with CO_2 loaded samples
Blue - indicates presence of water
Grey - indicates change of peaks in amine region

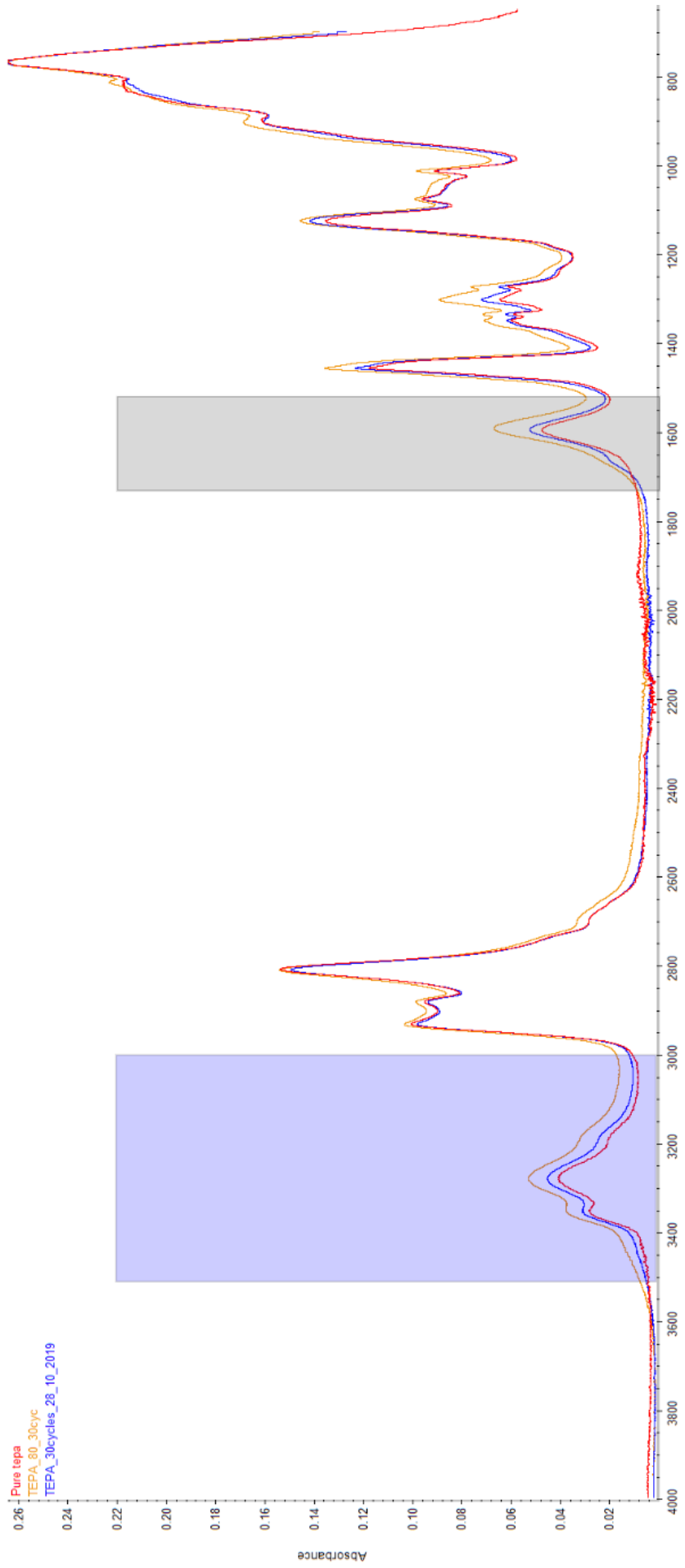

Figure C.10: FTIR results - TEPA cyclic experiments
Blue - indicates presence of water
Grey - indicates change of peaks in amine region

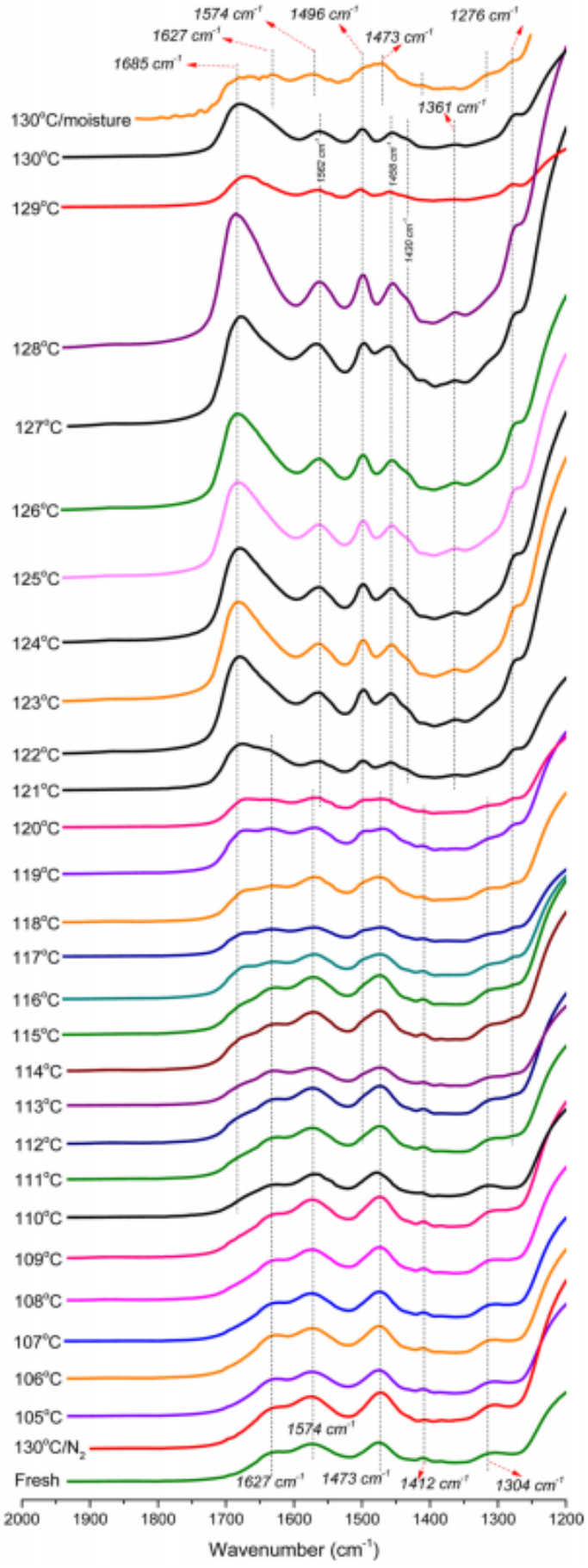

Figure C.11: FTIR analysis of PEI - Degradation study carried out by Li et al. [67]

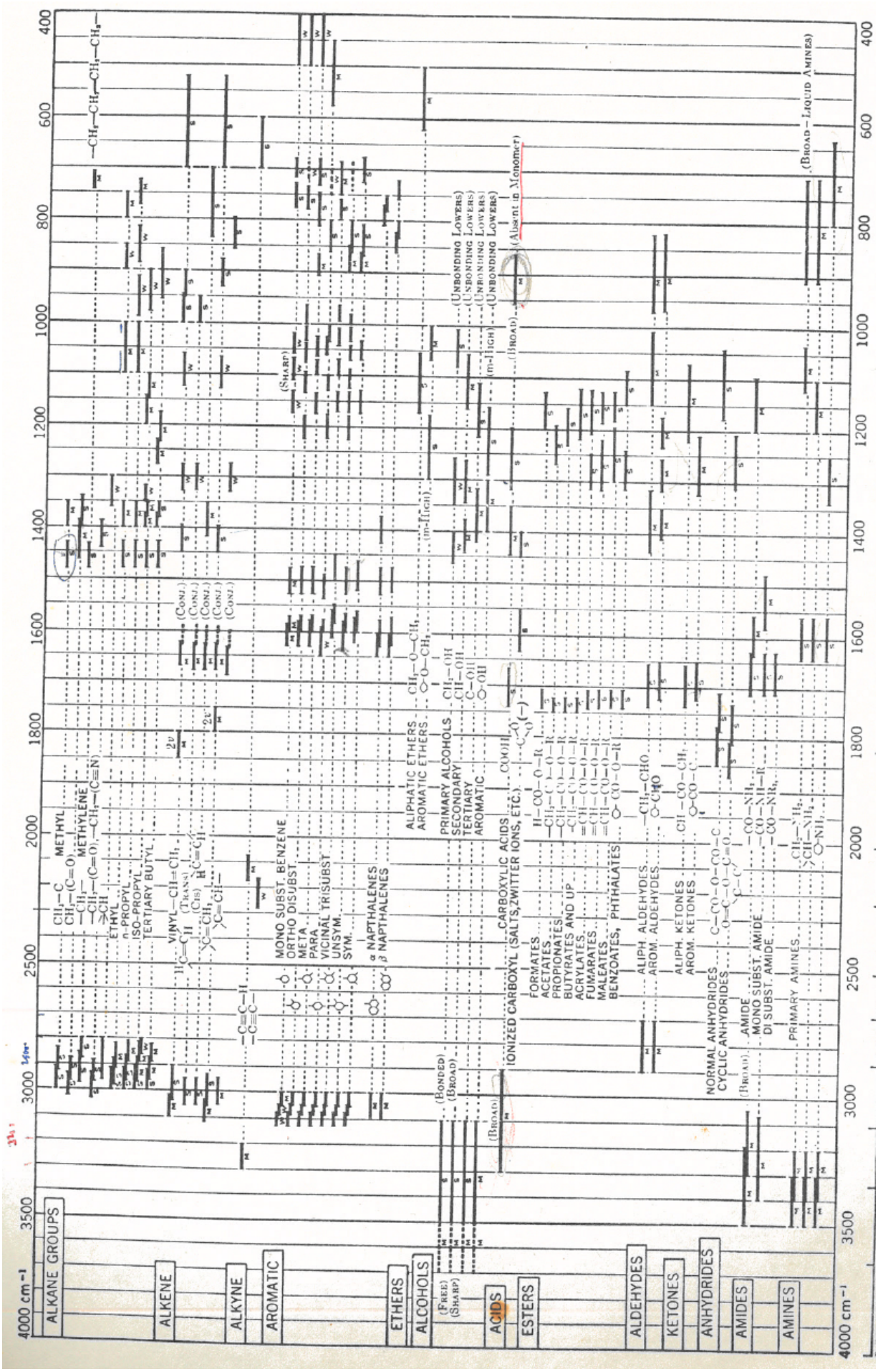

Figure C.12: Characteristic infrared group frequencies [91]

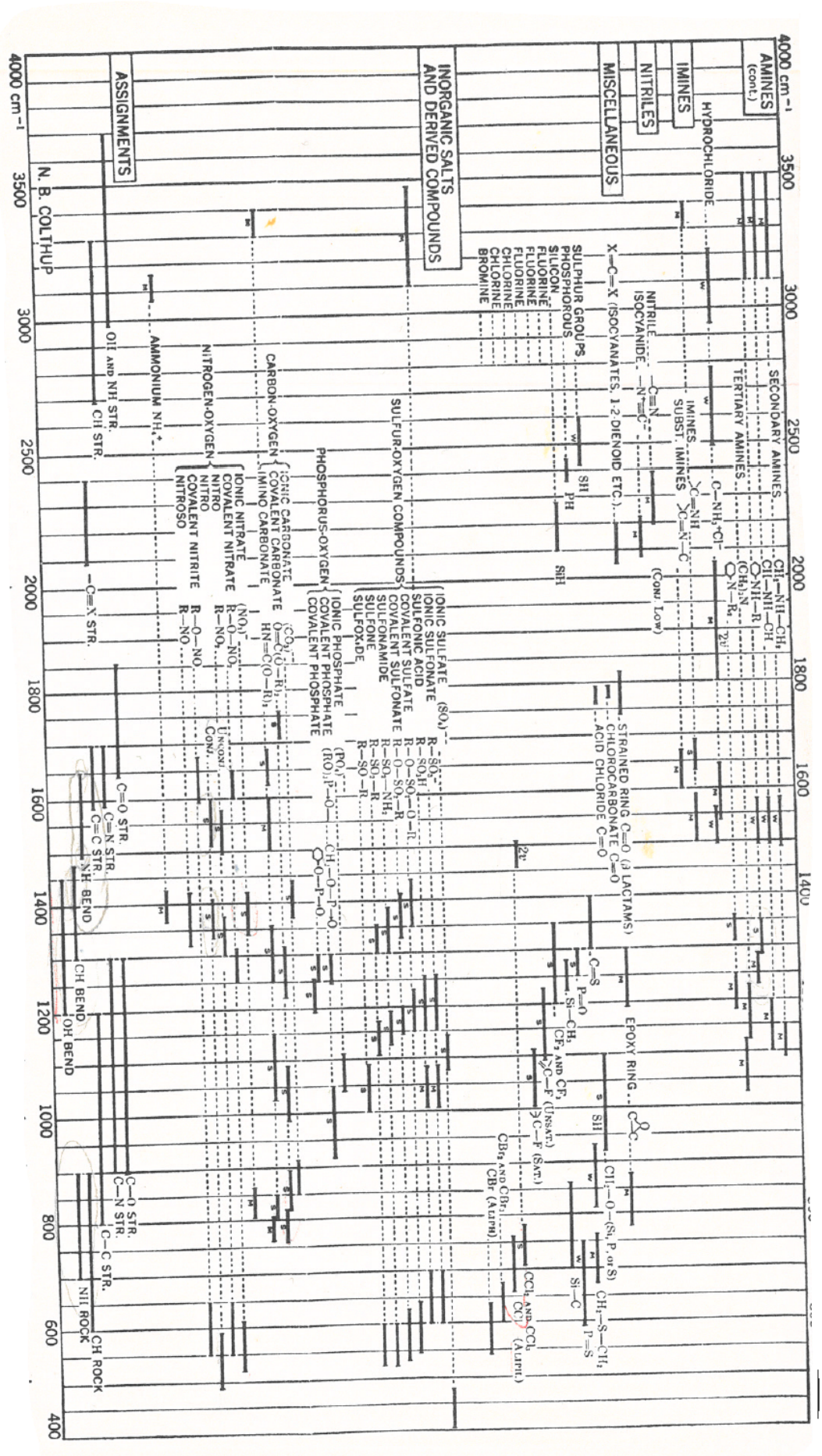

Figure C.13: Characteristic infrared group frequencies [91]